R. E. Babuilen

PROCEEDINGS

AMERICAN SOCIETY OF CIVIL ENGINEERS FOUNDED 1852

American Society
of
Civil Engineers

AUGUST
1935

Foundations
Cummings
823

VOLUME 61 NO. 6

PROCEEDINGS

OF THE

AMERICAN SOCIETY OF CIVIL ENGINEERS

VOL. 61 AUGUST, 1935 No. 6

TECHNICAL PAPERS

AND

DISCUSSIONS

Published monthly, except June and July, at 99–129 North Broadway, Albany, N. Y., by the American Society of Civil Engineers, Editorial and General Offices at 33 West Thirty-ninth Street, New York, N. Y. Reprints from this publication may be made on condition that the full title of Paper, name of Author, page reference, and date of publication by the Society, are given.

Entered as Second-Class Matter, December 28, 1931, at the Post Office at Albany, N. Y., under the Act of March 3, 1879. Acceptance for mailing at special rate of postage provided for in Section 1103, Act of October 3, 1917, authorized on July 5, 1918.

Subscription (if entered before January 1) $8.00 per annum. Price $1.00 per copy.

CURRENT PAPERS AND DISCUSSIONS

		Discussion closes
An Asymmetric Probability Function. *J. J. Slade, Jr.*	Oct., 1934	
Discussion	Dec., 1934, Jan., Feb., Mar., Apr., May, 1935	Closed
Analysis of Continuous Structures by Traversing the Elastic Curves. *Ralph W. Stewart*	Oct., 1934	
Discussion	Dec., 1934, Feb., Mar., May, 1935	Closed
Relation Between Rainfall and Run-Off from Small Urban Areas. *W. W. Horner and F. L. Flynt*	Oct., 1934	
Discussion	May, 1935	Sept., 1935
The Silt Problem. *J. C. Stevens*	Oct., 1934	
Discussion	Feb., Mar., May, 1935	Uncertain
Effect of Secondary Stresses Upon Ultimate Strength. *John I. Parcel and Eldred B. Murer*	Nov., 1934	
Discussion	Jan., Mar., Aug., 1935	Sept., 1935
The Springwells Filtration Plant, Detroit, Michigan. *Eugene A. Hardin*	Nov., 1934	
Discussion	Jan., 1935	Closed
Analysis of Multiple Arches. *Alexander Hrennikoff*	Dec., 1934	
Discussion	May, 1935	Sept., 1935
Rational Design of Steel Columns. *D. H. Young*	Dec., 1934	
Discussion	Mar., May, Aug., 1935	Sept., 1935
A Direct Method of Moment Distribution. *T. Y. Lin*	Dec., 1934	
Discussion	Mar., May, Aug., 1935	Sept., 1935
Elastic Properties of Riveted Connections. *J. Charles Rathbun*	Jan., 1935	
Discussion	Feb., May, Aug., 1935	Oct., 1935
Analysis of Thick Arch Dams, Including Abutment Yield. *Philip Cravitz*	Jan., 1935	Oct., 1935
Hydraulic Laboratory Results and Their Verification in Nature. *Herbert D. Vogel*	Jan., 1935	
Discussion	May, Aug., 1935	Oct., 1935
The Hydraulic Jump in Terms of Dynamic Similarity. *Boris A. Bakhmeteff and Arthur E. Matzke*	Feb., 1935	
Discussion	Mar., May, Aug., 1935	Oct., 1935
Frictional Resistance in Artificially Roughened Pipes. *Victor L. Streeter*	Feb., 1935	
Discussion	Aug., 1935	Oct., 1935
Stabilizing Constructed Masonry Dams by Means of Cement Injections. *D. W. Cole*	Feb., 1935	
Discussion	Aug., 1935	Uncertain
Weights of Metal in Steel Trusses. *J. A. L. Waddell*	Feb., 1935	
Discussion	May, 1935	Oct., 1935
Line Load Action on Thin Cylindrical Shells. *Herman Schorer*	Mar., 1935	Nov., 1935
Underground Corrosion. *K. H. Logan*	Mar., 1935	
Discussion	Apr., Aug., 1935	Nov., 1935
The Adjustment of a Level Net. *George H. Dell*	Apr., 1935	
Discussion	Aug., 1935	Nov., 1935
Structural Beams in Torsion. *Inge Lyse and Bruce G. Johnston*	Apr., 1935	
Discussion	Aug., 1935	Nov., 1935
Photo-Elastic Determination of Shrinkage Stresses. *Howard G. Smits*	May, 1935	Nov., 1935
The Shear-Area Method. *Horace B. Compton and Clayton O. Dohrenwend*	May, 1935	
Discussion	Aug., 1935	Nov., 1935

NOTE.—The closing dates, herein published, are final except when names of prospective discussers are registered for special extension of time.

CONTENTS FOR AUGUST, 1935

PAPERS

DISCUSSIONS

CONTENTS FOR AUGUST, 1935 (*Continued*)

For Index to all Papers, the discussion of which is current in PROCEEDINGS, *see page 2*

AMERICAN SOCIETY OF CIVIL ENGINEERS
Founded November 5, 1852
PAPERS

FLOOD-STAGE RECORDS OF THE RIVER NILE

By C. S. Jarvis,[1] M. Am. Soc. C. E.

Synopsis

The need for longer hydrographic records than are now available on American streams, as disclosed by recent investigations dealing with floods and their various characteristics, has led the writer to a study of the records of foreign rivers. The paper affords only a brief summary of outstanding records or evidences regarding stream-flow trends of European and Asiatic rivers, and then undertakes the presentation of stages of the Nile River at the Roda gauge, in Cairo, Egypt, covering a period of thirteen centuries. Additional data, such as those procured at Aswan, dealing with both stages and volumes, and various versions of divergent data, are added to make the graphic representation as nearly complete as is practicable on one continuous chart. No attempt is made at this time to evaluate the data, as they are too numerous and complex to permit ready appraisals. The main purpose is a presentation of records, or some kind of derivation from actual observations, as a preliminary to further study by the profession.

General Considerations

The study of flood frequencies and magnitudes by the United States Geological Survey in collaboration with, and under the sponsorship of, the Mississippi Valley Committee and its successor, the National Resources Board (Water Planning Committee), has advanced some interesting information relating to long-period records of river stages. These records were investigated with a view to furnishing a background for the interpretation of available hydrographic records in the United States, most of them covering relatively short periods.

A few American flood records extend intermittently into the Colonial era —notably the Ohio River, at Pittsburgh, Pa., and the James, Roanoke, Delaware, Mississippi, and other rivers at or near tide-water. In this manner a sketchy and somewhat uncertain notion may be derived as to the comparative

Note.—Discussion on this paper will be closed in November, 1935, *Proceedings*.

[1] Senior Hydr. Engr., U. S. Geological Survey, Washington, D. C.

river stages, or the corresponding discharges, where the channel sections and controls have not changed materially; but at best a period of only about 200 yr may be thus covered in this country from written records or satisfactorily authenticated marks.

The study of drift or débris deposits, the heights of mounds distributed along the flood-plains of rivers and presumably intended as islands of refuge (as on the Lower Mississippi and in the Nile Delta), the character of trees and other vegetation along various contours, the evidences of either channel scouring or filling, and consideration of other prominent geologic and geomorphic features may add significant items of information relating to the occurrence of floods in the past, possibly within a few hundred years.

What can be said more definitely of such floods as have left their marks, and of similar contemporaneous events of equal importance that have left no physical effects or record marks clear enough for recognition and separate interpretation? Some investigators have expressed the opinion that a continuous record of stages on a large stream, over a period of 500 or 1 000 yr, for example, might indicate more definitely the trends and cyclic or other recurrent periods of stages above or below normal than several shorter records of equal or greater aggregate length. Before such long-period records of foreign streams can serve a useful purpose most effectively, account must be taken of the differences in physical factors as affecting run-off habits. This applies particularly in the present study, which concerns flood frequencies and magnitudes, to those influences that would either retard, accelerate, augment, dissipate, or otherwise change, the discharge habits of the stream or modify the discharge capacity of the channel. Thus, the regimen of a river may be affected by: (*a*) Changes in the vegetative cover of a drainage area; (*b*) erosion; (*c*) increase or decrease of natural or artificial storage either in basins or on flood-plains; (*d*) diversion to other drainage basins by either natural or artificial means; (*e*) restriction of the river channel by levees; (*f*) facilitation of flow by dredging and removal of obstructions; or (*g*) formation or abandonment of auxiliary channels and by-pass areas. Furthermore, any one of Items (*a*) to (*g*) is likely to interfere with satisfactory interpretation of records.

What is more important, available human experience is often capable of making fairly intelligent approximations of such influences, as, for example, by recognizing that one factor may be additive, another may be subtractive, and the algebraic sum may be of small amount. Thus, it has been shown for several stations on large foreign rivers, and on the Upper Mississippi River, that the dredging of bars, removal of snags and other obstructions, rectification of alignment, and improvement of the hydraulic elements of the channel, tend to lower the river surface; whereas channel encroachments and the development and protection of great areas among the natural flood-plains cause a corresponding rise of stage. The actual effect is the resulting difference of these two factors, normally lowering the stages of low water and raising the stages of high water, the net effect being to increase the range of variation in stages, except where regulation works are used to produce opposite effects.

Flood Records of Rivers in Europe

Among the rivers of Europe, the Thames, the Seine, the Rhine, the Rhône, the Loire, the Po, and the Danube seem to afford the best information. It is realized that the progressive changes which these river channels and drainage systems have undergone may vitiate, more or less, the close comparability of stages as indexes of flood magnitudes over long periods; nevertheless, the study of outstanding flood catastrophes should afford a valuable record of experience. The floods of the Rhône, the Loire, and the Seine Rivers in the years 563, 572, and 583 A. D., respectively, have been described briefly in available records. Thereafter, until about 1 000 yr later, the published fragmentary data are qualitative rather than quantitative; certain outstanding inundations, which were equal to or worse than others, are designated by date or by year of occurrence. The usual standards for comparison seem to have been based on loss of life and damage to property, and in this connection the suddenness of flood rise without warning played a prominent part; therefore, the floods at unusual or unexpected seasons would naturally be mentioned.[2]

Within the last 300 yr the quantitative or magnitude relations of floods have entered into the records of European streams. Thus, the foregoing references, together with those listed by Kuichling,[3] show that the flood in the Seine River Valley on January 28, 1910, and that of February 27, 1658, at Paris, were of approximately the same stage (8.40 m and 8.81 m, or 27.6 ft and 28.9 ft, respectively, above the zero of the Pont de Tournelle); and that the maximum estimated discharges were of a similar order (88 300 and 84 500 cu ft per sec, respectively). The greater volume and lesser gauge height thus applied to the flood crest of 1910. No other floods on the Seine during a period of nearly 300 yr approached within 15% of the maximum recorded for 1910. The catastrophic occurrences during the period, 683 to 1658, A. D., probably included several of nearly the same order, to judge from descriptive accounts of complete submergence of homes, undermining of bridges and other structures, and general devastation, including the demolition of fortification walls during the flood and the accompanying earthquake. The question naturally arises as to whether the recorded earth tremors were the cause or the effect of the structural collapse.

The year 1012 A. D., witnessed intense rainfall and the "great flood" of the Danube River at Vienna; likewise, along the River Rhine, homes were inundated, and a multitude of people and their live stock were destroyed. The margins of forests intruding into the flood-plains were wiped out during a catastrophe that was without parallel in all the preceding history of that region. Prior to 1012 A. D., as in present times, the sub-normal river stages

[2] "Materiaux pour l'etude des calamities," 5e annee, nos. 17–20, Genéve, Soc. Géographic, 1928–29; "Les inondations en France," par Maurice Champanion, 6 vol., Paris, 1858–64 (deals with flood events from the Sixth Century to 1862); "Forests and Floods," by the late H. M. Chittenden, M. Am. Soc. C. E., *Engineering News*, October 29, 1908, p. 467 (discusses report of Ernst Lauda, Chief of the Hydrographic Bureau of the Austrian Government (Hydrographischen Dienst in Osterreich: Beitrage Hydrographic Osterreichs, Heft 4, pp. 155–162, Wien, 1900)); "Le Seine," par E. Belgrand, Inspector General, Ponts et Chaussées, 1869. (Includes a discussion of notable floods beginning with 1649); and *Engineering News*, Vol. 63, p. 327, 1910.

[3] "Flood Flows," by W. E. Fuller, M. Am. Soc. C. E.; discussion by the late Emil Kuichling, M. Am. Soc. C. E, *Transactions*, Vol LXXVII (1914), p. 643.

of successive years created a false sense of security that left the people unprepared for the eventual torrent.

The Danube flood of 1342 was reported to have caused the loss of 6 000 human lives. In the flood of 1501 on the Danube several marks were established on monuments and are still preserved as permanent records. Comparison of this event with another devastating flood, in 1899, at fourteen stations in the same valley, shows that the range above low-water stage was 7.24 to 16.58 m (23.8 to 54.4 ft) in 1501 and only 6.52 to 13.18 m (21.4 to 43.2 ft) in 1899, the lower stages perhaps being due in part to channel improvements in the interest of navigation.

The scattered references in early records show that flood heights above either normal or low-water stages are so nearly comparable with those of later centuries as to give support to the opinion that no radical progressive changes of intensities or frequencies of floods and droughts have taken place in historic times on any extensive river systems, except as logical consequencies of regulation, diversion, utilization, or other activities of Man. On the other hand, no direct proof is available regarding the trends of climate and rainfall throughout historical periods, such evidence as exists being based on considerations other than physical measurements. On extending the period considered into geologic time, however, it is indisputably established that marked changes in both temperature and rainfall have taken place by gradual processes.

Flood Records of Rivers in Asia

Traces of irrigation, regulation, channel-training, and flood-protection works have survived from early centuries of historical epochs in various civilizations, or even from times before the earliest records now available for some countries, particularly in Asia. These remnants of a past civilization seem to supply indisputable proof of a long-continued similarity of climatic, rainfall, and run-off habits. The only possible explanation and justification for such engineering works must be found in deficient local rainfall and in reliable stream flow, even when the discharge was flashy and irregular. This combination of circumstances presumably reflects the occurrence of storms among the head-waters and intervening catchment areas, or the thawing of snow and ice accumulations.

The records of several Asiatic rivers, although enveloped in vagueness, extend back to remote periods of history. Thus, the series of irrigation canals in Mesopotamia, with combined original capacities much greater than the reliable flow of the Euphrates and Tigris during recent times, do not necessarily betoken a shrinkage of water supply since they were built. According to opinions of engineers who have studied the situation on the ground,[4] new canals were established as the irrigated tracts under the older projects became water-logged and overcharged with alkali, for want of systematic drainage, as often happens under modern practice. The important facts to note, however, are that the rainfall was deficient throughout the historical period of Babylon, Nineveh, and neighboring cities, and that the rivers were both fairly stable

[4] "Euphrates River and Valley," by Francis Rawdon Chesney, Lond., 1868.

and reasonably tractable, to permit such bridging, navigation, and diversion for irrigation at that time. It is plain that irrigation was found necessary to raise crops and to sustain life in that country, and that the rivers were fairly reliable sources of supply. During the festival in November, about 539 B. C., Cyrus, the Persian, captured Babylon by the simple expedient of diverting the Euphrates River into the desert through one or more canals and marching his troops through the walls along the channel thus made available. This feat is quite consistent with the known habits and volume of discharge of the Euphrates as observed during the Nineteenth Century.

Confirmatory evidence concerning both the variations and the stabilization of water resources lies in the rainfall records extending back more than 200 yr at a few stations, mainly in Europe, and considerably more than 100 yr at many other places. These records parallel the meager hydrographic records, and both sources furnish valuable interrelated and, therefore, mutually supporting data.

Tradition and history combine to give descriptive accounts of notable floods and droughts in India and in China. The 1930 report of the Huai River Commission, Bureau of Engineering,[5] lists the floods of 1649, 1741, 1879, and 1921 as the outstanding ones on this important northern tributary of the Yangtze River. They were measured indirectly by the extent of the inundation on populated land, the total number of "districts" inundated being reported as 5, 11, 6, and 10, respectively, whereas the usual damaging inundations affect only 3 or 4 such districts. With all available data before it, the Commission adopted the flood of 1921 as the basis for designing the Huai River regulation. Presumably, this decision was not entirely due to the high discharge rate, but also to the sustained volume, which was reported as having inundated 11 740 sq km (4 533 sq miles) to a depth of 1 to 4 m (3.3 to 13.1 ft). It is noteworthy that the expected 100-yr flood on the Huai derived from a study of rainfall, is 15 500 cu m per sec, whereas Fuller's formula gives only 11 700 cu m per sec. Reduced to English units, these rates become 548 000 and 414 000 cu ft per sec, respectively, or 8.55 and 6.46 cu ft per sec per sq mile. The maximum recorded flood discharge, which occurred in 1916, was 12 900 cu m per sec (455 000 cu ft per sec, or 7.10 cu ft per sec per sq mile), perhaps representing a 30 or 35-yr average frequency. The failure of levees during the more severe flood of 1921 prevented even approximate measurement of the maximum discharge.

The River Nile in Egypt

It is freely admitted that the foregoing brief references to available long-period river-stage records and to what these data seem to show, should be supplemented by further research in this inviting field perhaps in a separate paper. The presentation of fairly complete river-stage data, so far as they are now available and capable of interpretation, is limited herein to the Nile River, in Egypt.

The nilometer records are most notable with respect to antiquity, continuity, and permanence. The annual inundation of the Nile Valley in

[5] "Projects of Flood Control and Irrigation for the Huai River System," Official Tech. Rept. 1, p. 23, Huai-Yin, China, 1930.

the late summer generally supplied enough moisture to the soil to insure fair crops in the fall and winter. A subnormal flood meant restricted plantings and deficient harvests; and well-sustained high water, at or above "wafa"—the stage insuring plenty—meant bounteous crops on more and more of the fertile alluvial land, as long as the stage did not overtop the protective works and islands of refuge. Thus, it happened that the most important annual event in Egypt was the Nile flood; and, therefore, records were engraved on the cliff walls in various places, notably at Semna, a section of the Second Cataract. In this locality, 179 distinct markings have been discovered dating back to about the 12th Dynasty; that is, 1 750 to 1 800 yr B. C., or earlier. Of these markings 18 on the west bank are about 8 m, or nearly 27 ft, above the flood range of recent centuries, but the difference probably reflects to a considerable degree the erosion in both channel walls and floor and does not necessarily indicate any pronounced or progressive change in discharge from century to century.

On that fragment of an ancient inscribed monument known as the "Palermo stone," because it now reposes in the Palermo Museum, in Sicily, there are notations regarding the successive ruling monarchs of the first five dynasties, dating back to between 3 000 and 3 500 yr B. C.; there are also records of such important events as military campaigns and public festivals. These notations include mention of the rise of the Nile during several consecutive years, apparently recording a range between 1 and 8 cubits (2 to 14 ft) somewhere in the Delta,[6] but with gauge readings usually about midway. Although it is difficult to tie these records to any particular section of the Nile Valley, they establish the importance of the Nile flood in making Egypt the never-failing storehouse of grain for export, especially in periods when droughts and famine prevailed in neighboring countries. Likewise, they indicate the irregular distribution of flood heights over a range quite comparable with that observed in the past century, prior to the construction of large regulative works.

Fortunately, several sections of nilometers, at various points along the stream channel, have been discovered, and their inscriptions have been deciphered and correlated. Capt. H. G. Lyons[7] states that the height above sea level of corresponding points of the ancient nilometers in Egypt and Nubia have been determined with the aid of bench-marks of the Irrigation Department, and that the zero points of the nilometer scales were found to lie in a line inclined to the north. In Nubia, according to Lyons, the line is sensibly parallel to the water slope, but north of Aswan it is considerably less inclined than the flood slope. As a consequence, a flood was indicated by a higher reading on the nilometer at Aswan than on that of Roda, at Cairo. This is offered as an explanation of the statement found in the Egyptian inscriptions and the works of the Greek and Roman authors that, in very good years, the Nile River rose 28 cubits (46.5 ft) at Elephantine, 21 cubits (36.12 ft) at Koptos, 14 cubits (24 ft) at Roda, and 7 cubits (12 ft) in the Delta. The altitude of the zero point of the ancient nilometer at Roda may be obtained

[6] "Egypt," by James H. Breasted. Vol. 1, p. 51 *et seq.*, Univ of Chicago Press, 1906.
[7] "Physiography of the River Nile," by H. G. Lyons, pp. 316 *et seq.*, Cairo, 1906.

approximately from the slope of the line determined by the zero points of the remaining nilometers. After computing the secular rise of the bed one can conclude that the flood levels about 3 000 B. C. (which are recorded on the Palermo stone) and the later data concerning Nile floods given by the Greek and Roman authors agree well with those of to-day.

From the evidence he studied, Lyons was convinced that about 100 A. D. the Nile often rose to 24 cubits (41 ft) and sometimes to 25 cubits (43 ft) on the nilometer scale on Elephantine Island, at Aswan, below the First Cataract so that the high floods of that time reached the level of 91 m (299 ft) above sea level. In 1874 they reached 94 m (308 ft) or 3 m (10 ft) above the level of about 1 800 yr earlier which corresponds to a rise of the bed of 0.17 m (6.7 in.) per century at this point. If the mean flood level of the period, 1870 to 1906, is taken, the height becomes 93 m (305 ft) and the rise, 0.11 m (4.3 in.) per century. Quoting Lyons:[7]

"At Karnak in 1895 M. LeGrain found a series of 40 high Nile levels marked on the quay walls of the great temple. They date from about 800 B. C., and the mean altitude given by them for a high Nile is 74.25 meters [243.60 ft] above sea-level, while that of today is 74.93[8] [1906], showing a rise of the river-bed of 2.68 meters [8.8 ft] in 2 800 years, or at the rate of 0.096 meters [3.8 in.] per century."

In 1935, 76.93 m (252.3 ft) seems to be a better elevation than that reported by Lyons (74.93 m, or 245.8 ft) in 1906. If 0.15 m (5.9 in.) in a century is assumed as the average rate of rise of the Nile flood-plain, due to overflow and sedimentation, the 10-m (33-ft) average thickness of observed alluvial deposits might represent about 67 centuries of growth. Other methods of reckoning based, for example, on the maximum thickness of sediment, or the extension of the delta seaward, almost invariably indicate much longer periods of geomorphic development.

Similar conclusions regarding the rate of sedimentation follow the comparison of maximum flood height during the reign of the Roman Emperor Severus (about 200 A. D.), and the maximum flood mark noted by the French savants during the Napoleonic Invasion, in 1800 A. D., was 2.11 m (6.9 ft) higher.[9] If those two floods and their available channels were comparable, the rate of aggradation of the Delta was $\frac{2.11}{16} = 0.132$ m (5.2 in.) per 100 yr. Incidentally, that rate seems to be slightly greater than the rate of erosion at the First Cataract, about 600 miles above Cairo, derived by a comparison of maximum flood crests, on the assumption that they were of almost equal magnitude near the beginning and the end of the last 1 900 yr.

The durable outcropping ledge of Syene granite (syenite) forming the First Cataract, at Aswan, from which great obelisks and other monuments were quarried for Lower Egypt and eventual transfer to other countries, accounts for the relatively slight erosion here compared with 8 m (26 ft) in about 3 700 yr, or an average of 0.22 m (8.7 in.) per century, at Semna, on

[8] 74.25 + 2.68 = 76.93 m which presumably was intended.

[9] "The Nile in 1904," by Sir William Wilcocks, p. 48.

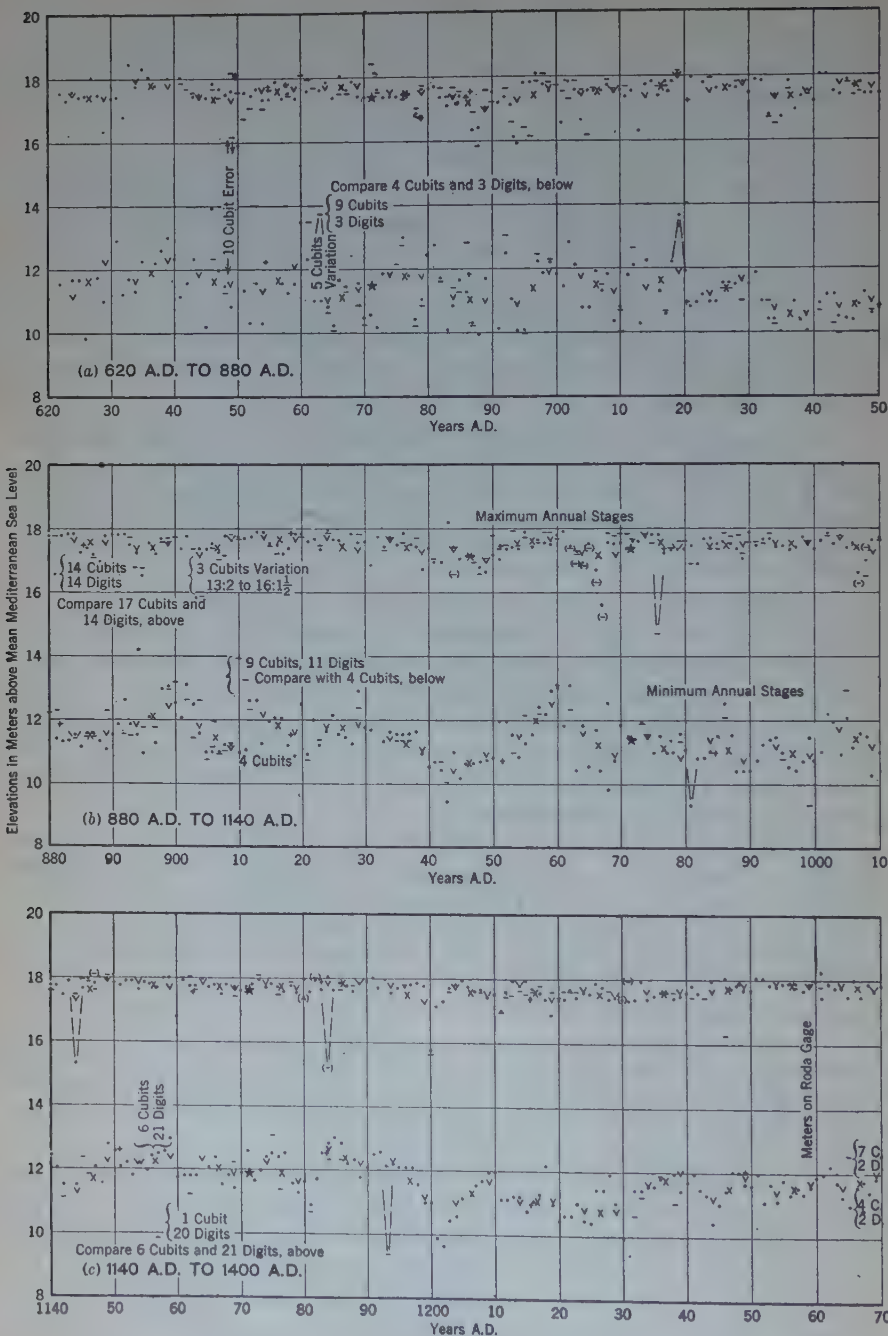

FIG. 1.—MAXIMUM AND MINIMUM STAGES OF THE

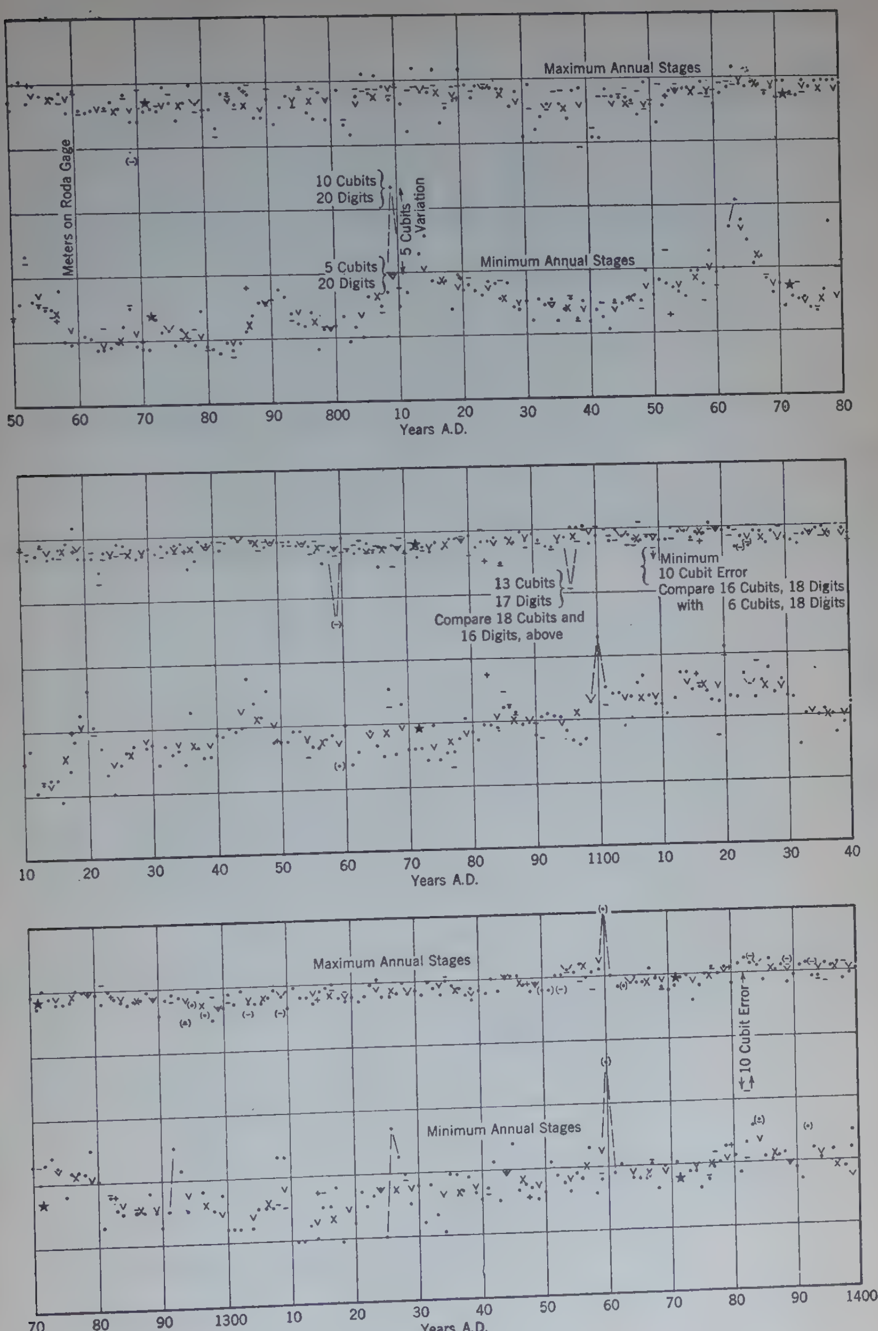

NILE RIVER IN EGYPT, FROM ALL AVAILABLE RECORDS

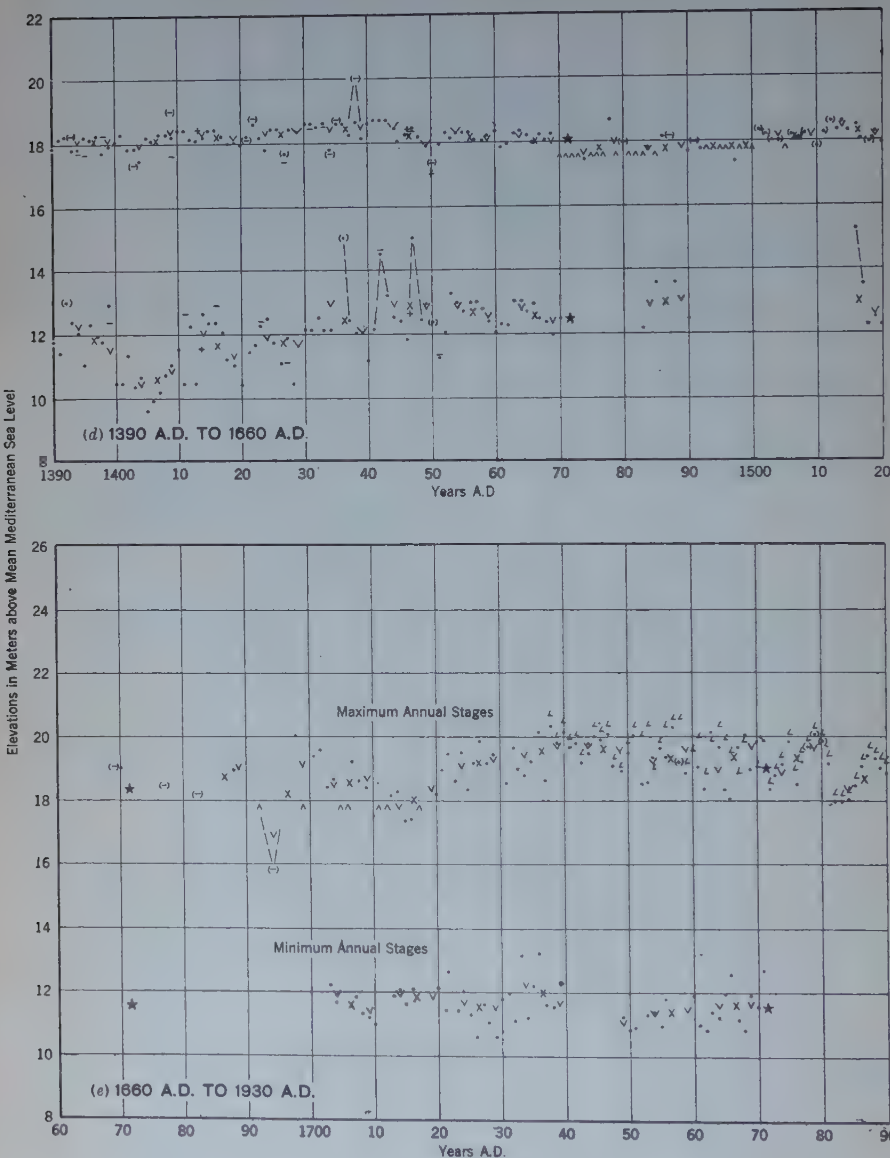

FIG. 1 (*Continued*).—MAXIMUM AND MINIMUM STAGES OF

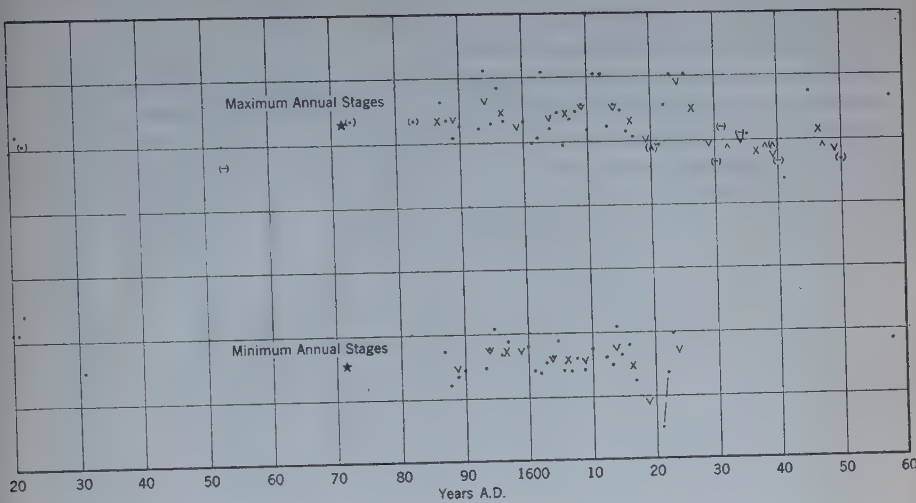

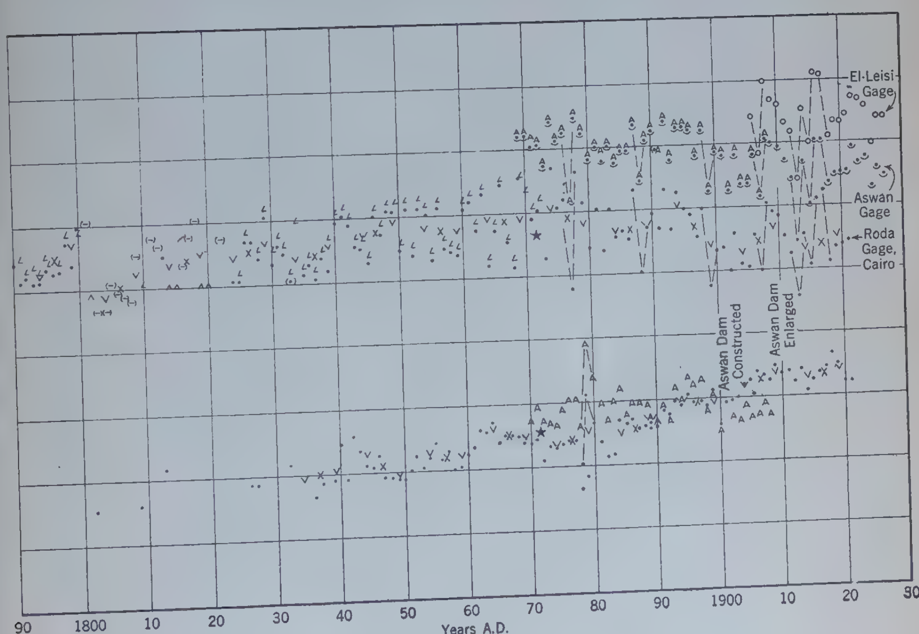

THE NILE RIVER IN EGYPT, FROM ALL AVAILABLE RECORDS

the Second Cataract, where the outcropping stone is not so durable and where sandstone or other sedimentary formations predominate along the canyon walls.

The only long-period continuous records now available for the Nile relate to the Roda gauge, at Cairo. There is fair assurance that the gauge datum has been maintained throughout the thirteen centuries of record without change, unless the Temple of Roda, in which the nilometer column is located, has settled into the alluvium. The depth of the temple foundation, and the tradition that the gauge which was used throughout most of the Arabian epoch and thereafter, was referred to the datum and site of a much older structure, are items of evidence tending to insure the stability of the foundation.

Incidentally, the graduation of the masonry column into plainly marked cubits, with the zero of the scale somewhat lower than was ever attained (according to the available records) in the 1 300 yr following 622 A. D., is indirect evidence of its antiquity, if the zero represented the lowest previously observed and recorded stage. During the first 1 000 yr of this record the lowest annual stages approached within about 2 ft of the zero only five or six times, depending on which tabulation is adopted; but in 1531 and in 1621 the recorded low stage was only 9 digits, or 8 in., above the zero. Moreover, the graduations between the sixteenth and twenty-second cubit marks on the column are half cubits, whereas above 22 cubits (38 ft) they resume the full measure. This is explained by Lyons on the ground that the canals were opened at 16 cubits (27.5 ft), as was customary at the beginning of the Arabic epoch, about 641 A. D., and a half-unit rise at Roda meant a full-unit rise above the canal diversions; but at 22 cubits, the irrigation basins were ordinarily full, and no further diversion was necessary. As a further assistance in visualizing the units of the paper, roughly, in terms of their English equivalents, Fig. 2 includes three general conversion scales.

It is understood that most of the records had a common origin, but the originals are not known to exist at the present time. There are various versions of parts of the records, transcribed by different authors either from the original documents or from other transcriptions. Volumes 4 and 9 of the *Memoirs* of the Institute of Egypt (published in French by Prince Omar Toussoun during the period, 1923 to 1925) afford three different sources of data, all more or less interrelated, yet not identical. Ibn Iyas and others have compiled voluminous textual notes, which appear in part in Volume 9 of the *Memoirs* and from which many data may be derived for various years from 769 to 1878 A. D. Some of these data confirm similar figures in tabulated form; others differ; and still other significant notes make cross-references that agree with previous records and supply data for many years which are omitted in the tabulations.

The record of Aboul Mehasin in Volume 4 of the *Memoirs* extends from the year 20 to 855 of the Hegira, or 641 to 1451 A. D., but all according to Mohammedan years of 12 lunar months, which are thus 11 days shorter than the solar years. Therefore, there are 103 yr per century of the present-day mode of reckoning. The longer tabulation published in Volume 9, in

1925, or two years later than that of Aboul Mehasin, gives 1 108 maximum annual stages and 1 025 corresponding annual minima during the 1 300-yr period from 622 to 1921 A. D.

There would be definite advantages in publishing these tabular data, in pics and kirats, coudees and doights, or cubits and digits, according to the various transcriptions, with their equivalents, in meters, above mean sea level; but they are too voluminous to present in this manner, especially for all three main sources of data mentioned herein. The use of a chart on which all the data could be shown, and their trends compared, century by century, by connecting successive century or other averages of maximum or minimum stages, has seemed to be a more acceptable method of presentation. Naturally, the longer tabulation, representing the latest and most nearly complete version of available data regarding Nile River stages, was adopted as the one to be given preference.

In Fig. 1, the various plotted points may be identified as follows:

Applying to All the Records:

∨ = five-year average for the data shown by dots, supplemented by — or (—) when the location of the dot is not given;

× = ten-year average for data shown by dots, supplemented by — or (—) when the location of the dot is not given; and,

★ = one hundred-year average.

Applying to the Roda gauge, at Cairo:

• = records compiled by Omar Toussoun[10] covering the 1 300-yr period from 622 to 1921 A. D.;

(•) = confirmation from textual notes for the records compiled by Omar Toussoun; when — is lacking an agreement is indicated between all three sources;

— = records compiled by Aboul Mehasin,[11] covering the period, 20 to 855 of the Hegira, or 641 to 1451 A. D., a total of 811 years. A small + indicates extra data, representing 25 surplus years of Mohammedan reckoning;

(—) = records from notes compiled by Ibn Iyas and others,[12] for the period 769 to 1878 A. D.

∠ = records by Lyons;[13] and,

∧ = records indicating "wafa," or the stage that assures plenty, at which the canals were opened to supply the basins; the maximum flood stage, ordinarily, was somewhat higher.

Applying to the gauge down stream from Aswan Dam:

△ = maximum annual river stages at the Aswan gauge above the assumed datum, 71.0 m, or 232.9 ft, above mean Mediterranean Sea level;

◉ = maximum ten-day, average gauge heights, and, therefore, somewhat below the actual maximum.

Applying to the El-Leisi gauge, 37 miles up stream from Cairo:

○ = maximum ten-day average gauge heights, and, therefore, somewhat below the actual minimum.

---

[10] *Memoirs*, Inst. of Egypt, 1925, Vol. 9.
[11] *Loc. cit.*, 1923, Vol. 4.
[12] *Loc. cit.*, 1923 and 1925, Vol. 4 and 9.
[13] "The Nile Flood in 1905," by Capt. H. G. Lyons.

The gauge heights plotted as ordinates in Fig. 1 are readings from the Roda gauge on the Nile River, at Cairo. The exceptions, marked *A* or *J*, refer to readings of the Aswan gauge and those marked *O* refer to readings of the El-Leisi gauge, 37 miles above Cairo. In all cases the readings are the mean Mediterranean Sea level elevations, at Alexandria.

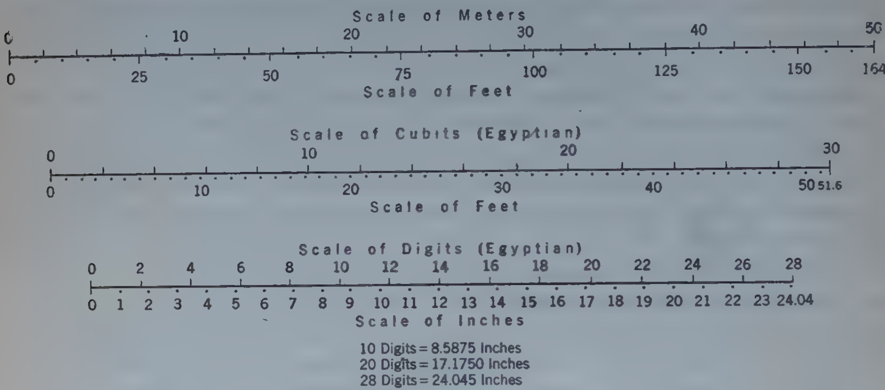

Fig. 2.—Conversion Scales

Fig. 1 probably includes many items that represent river stages at the time of the festival attending the opening of canal gates, after which the flood ordinarily continued to rise to varying heights. According to tradition and historical references, furthermore, some of the flood heights were increased falsely in the records for the purpose of adding to the revenues from land taxation. There appear to be good reasons for expecting fully as wide ranges of variation for the maximum annual gauge heights as for the minima, except as the former may be affected by valley storage and flood-plain discharge.

The data from Aboul Mehasin's tabulation that differed by measurable amounts (say, 3 in., or more, on the adopted scale) are shown as short dashes crossing the grid lines; and those derived from or confirmed by textual notes are shown within parentheses. In this manner, it was found possible to supply about 65 additional maxima, so that a total of 1 173 out of a possible 1 300 are plotted, some with more than one value owing to the unexplained discrepancies among the records. These differences may reach 3, 4, 5, or even 10 cubits, but usually are less than 1 cubit. The data for the extra 25 yr of Mohammedan reckoning are shown as short dashes between grid lines.

For the 811 yr of concurrent record covered by the aforementioned two tabulations, about one-fourth the maxima and one-half the minima coincide, but if those in practical agreement or those differing by only a few inches are included, the proportions increase to about one-half and three-fourths, respectively. The textual notes of Ibn Iyas, El Gabarti, and others provide several coincidences of both maxima and minima, as well as at least an equal number of measurable divergences. Furthermore, they supply the sixty-five yearly maxima not found in either of the long tabulations. All these new data are shown in Fig. 1 as short dashes enclosed in parentheses. Agreement of textual notes with the data from the longer tabulation is indicated by paren-

theses around the individual dots or small groups of dots. Such a symbol for any year between 641 and 1451 A. D., without a dash, indicates agreement of all three sources, as explained in the foregoing list of symbols.

It seems to be fairly well established, by tradition as well as by historic references, that the records of some of the sub-normal Nile flood stages were increased arbitrarily by order of unscrupulous rulers whose prospects of land revenues had been adversely affected by the drought. In years of assured plenty, or abundant water supply, such sordid motives for falsification of records would seem to be lacking. However, there is considerable evidence that a record was sometimes made of the stage at which the canal gates were opened, upon the assurance of a satisfactory water supply, after which the river may have continued its rise in varying unrecorded amounts. Furthermore, a sudden or early recession of the flood from what was at first considered to be a stage assuring plenty, or "wafa," was occasionally followed by a partial famine, due to the brief duration of high flood. Obviously, any neglected maximum stages would tend to counterbalance the artificial increase of sub-normal stages as expressed in trends.

With full recognition of the obvious discrepancies in the records and the likelihood that many other errors and inaccuracies were incorporated which may never be detected (or at least are not detectable at this time) it is truly remarkable, nevertheless, how nearly the computed trends of rise apparently ascribable to sedimentation, ranging from 0.10 to 0.15 m (3.9 to 5.9 in.) per century, are reflected in Table 1.

TABLE 1.—COMPUTED TREND OF RISE, FLOOD STAGES OF THE NILE, ASCRIBABLE TO SEDIMENTATION

Years of Record (A. D.): From	Years of Record (A. D.): To	Cumulative interval, in years	Average Annual Low-Water and Flood Stages, Above Mean Mediterranean Sea Level at Alexandria, Egypt: In Meters Above: Minimum	In Meters Above: Maximum	In Feet Above: Minimum	In Feet Above: Maximum	Average Rise for the Cumulative Interval: In Meters per Century: Minimum	In Meters per Century: Maximum	In Inches per Century: Minimum	In Inches per Century: Maximum
(1)	(2)	(3)	(4)	(5)	(6)	(7)	(8)	(9)	(10)	(11)
622	721	100	11.51	17.50	37.8	57.4	......	......	......	......
1 422	1 521	900	12.52	18.21	41.1	59.7	0.13	0.09	5.12	3.54
1 522	1 621	1 000	11.09	18.71	36.4	61.3	—0.05	0.13	—1.97	5.12
1 522	1 721	1 100	11.66	18.34	38.3	60.2	0.015	0.084	0.59	3.23
1 722	1 821	1 200	11.66	19.06	38.3	62.5	0.014	0.14	0.55	5.51
1 822	1 921	1 300	13.19	19.33	43.3	63.4	0.14	0.15	5.51	5.91

The year 1834 marks the construction of a main barrage below Cairo and the beginning of perennial irrigation in Egypt. The effect of this development soon after the severe drought that culminated in 1833, is more marked in the trend of minima than in that of maxima. The barrages raised the river bed, the release of storage water augmented the minimum flow, and the storage of a portion of the flood flow necessarily tended to decrease the peak stages. A study of the trends on the graphic composite record covering 1 300 yr, especially between successive century averages (marked

* in Fig. 1), shows unmistakably why the flood stages that indicated an assurance of plenty progressed gradually from 16 to 20 cubits (28 to 35 ft) on the Roda gauge and then, during the final century of record, increased nearly another 6 cubits (10.3 ft), owing to increased usage of water and to the construction of the main barrage or diversion dam about 15 miles below. This was designed to raise the low-water surface about 3.2 m, or 10.5 ft, or 6 cubits (10.3 ft), and it actually raised the flood crests about 0.75 m (29.5 in.) at the barrage, even with all gateways open; or 0.25 to 0.75 m (9.8 to 29.5 in.) at the Roda gauge.[14]

The first notable effort toward providing a reliable perennial irrigation supply for Egypt was evidently the Lake Moeris Reservoir project, described by Herodotus after his personal visit to Egypt about 450 B. C. The site has been identified definitely as the fertile Fayum Basin of the present day, with its saline lake occupying the lowest part of the valley, 140 ft below sea level, in a manner similar to the Salton Sea in Imperial Valley, California. The width of the canal supplying the reservoir was given as the equivalent of about 300 ft. With an average depth of 25 ft during high flood and a mean velocity of 4 ft per sec, the discharge would have been 30 000 cu ft per sec, or 60 000 acre-ft per day, thus requiring approximately 17 days of continuous flow to deliver 1 000 000 acre-ft. It is plain that both the diversion and the storage quantities might have been considerably greater or less than these values, but they afford at least an idea of the possibilities in the light of modern practice.

Sir R. Hanbury Brown[15] derived the available storage depths and capacities for Lake Moeris which are used in the following comments: Taking into account the present contours of the Fayum Basin, enclosing an area of fully 630 sq miles under the level of ancient lake shells, or 22.5 m (74 ft) above mean sea level, and assuming the depth of usable storage for return to the Nile to augment the low flow, as 10 ft, intermediate between the high-water and low-water stages of the adjacent Nile channel, the net available volume is found to have been about 3 000 000 acre-ft, or nearly the usable capacity of the Aswan Reservoir from 1912 to 1930, after the first enlargement and before the recent one. The storage and release of this water, therefore, must have modified the Nile discharge at Cairo, about 80 miles below the diversion canal leading to the Fayum Basin; but it appears that before 622 A. D., the beginning of the nilometer record herein presented, Lake Moeris had been abandoned as a storage project, and the rich alluvial lands of its bed had been devoted to agricultural use, such as prevails to this day. In addition to this storage, the chains of natural lakes were doubtless operating as effectively in those ancient times as at the present, if not more so. Presumably, the natural processes of erosion and sedimentation would have tended to enlarge the lake outlets and to convert the shallower lakes or portions of them into marsh land, such as now prevails on the White Nile above Khartoum.

From what seems to be the best information and opinions thus far published and discovered in the present research, it appears that the storage

[14] "The Delta Barrage," by Sir R. Hanbury Brown, Cairo, 1902.

[15] "The Fayum and Lake Moeris," by Sir R. Hanbury Brown, Lond., 1892, p. 80.

and regulative features of the Nile were not greatly changed during the first 1 200 yr of the record plotted herewith; but that the developments during the final century of this record at least restored the quantity of storage and regulation provided by Lake Moeris for possibly sixteen centuries before, and more than a century after, the visit of Herodotus, about 450 B. C.

In spite of all the changing, uncertain, and erroneous factors that must be considered in connection with the records of stages of the Nile River, it is believed that they disclose some important information; and there is a fair prospect that they may yield more data with further study and the cumulation of ideas of various students.

It is readily apparent that the use of records covering only a single early century might yield an unreliable estimate of the frequency characteristics of the maximum stages for the total period. On the other hand, it is believed that, after eliminating the obvious errors in Fig. 1, such as 3, 5, or 10 cubits (5, 8.5, or 17 ft), and some lesser ones, and then applying an average rate of rise per century to indicate the increase of sedimentation on the flood-plains and the resultant rise of flood stages, any one of the first twelve centuries of record may be found to qualify as a rough indicator of what should be expected during a longer period, such as 500 or 1 000 yr. Furthermore, the comparison of the Toussoun data (plotted as dots in Fig. 2) and the Lyons data (marked ∠ in Fig. 1) for the two centuries ending in 1902, shows several measurable differences, some of them systematic and nearly constant, and others of irregular amounts and sign; that is, alternating as positive and negative variations. In view of such discrepancies, of the ease with which a "3" may be read as an "8," or a single unit changed in the 10's column in Arabic numerals, and of the chance of other errors of transcription, it is not surprising that about 5 or 10 digits or cubits or other differences exist in the two tabulations covering 811 yr concurrently. The greater occasion for surprise seems to lie in the possibility of synchronizing the two time scales (Mohammedan and solar years), which has been done in such a way that a majority of the items are in actual or substantial agreement, for both maximum and minimum annual stages.

This presentation of what purport to be records or data derived in some way from actual records, is made with the hope that others may be spared the tedious work of computation, co-ordination, and plotting of the various items. Perhaps it may serve as a kind of groundwork on which comparison may be made between segments of this record, or between these data and others for rivers in the United States, proper account being taken, of course, of differences in drainage-basin characteristics and river regimen.

It seems important to observe that the site of the Roda gauge, at Cairo, is virtually at the apex of the Nile Delta cone and that the opportunity of the stream to spread through a wide angle resulted in various conditions regarding the number of outlet channels. Thus, some of the early maps outline six distinct outlet branches; others show three or four; and now there are only two well-established natural channels. Perhaps the combined capacities of the various canals in Lower Egypt, or even those restricted to the Delta itself,

would account for the equivalent of one or more of the abandoned channels. It is quite probable that under such conditions as are known to have existed some of the annual flood heights were affected more by channel changes than by variations in rates of flow. For example, a devastating flood may have lowered the river heights temporarily as a result of scouring, or an obstruction may have increased them. The transfer of the main gauging operations, about 1870, to the Aswan site, below the First Cataract, avoided some of the disturbances that have been felt at Cairo from new irrigation developments since the British occupation. These Aswan gauge heights, above an assumed datum, are superimposed on Fig. 1 with Roda gauge readings.

Attention is also invited in Fig. 3 to the plotted records of both annual volumes and 4-month flood volumes at Aswan, beginning with 1870, as deter-

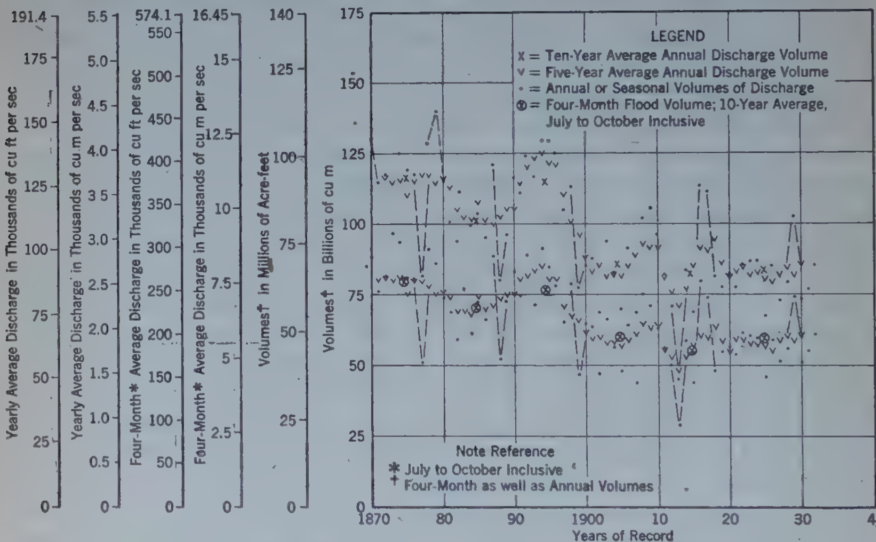

FIG. 3.—FLOOD DISCHARGE AND VOLUMES OF THE NILE RIVER AT ASWAN

mined from the records of the Ministry of Public Works, of Egypt.[16] These values may be read from the various scales in almost any desired unit of measure in common use. The decrease from the first to the latest decade of record seems to be due, in part, to climatic trends over the period of record, but perhaps it may reflect also the increased use of water in Upper Egypt and the increased losses in storage or in transit due to recent works.

Probably the most authoritative appraisal is that of the Physical Department, Egyptian Ministry of Public Works, as expressed[17] by H. E. Hurst, Director General, and P. Phillips, Director of the Hydrological Service:

"One series of maxima and minima at Cairo extending from 641 A. D. to 1450 A. D. is fairly complete. The outstanding feature of these is that over considerable periods, sometimes as long as 50 years, floods are above the

[16] Physical Dept. Papers, Nos. 29 and 31; also "The Nile Basin," Vol. III and IV (Supplement).

[17] "The Nile Basin," Vol. 1, p. 20, 1931.

average, while over other periods they are below the average. It is also the case that very low floods may occur amongst a high series and *vice versa*. These records have been analyzed for periodicities, and periods of small amplitude have been found. They are, however, so masked by irregularities as to be useless for forecasting purposes."

Despite the obscuring effects of errors, uncertainties, and difficulties attending these records of Nile River stages, it seems probable that the concentrated attention of members of the Engineering Profession who are so inclined may yet bring into view many facts and relationships to build up a better background of experience and to afford perspective covering long-time trends of river behavior. Throughout the notable long-period records recently investigated on both American and foreign rivers, aggregating thousands of years in length, it appears that no single flood event is completely at variance or out of character with what appear to be the natural and reasonable potentialities of that particular basin or river system, as indicated by other similarly outstanding events of record.

Acknowledgments

A wide circle of associates and advisers have been most helpful in the conception and development of the plan for this paper, and in reviewing or contributing ideas to be included. Especial mention should be made of the personnel of the U. S. Geological Survey and that of the Society's Committee on Flood Protection Data; and, particularly, to N. C. Grover, H. T. Cory, R. W. Davenport, J. C. Hoyt, Gerard H. Matthes, and Thorndike Saville, Members, Am. Soc. C. E., for their direct contributions and co-operation.

AMERICAN SOCIETY OF CIVIL ENGINEERS

Founded November 5, 1852

PAPERS

DISTRIBUTION OF STRESSES UNDER A FOUNDATION

By A. E. Cummings,[1] Assoc. M. Am. Soc. C E.

Synopsis

The question of the distribution of stress in the ground under a foundation has engaged the attention of engineers for many years. The problem has been studied both theoretically and experimentally and it is the purpose of this paper to compare theory and experiment and to indicate several important factors which must be considered when problems of this kind are being analyzed. The symbols in this paper are introduced in the text as they occur and are summarized for reference in the Appendix. An effort has been made to conform essentially with "Symbols for Mechanics, Structural Engineering, and Testing Materials"[2] compiled by a Committee of the American Standards Association, with Society representation, and approved by the Association in 1932.

The Theory

The problem of determining the distribution of stresses and strains in a semi-infinite, elastic, isotropic solid, bounded by a plane and loaded at a point on that plane by a single concentrated force, was first solved by Lamé and Clapeyron[3] not long after the discovery by Navier of the differential equations of elastic equilibrium. Their solutions in the form of quadruple integrals are of little use for practical calculations. More recently the problem was developed in considerable detail by Boussinesq.[4] His solutions are much more usable than those of the older elasticians and have become so well known that the entire problem is often referred to as the "problem of Boussinesq."

Fig. 1 shows the distribution of stresses across planes parallel to the surface as given by Boussinesq. The external force, P, applied perpendicularly

Note.—Discussion on this paper will be closed in November, 1935, *Proceedings.*

[1] Dist. Mgr., Raymond Concrete Pile Co., Chicago, Ill.

[2] A. S. A.—*Z* 10 *a*—1932.

[3] "Sur l'équilibre intérieur des solides homogènes," Savants étrangers de l'Académie des Sciences de Paris, 1833, Tome IV, p. 541.

[4] "Application des Potentiels a l'Étude de l'Équilibre et du Mouvement des Solides Élastiques," Paris, 1885.

to the plane boundary of the semi-infinite solid produces a stress in the direction of the radius vector, R, the magnitude of which per unit of area on any plane parallel to the surface is given by the expression,

$$p = \frac{3\,P\,z^2}{2\,\pi\,R^4} \qquad \text{.........................(1)}$$

in which z is the depth from the surface to the plane for which the calculation is being made, and $R = \sqrt{x^2 + y^2 + z^2}$. At the point of intersection

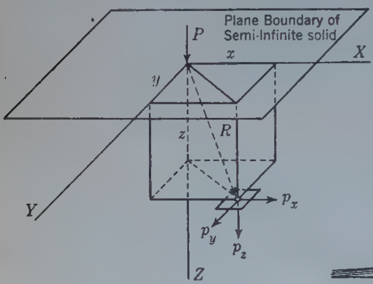

FIG. 1.

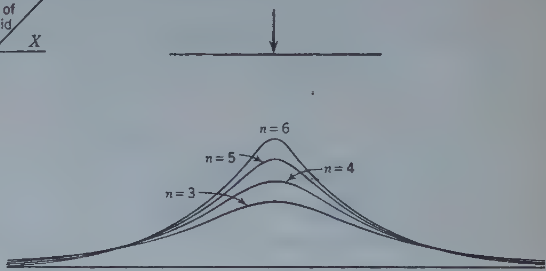

FIG. 2.—RELATIVE FORMS OF STRESS SURFACE FOR DIFFERENT VALUES OF n.

of R with any plane parallel to the surface, this stress may be resolved into three components as shown. The equations for these components as given by Boussinesq[5] are, as follows:

$$p_x = \frac{3\,P}{2\,\pi} \times \frac{z^2}{R^4} \times \frac{x}{R} \qquad \text{.....................(2a)}$$

$$p_y = \frac{3\,P}{2\,\pi} \times \frac{x^2}{R^4} \times \frac{y}{R} \qquad \text{.....................(2b)}$$

and,

$$p_z = \frac{3\,P}{2\,\pi} \times \frac{z^2}{R^4} \times \frac{z}{R} \qquad \text{.....................(2c)}$$

It is evident from Fig. 1, that the two horizontal components, p_x and p_y, are shears and that the vertical component, p_z, is a normal stress. It is also to be noted from Equations (2) that no elastic constants are involved. In connection with these two facts a little further explanation seems desirable.

The three stress components given by Equations (2) apply only to horizontal planes, that is, planes parallel to the boundary plane of the semi-infinite solid. For planes having other directions the stress distribution depends on the elastic properties of the material. In the general case the complete specification of stress at a point within the solid would require six components of stress, three being normal stresses and three being shears, and the elastic constants of the material appear in some of these equations. Because of the fact that Equations (2) do not include any elastic constants, the statement

[5] "Application des Potentiels," p. 104.

is sometimes made[6] that the distribution of stress is independent of the type of material. This is not exactly true and Boussinesq himself, after calling attention to the non-appearance of elastic constants in the equations, stated[7] that the distribution of stress across planes parallel to the surface is the same in all isotropic solids.

As long ago as 1897, August Föppl[8] arrived at the conclusion that the behavior of earths under load was not exactly in accordance with the theory of elasticity. He attributed this to the fact that the stresses and strains in earths are not proportional in the manner required by the assumptions on which that theory is based. In 1929, John H. Griffith,[9] M. Am. Soc. C. E., and, in 1932, Dr. Ing. O. K. Froehlich,[10] published stress equations involving a parameter which may be adjusted to suit materials other than the elastic isotropic solids. The two derivations differ in several important respects, but each makes use of the necessary condition of equilibrium between the summation of the vertical forces within the solid and the load applied at the surface. In the notation of Fig. 1, the equation given by these writers for the vertical normal stress is,

$$p_z = \frac{n\ P}{2\ \pi\ R^2} \times \frac{z^n}{R^n} \quad \ldots\ldots\ldots\ldots\ldots\ldots (3)$$

in which n is a parameter that may have different values for different soil structures and loading conditions. When $n = 3$ Equation (3) is exactly the same as Equation ($2c$). In other words, for elastic isotropic solids stressed within their elastic limits, the value of the parameter, n, is 3. It is also obvious from Equation (3) that the stress on the vertical center line of the load is directly proportional to n since the ratio, $\frac{z}{R}$, is 1 on this line. The general form of the bell-shaped stress surfaces computed from Equation ($2c$) is well known, and Fig. 2 shows the effect produced on these surfaces by varying the value of n. Because of this effect, n is sometimes called a concentration factor. It is of considerable importance in problems relating to earths and deserves much more attention than it has received.

It is generally conceded that the vertical normal stress, p_z, is the only one that needs to be considered as far as practical problems relating to the settlements of foundations are concerned. Its maximum values occur at points on the vertical center line of the loaded area ($x = 0$ and $y = 0$), where the shears vanish entirely. In the analysis which follows only the vertical normal stress on the vertical center line of the load will be considered.

The factor, P, in Equations (1), (2), and (3), is a concentrated load applied at a single point on the plane boundary. In practical problems relating to foundations it is necessary to calculate with loads distributed over a certain part of the plane boundary. Boussinesq[11] discussed a number of cases

[6] Progress Report of the Special Committee on Earths and Foundations, *Proceedings*, Am. Soc. C. E., May, 1933, p. 780.

[7] "Application des Potentiels," p. 106.

[8] "Versuche über die Elastizität des Erdbodens," *Zentralblatt der Bauverwaltung*, 1897.

[9] "Pressures under Substructures," *Engineering and Contracting*, March, 1929, pp. 113–119.

[10] "Drukverdeeling in Bouwgrond," *De Ingenieur*, April 15, 1932, p. B-52.

[11] "Application des Potentiels," pp. 139–179.

of distributed loads and there have been additional contributions to the subject by later writers. The simplest case is that of a load uniformly distributed over a circular area. For bearing areas other than circles and for loads non-uniformly distributed the integrations become increasingly difficult. Inasmuch as the experiments discussed subsequently herein were made with circular plates, the theoretical analysis will be made for the circular bearing area. Two types of loading—uniform and parabolic— will be considered.

Fig. 3(*a*) is a representation in plan and section of a load uniformly distributed over a circular bearing area; and Fig. 3(*b*) is a similar representation

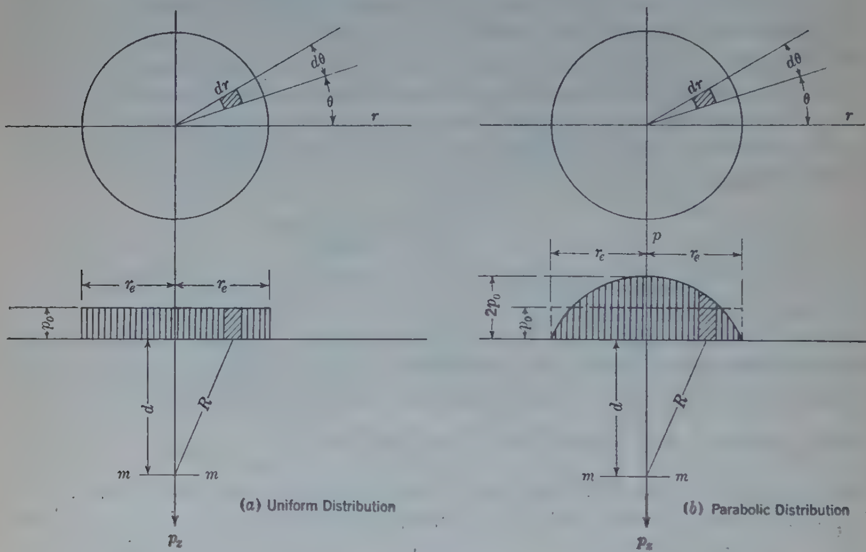

FIG. 3.—LOAD DISTRIBUTION ON A CIRCULAR BEARING AREA.

of a parabolic distribution that is maximum at the center and zero at the edges. Four different cases will be analyzed and in each case a formula will be derived for the vertical normal stress on the vertical center line of the load on a small element of area (Plane *m-m*, Fig. 3), at a depth, *d*, below the plane of the load.

Case I.—Uniform Distribution (n = 3).—This case has been developed by Föppl.[12] The formula for the vertical normal stress produced by a concentrated load is expressed by Equation (3) when $n = 3$ and $z = d$.

Using the polar co-ordinates, r and θ, as shown in Fig. 3, the total load distributed over the circular area will be given by,

$$P = \int_{r=0}^{r=r_e} \int_{\theta=0}^{\theta=2\pi} p_0 \, r \, dr \, d\theta \qquad \ldots\ldots\ldots\ldots\ldots\ldots (4)$$

[12] "Drang und Zwang," Vol. 2, p. 205.

in which p_o is the density of the uniformly distributed load. It should be noted that Equation (4) gives the volume of the circular disk of height, p_o. From Fig. 3 there is also the obvious relation,

$$R^2 = d^2 + r^2 \qquad (5)$$

Substituting Equations (4) and (5) in Equation (3), with $n = 3$ and $z = d$;

$$p_z = \int_{r=0}^{r=r_e} \int_{\theta=0}^{\theta=2\pi} \frac{3\,p_o}{2\,\pi} \frac{d^3}{(d^2 + r^2)^{\frac{5}{2}}}\, r\, dr\, d\theta \qquad (6)$$

Integrating and simplifying:

$$p_z = p_o \left[1 - \left(\frac{1}{1 + \left(\frac{r_e}{d}\right)} \right)^{\frac{3}{2}} \right] \qquad (7)$$

Case II.—Uniform Distribution (n = 6).—Equations (4) and (5) also apply in this case and they may be substituted in Equation (3) when $n = 6$ and $z = d$; thus:

$$p_z = \int_{r=0}^{r=r_e} \int_{\theta=0}^{\theta=2\pi} \frac{3\,p_o\,d^6}{\pi\,(d^2 + r^2)^4}\, r\, dr\, d\theta \qquad (8)$$

Integrating and simplifying as in Case I, the resulting formula is identical with Equation (7), except that the three-halves power becomes the third power; that is, the quantity is simply cubed.

Case III.—Parabolic Distribution (n = 3).—The equation for the vertical normal stress due to a concentrated load is again expressed by Equation (3) when $n = 3$ and $z = d$. In order that Case III may be comparable to Case I, it is necessary to find a paraboloid of revolution with a volume equal to that of the circular disk of Case I. These volumes represent the total load on the bearing area. The equation of the parabola (Fig. 3(*b*)) will be taken as:

$$p = 2\,p_o \left(1 - \frac{r^2}{r_e^2} \right) \qquad (9)$$

The volume of the paraboloid is then:

$$V = \pi \int_{p=0}^{p=2p_o} \left(r_e^2 - \frac{r_e^2\,p}{2\,p_o} \right) dp = p_o\,\pi\,r_e^2 \qquad (10)$$

which is also the volume of the disk. Using the polar co-ordinates, r and θ, the total load is now given by,

$$P = \int_{r=0}^{r=r_e} \int_{\theta=0}^{\theta=2\pi} 2\,p_o \left(1 - \frac{r^2}{r_e^2} \right) r\, dr\, d\theta \qquad (11)$$

Equation (5) applies also to this case and, when Equations (5) and (11) are substituted in Equation (3) (with $n = 3$ and $z = d$), the formula for the vertical normal stress becomes,

$$p_z = \int_{r=0}^{r=r_e} \int_{\theta=0}^{\theta=2\pi} \frac{3}{2\pi} \frac{d^3}{[d^2 + r^2]^{\frac{5}{2}}} \, 2\, p_o \left(1 - \frac{r^2}{r_e^2}\right) r\, dr\, d\theta \quad \ldots\ldots.(12)$$

Equation (12) may be integrated by expanding the quantity in the square brackets as a binomial series, then multiplying, and, finally, integrating term by term. This process leads to the equation,

$$= p_o \left[\frac{3}{2} \left(\frac{r_e}{d}\right)^2 - \frac{5}{4} \left(\frac{r_e}{d}\right)^4 + \frac{5 \times 7}{4 \times 8} \left(\frac{r_e}{d}\right)^6 - \frac{5 \times 7 \times 9}{4 \times 8 \times 10} \left(\frac{r_e}{d}\right)^8 + \frac{5 \times 7 \times 9 \times 11}{4 \times 8 \times 10 \times 12} \left(\frac{r_e}{d}\right)^{10} - \ldots + \right] \quad \ldots\ldots\ldots\ldots(13)$$

which infinite series is convergent only for $d > r_e$ and, therefore, can be used only at depths greater than the radius of the loaded area.

Case IV.—Parabolic Distribution ($n = 6$).—Equations (5) and (11) apply to this case, and they may be substituted in Equation (3) (with $n = 6$ and $z = d$), giving,

$$p_z = \int_{r=0}^{r=r_e} \int_{\theta=0}^{\theta=2\pi} \frac{3}{\pi} \frac{d^6}{[d^2 + r^2]^4} \, 2 p_o \left(1 - \frac{r^2}{r_e^2}\right) r\, dr\, d\theta \quad \ldots\ldots.(14)$$

and simplifying as in Case III, the resulting formula is identical with Equation (13), except that the numerical coefficients of corresponding quantities become 3, 4, 5, 6, 7, etc. This series is also convergent only for $d > r_e$. By a transformation to trigonometric functions, Froehlich[13] has derived expressions similar to Equations (12) and (14) in a closed form instead of the infinite series of Equation (13) and its parallel in Case IV.

Equations (7) and (13) and their respective parallels in Cases II and IV may be used to make theoretical calculations for comparison with the stresses measured in the experiments.

The Experiments

Among the earliest experiments made to determine the distribution of vertical normal stresses on horizontal planes at various depths beneath a loaded disk, were those of Steiner-Kick[14] at Prague, in 1879 (see Table 1(*a*)). These experiments were made with sand and the bearing area was a circular disk 10 cm in diameter. In 1909, at Graz, Austria, Strohschneider[15] experimented with small circular disks 1.5 cm in diameter, subjecting them to loads of a few kilograms (Table 1(*b*)). He made his experiments with sand and measured the vertical normal stress on horizontal planes at depths to about 4 cm

[13] "Druckverteilung im Baugrunde," Julius Springer, Vienna, 1934.

[14] Handbuck der Ingenieurwissenschaften, 1 Aufl., II. Bd.; *Der Brückenbau*, 2 Abt., S. 195, Leipzig, 1882.

[15] "Elastische Druckverteilung," *Sitzungsberichte* d. Kais. Akad. d. Wissenschaften in Wien, Vol. 71, Abt. IIa, February, 1912, p. 299.

below the plane of the disk. A. T. Goldbeck, M. Am. Soc. C. E., made similar experiments,[16] in 1917, at the United States Bureau of Public Roads (Tables 1(*f*) and 1(*g*)). For bearing areas Goldbeck used circular disks of different diameters (8 in. and 13.5 in.) and measured the stresses transmitted through

TABLE 1.—COMPARISON OF RESULTS; DISTRIBUTION OF VERTICAL NORMAL STRESSES BENEATH FOUNDATIONS

Depth, d, Measured in: Centimeters (1 (*a*))	Depth, d, Measured in: Inches (1(*b*))	Diameter, $D = 2\,r_e$, of the Loaded Plate, Measured in: Centimeters (2 (*a*))	Diameter, $D = 2\,r_e$, of the Loaded Plate, Measured in: Inches (2(*b*))	Ratio, $\frac{d}{r_e}$ (3)	Values of p_z expressed as percentages of p_o (4)
(*a*) STEINER-KICK					
8.0	3.1	10.0	3.9	1.60	107.2
13.2	5.2	10.0	3.9	2.64	43.0
(*b*) STROHSCHNEIDER					
2.0	0.8	1.5	0.6	2.67	38.3
3.0	1.2	1.5	0.6	4.00	17.8
4.0	1.6	1.5	0.6	5.33	9.9
(*c*) KÖGLER AND SCHEIDIG; SERIES I					
20.0	7.9	33.9	13.3	1.18	128
30.0	11.8	33.9	13.3	1.77	76
40.0	15.7	33.9	13.3	2.36	41
50.0	19.7	33.9	13.3	2.95	30
60.0	23.6	33.9	13.3	3.54	21
(*d*) KÖGLER AND SCHEIDIG; SERIES II					
10.0	3.9	45.0	17.7	0.45	220
20.0	7.9	45.0	17.7	0.89	100
30.0	11.8	45.0	17.7	1.33	80
40.0	15.7	45.0	17.7	1.78	65
50.0	19.7	45.0	17.7	2.22	48
60.0	23.6	45.0	17.7	2.67	31

Depth, d, measured in inches (1)	Diameter, $D = 2\,r_e$, of the loaded plate (2)	Ratio, $\frac{d}{r_e}$ (3)	Values of p_z expressed as percentages of p_o (4)
(*e*) M. L. ENGER			
38	36	2.11	50
30	36	1.67	74
24	36	1.34	111
18	36	1.00	160
12	36	0.67	184
30	30	2.00	64
24	30	1.60	101
18	30	1.20	136
12	30	0.80	199
38	21	3.62	18
30	21	2.86	38
24	21	2.28	72
18	21	1.72	108
12	21	1.14	139
(*f*) A. T. GOLDBECK; SERIES I			
12	13.5	1.78	79.5
12	13.5	1.78	75.7
12	13.5	1.78	81.5
12	13.5	1.78	89.1
Average	....	....	81.5
24	13.5	3.56	19.8
24	13.5	3.56	26.7
24	13.5	3.56	25.7
Average	....	....	24.1
36	13.5	5.33	8.7
36	13.5	5.33	9.1
36	13.5	5.33	10.7
Average	....	....	9.5

Depth, d, measured in inches (1)	Ratio, $\frac{d}{r_e}$ (3)	Values of p_z expressed as percentages of p_o (4)
(*f*) A. T. GOLDBECK; SERIES I (*Continued*) ($D = 13.5$ INCHES)		
48	7.11	3.96
48	7.11	4.28
48	7.11	4.28
Average	....	4.17
60	8.89	2.38
60	8.89	2.86
60	8.89	2.29
Average	....	2.51
(*g*) A. T. GOLDBECK; SERIES II ($D = 8.0$ INCHES)		
6	1.5	116.5
6	1.5	98.3
6	1.5	93.9
6	1.5	94.5
6	1.5	94.3
Average	....	99.5
12	3.0	36.7
12	3.0	49.1
12	3.0	45.5
12	3.0	45.0
Average	....	44.1
24	6.0	8.33
24	6.0	8.33
24	6.0	7.22
24	6.0	8.75
24	6.0	8.56
Average	....	8.24
36	9.0	3.33
36	9.0	3.33
36	9.0	3.93
Average	....	3.53

sand at depths to 60 in. below the plane of the load. At the University of Illinois, M. L. Enger, M. Am. Soc. C. E., conducted further experiments[17] of the same kind, using circular plates of various sizes to 36 in. in diameter (Table 1(*e*)). At Freiburg, Germany, Kögler and Scheidig have concluded an extensive experimental program[18] which included the measurement of stresses produced in sand fills by loaded plates on top of the sand (Tables 1(*c*) and 1(*d*)).

[16] "Distribution of Pressures through Earth Fills," *Proceedings*, Am. Soc. for Testing Materials, Vol. 17, 1917.

[17] Second Progress Report of the Special Committee on Stresses in Railroad Track, *Transactions*, Am. Soc. C. E., Vol. LXXXIII (1919–1920), p. 1409, and Vol. 93 (1929), p. 372.

[18] "Druckverteilung im Baugrund," *Die Bautechnik*, 1927, Heft 29 und 31; 1928, Heft 15 und 17; 1929, Heft 18 und 22.

Values in Column (4), Table 1, are the measured vertical normal stresses on the vertical axis of the loaded area, expressed as a percentage of the average load on the bearing area. The average load is simply the total load applied to the plate divided by the area of the plate.

Fig. 4 is a graphical representation of these experimental results, together with the four theoretical curves represented by Equations (7), and (13) for

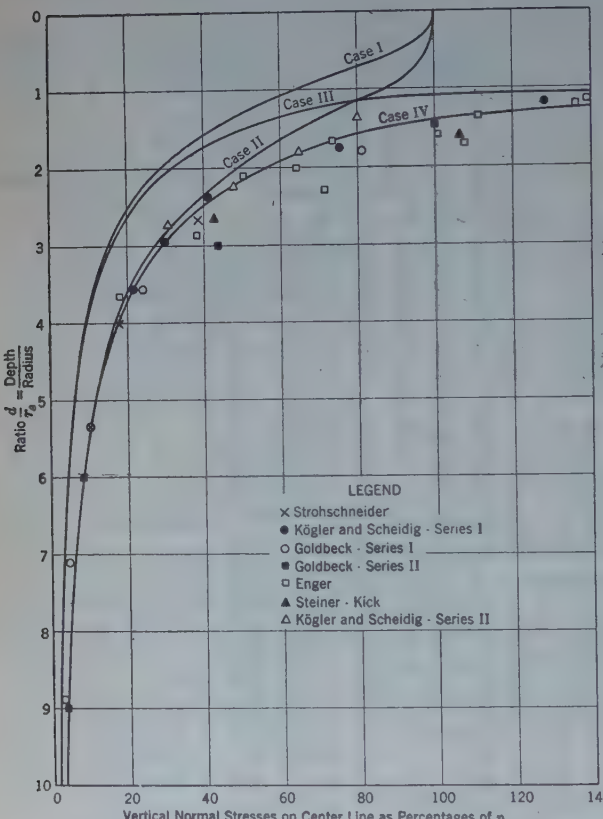

FIG. 4.

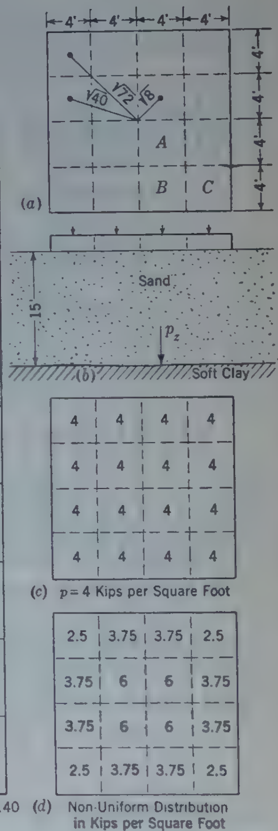

FIG. 5.—NUMERICAL EXAMPLE (1 KIP = 1 000 POUNDS)

Cases I and III, and their parallels for Cases II and IV. Before considering the relationship between the curves and the experimental points, it is desirable to notice several remarkable facts about the experiments themselves. In time, they cover a period of about fifty years. Geographically, they represent several places on two continents. The sands that were used came from various sources and the stress-measuring devices were of different kinds. The apparatus ranged from the miniatures used by Strohschneider to the large plates used by Enger. Notwithstanding these many possible variables, there is a most noticeable uniformity in the results of the experiments.

The theoretical curves show several interesting facts. For a uniform distribution of surface pressure (Cases I and II) the curves show a stress under the center of the plate at the surface equal to 100% of this pressure. This is in accordance with the assumptions made in the analysis. For a parabolic distribution (Cases III and IV) the curves continue out toward the right and these particular curves plotted from the infinite series of Equation (17) and its adaptation to Case IV become asymptotic to the line, $\frac{d}{r_e} = 1$. With the finite integrals obtained by Froehlich[19] for the parabolic distribution, the curves turn upward and give a stress under the center of the plate at the surface which is 200% of the average surface pressure. In the region represented by Fig. 4, Froehlich's integrals and the infinite series give the same results. The importance of the parameter, n, of Equation (3) is clearly indicated by the curves. Stress calculations based on the theory of elasticity in which n is 3 (Cases I and III), give results at any depth on the vertical center line which are much smaller than those calculated with $n = 6$ (Cases II and IV). The character of the pressure distribution at the surface (uniform or parabolic) is especially important near the surface but loses its importance as the depth increases. This is evident from the fact that the curve of Case I (uniform) is the same as the curve of Case III (parabolic) at depths greater than about twice the diameter of the loaded area. The same phenomenon applies to the other pair of curves.

It is easy to note which of the four theoretical curves gives the best interpretation of the experiments. The distribution of pressure at the under side of these test plates was approximately parabolic and the parameter, n, was approximately 6. Both these factors are required to account for the measured stresses.

It seems desirable to point out the fact that the distribution of pressure on the surface is not necessarily parabolic in the manner shown in Fig. 3(b). The surface pressure might be a maximum at the center and zero at the edge, but it can vary from this range to a distribution that would be a minimum at the center and infinite at the edge. Boussinesq[20] has discussed several of these possible surface distributions and, in general, they depend on the relative elastic properties of the two bodies in contact. For a square or a rectangular area the distribution of pressure at the ground surface can be fairly complicated as has been shown experimentally by Frederick J. Converse,[21] Assoc. M. Am. Soc. C. E. A. E. H. Love[22] has given a theoretical analysis of the problem for both uniform and variable pressures over rectangular bearing areas. In most practical problems involving large bearing areas, it is customary to divide the large area into a number of small areas and then to make the stress calculation for each of the small areas and add the results. A non-uniform distribution can be treated in this manner by varying the

[19] "Druckverteilung im Baugrunde," p. 52.

[20] "Application des Potentiels," pp. 149–166.

[21] "Distribution of Pressure Under a Footing," *Civil Engineering*, April, 1933, Vol. 3, No. 4, p. 207.

[22] *Philosophical Transactions*, Royal Soc. of London, Vol. 228, Series A, 1929, p. 377.

load on the several small areas in accordance with the non-uniformity of the surface distribution.

Very little experimental work has been done for the purpose of determining the distribution of pressure in the contact area between the plate and the sand-fill. However, it is very probable that this pressure distribution varies to some extent with the load itself. For very slight loads or for very large bearing areas the pressure is approximately uniform and the parameter, n, is approximately 3. As the load is increased or as the size of the bearing area is decreased the pressure at the contact plane becomes non-uniform and, at the same time, the value of n increases to 6 if not higher. The value of n also depends to some extent on the elastic properties of the soil. A value of 3 can be used only for elastic isotropic solids stressed within their elastic limits. A very hard dry clay, not too heavily loaded, would behave approximately as an elastic solid, and $n = 3$ would be nearly correct for this kind of material. Granular soils offering almost no resistance to tension cannot act as elastic solids and, in such materials, n has values which may be as great as 6.

Numerical Example

Figs. 5(a) and 5(b) show a footing 16 ft square which is to be built on a 15-ft stratum of sand, overlying soft clay. It is desired to know the vertical normal stress that will be exerted on the top surface of the clay. The footing is subdivided into small squares each 4 ft on a side and because of symmetry there will be only three types of squares, designated A, B, and C. The load will be assumed as concentrated at the center of gravity of each square, and the horizontal distances from the center of the footing to these centers of gravity are shown in Fig. 5(a). Fig. 5(c) shows this footing with a uniform distribution of surface pressure of 4 000 lb per sq ft. The total load is 1 024 000 lb. Fig. 5(d) shows the footing with a non-uniform distribution of pressure similar to the experimental determination of Converse.[21] The pressure is more than the average in the center squares and less than the average in the middle of the sides and in the corners. The total load for Fig. 5(d) is also 1 024 000 lb.

TABLE 2.—Stress Computation; Numerical Example
($z = d = 15.0$ feet)

Type (see Fig. 5 (a))	Number of acres	Radius vector, R, in feet	(a) Uniform Load			(b) Non-Uniform Load		
			Concentrated load, P, in pounds	Vertical Normal Stress, in Pounds per Square Foot: By Equation (3)*	Vertical Normal Stress, in Pounds per Square Foot: Total (Column (2)) × (Column (5))	Concentrated load, P, in pounds	Vertical Normal Stress, in Pounds per Square Foot: By Equation (3)†	Vertical Normal Stress, in Pounds per Square Foot: Total (Column (2)) × (Column (8))
(1)	(2)	(3)	(4)	(5)	(6)	(7)	(8)	(9)
A......	4	15.3	64 000	123	492	96 000	349	1 396
B......	8	16.3	64 000	90	720	60 000	131	1 048
C......	4	17.2	64 000	68	272	40 000	57	228
Total...	....	......	....	....	1 484	....	....	2 672

* $n = 3$ † $n = 6$

Table 2 gives the stress calculations in condensed form. Table 2(a) refers to Fig. 5(c); and, in addition to the uniform distribution of pressure at the surface, it is assumed that the distribution of stress through the sand is in accordance with the theory of elasticity; that is, $n = 3$. The total stress exerted on the top surface of the clay on the vertical center line of the footing is 1 484 lb per sq ft. Table 2(b) refers to Fig. 5(d); and, in addition to the non-uniform pressure distribution, it is assumed that $n = 6$. The calculated stress is 2 672 lb per sq ft, which is almost twice that of the other assumption.

Summary and Conclusions

In most problems of soil mechanics dealing with the probable behavior of foundations, the first requisite is a calculation of the stresses produced in the underlying strata by the foundation loads. The accuracy of the subsequent calculation of the effects produced by these stresses will depend on the degree of approximation obtained in the calculation of the stresses themselves. For the problem of the calculation of the stresses, it is believed that the foregoing analysis leads to two important conclusions: (1) The manner in which the pressure is distributed over the contact surface must be considered; and (2) the equations of the theory of elasticity must be modified before they can be applied to soils.

Conclusion (1) is particularly true when the depth for which the computation is being made is equal to, or less than, the diameter of the loaded area. It is to be understood that Equations (7) and (13) for Cases I and III, and their adaptation to Cases II and IV, are not offered for immediate use in the solution of practical problems. These formulas can be used only when the practical problem fulfills all the conditions under which they were derived. Most practical problems involve bearing areas other than circles and the distribution of pressure under the foundation is neither perfectly uniform nor parabolic. However, a reasonably accurate determination of the stresses can be expected only after a careful consideration of the probable pressure distribution at the contact surface and a proper choice of the value of the parameter, n. As a general rule, it is not satisfactory to assume that the pressure at the surface is uniformly distributed and that the equations of the theory of elasticity can be used without modification.

APPENDIX

Notation

d = depth from ground surface to a given plane.
e = a subscript denoting "edge."
n = a parameter with values that vary with different conditions; a concentration factor.
o = a subscript denoting uniform distribution.

p = pressure per unit area; p_o = intensity of pressure under a uniformly distributed load; p_x, p_y, and p_z = components of unit stress at a given horizontal plane, distant $z = d$ below the ground surface.

r = variable radius; r_e = radius to the edge of a circular foundation.

z = a variable distance measured parallel to the Z-axis; the depth, d, from the ground surface to the plane for which a given computation is made.

D = diameter of circular foundation = $2r_e$.

P = externally applied, concentrated load.

R = a radius vector.

V = volume.

θ = angular distance.

AMERICAN SOCIETY OF CIVIL ENGINEERS

Founded November 5, 1852

PAPERS

SOME LOW-TEMPERATURE CHARACTERISTICS OF BITUMINOUS PAVING COMPOSITIONS

By Hugh W. Skidmore,[1] Assoc. M. Am. Soc. C. E.

Synopsis

Stability at temperatures approximating hot-weather temperatures in the pavement has become thoroughly established as a basic requirement of bituminous compositions. Means of measuring and rating this important property have been perfected as a result of laboratory experiments and have been proved sound through several years of practical application. Two contemporary tests have evolved with resistance to shear the basic principle of both: In one (the extrusion test) the shear is measured indirectly and in the other (the direct test), simple shear is measured directly, and values are expressed in pounds per square inch. The latter method is distinctly convenient in comparing a variety of compositions which may have been tested in cylinders of from 1 in. to 6 in., or more, in diameter, since values by the extrusion test are not reducible to unit loads.

Although much work has been done in connection with summer temperature characteristics, with the result that the elements of mixture design involved have become thoroughly understood, little, if any, study has been made concerning low-temperature performance in paving compositions. With the thought that such an investigation should throw much light upon several questions that have long been unanswered and have given engineers much concern, the results of a systematic course of study, begun in 1931, are reported in this paper.

Introduction

It was recognized that some engineers have avoided the use of bituminous pavements because they were not always certain of the capacity of these types to withstand winters, although it is well known that many bituminous compositions have withstood severe low temperatures for long periods. Just why

Note.—Discussion on this paper will be closed in November, 1935, *Proceedings*.

[1] Pres., Chicago Paving Laboratory, Chicago, Ill.

some pavements have failed to do so has never been clearly explained. Aside from failures definitely attributable to base or to sub-grade, bituminous compositions may crack too profusely, or they may become brittle, and ravel at low temperatures. Definite means of avoiding these faults have not been at hand because scientific data have not been available with reference to the characteristics of bituminous paving compositions over a wide range of temperatures, particularly low temperatures.

One of the early disclosures in experimental work with stability at temperatures above normal air temperature was that mixture resistance to shearing forces mainly resided in the mineral structure (especially the finely divided mineral filler) and that the bituminous cement was of decidedly secondary importance. Although there were noticeable differences between various cements in a given mineral structure, and although differences in consistency of a cement accounted for some change in stability, these differences were of minor importance as compared with those in stability that were due specifically to changes in mineral composition.

One of the first items of significance encountered in studying mixtures at low temperatures was the important rôle of the bitumen in such mixtures, both with respect to its normal consistency and to its inherent qualities, such as may result from refining methods or from the parent crude oil. As the temperature is reduced, the bituminous cement becomes more and more the outstanding factor in the strength of the composition. For example, there are obvious characteristic differences between straight-run materials and cracked or oxidized cements; and there are equally as distinctive differences between tar and some asphalts and between asphalts from mid-Continent, California, and South American sources. Such facts were suspected, but certainly they were not actually known until the studies were undertaken.

Although the data reported herein pertain to sheet asphalt mixtures of the hot-mix type, sufficient work has been done with other compositions to demonstrate that typical characteristics as disclosed by these studies are common to bituminous paving compositions in general. Important avenues of further investigation with reference to specific differences between fine and coarse aggregate mixtures, hot and cold-mix types, and other such comparisons, are clearly indicated.

Composition of Mixtures Studied

In order to develop a general comparison of the twenty or more cements included in this study, a normal sheet asphalt composition was chosen, with the bitumen the only variable. The commonly used consistency of 50 to 60 penetration was selected, with a few examples of a given cement over a complete range of consistencies from low to high penetration. Normal mixtures were designed with bitumen filling the voids in the dry, compacted, mineral aggregate. Variations from normal design were also studied with the bitumen content both less and more than mineral voids. A moderate filler content of 20% by weight of total mineral aggregate (about 14% of mineral passing a 200-mesh sieve in the finished mixture) was used in the main group, with more, and less, filler used in one group to determine

the general effect of variations in filler content. Thus, a fairly wide scope of possible variables applicable to fine aggregate compositions was covered by these studies.

Mineral Aggregates

Sand.—In order to eliminate possible sources of uncontrolled variables, a sand of controlled grading, obtained from a single source, was selected. It is recognized that, in all likelihood, similar mixtures with sands from other sources and gradations would produce different values, but extensive investigations in the past have indicated quite conclusively that there is a characteristic order of values for any given aggregate material and that, in so far, as practical sheet asphalt gradations are concerned, the order of stability is rather well defined, depending mainly upon filler content for marked increases or decreases. Hence, it was felt that although the studies of a variety of sands and fillers would be interesting academically, the chances were slight that any really vital information would be developed by such studies.

The Lake Michigan sand that was selected is common to the territory in the Great Lakes region, and has been used for many years in asphalt paving construction. Although it is not the best sand encountered, it has the advantage of extreme cleanliness, uniformity of composition, grain shape, and size within the range of material passing any given sieve opening. The sand was separated on the 10, 40, and 80-mesh sieves and recombined to a definite grading as follows:

Percentage passing the 80-mesh sieve, and retained on the 200-mesh sieve..........	21.6
Percentage passing the 40-mesh sieve and retained on the 80-mesh sieve...........	47.3
Percentage passing the 10-mesh sieve and retained on the 40-mesh sieve...........	31.1
Total (percentage)..................	100.0

The specific gravity of this sand was 2.65.

Mineral Filler.—The limestone dust filler has also been used extensively in the Chicago area for many years. It is made by pulverizing a hard, durable white limestone and, in the tests, had the following characteristics:

Percentage passing a 325-mesh sieve.......	61.3
Percentage passing a 200-mesh sieve and retained on a 325-mesh sieve...........	15.0
Percentage passing a 80-mesh sieve and retained on a 200-mesh sieve...........	23.7

The specific gravity in this case was 2.71.

Sand-Filler Aggregate.—Voids were determined[2] for several sand-filler proportions such as 0, 12, 20, 25, 30, and 100% of filler. Fig. 1, which is the voidage curve for these two minerals, is the basis for calculating the bitumen

[2] Symposium on Mineral Aggregates: "Fine Aggregate in Bituminous Mixtures," by Hugh W. Skidmore, *Proceedings*, Am. Soc. for Testing Materials, 1929, p. 788 (also reprinted in *Roads and Streets*, October, 1929); "Sheet Asphalt Mixture Research," by Hugh W. Skidmore, *Proceedings*, Wisconsin Eng. Soc., 1925 (also reprinted in *Roads and Streets*, April, 1925).

required in the mixtures. Because this curve was so typical for the materials, points intermediate between 30 and 100% of filler are omitted, since more than 30% of filler is rarely used in practice.

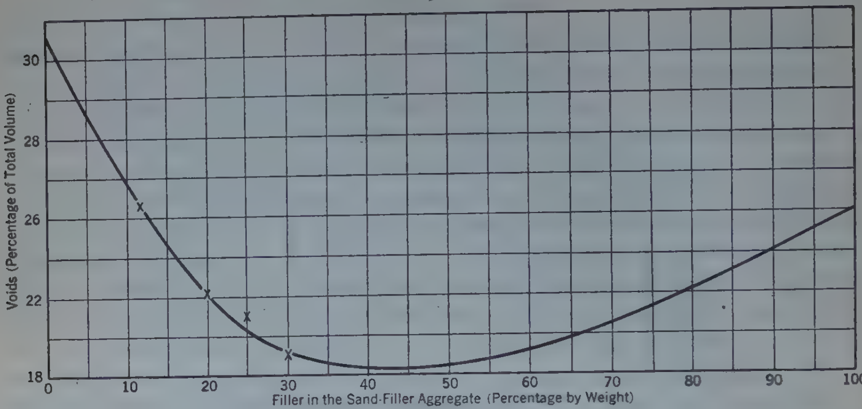

FIG. 1.—VOIDAGE CURVE; MINERAL COMPACTED DRY, TO REFUSAL.

Bituminous Materials.—The characteristics of the twenty-four cements in the main group of mixtures are detailed in Table 1, together with such addi-

TABLE 1.—CHARACTERISTICS OF BITUMINOUS CEMENTS

Specimen	Source	Method of refining	Penetration			Ductility			Cementation Values ‡		Specific gravity	Bitumen; solubility in carbon disulphide
			At 77° F; 100 g, 5 sec	At 32° F; 200 g, 60 sec	At 115° F; 50 g, 5 sec	At 77° F; 5 cm, 60 sec	At 32° F; 0.25 cm, 60 sec	At 41° F; 5 cm, 60 sec	Kilogrammeters at 41° F	Elongation, in centimeters		
1	California......	Steam............	54	11	400†	150†	14.5	0	0.377	15	1.014	99.9†
2	California......	Vacuum and steam	53	8	400†	150†	....	0.5	.....	....	1.020	99.9†
3	California......	Steam............	52	7	400†	150†	11.0	0	0.430	17†	1.019	99.9†
4	Coal tar.........	Steam............	56	1	400†	121	0	0	0.045	0.75	1.181	93.2
5	Pennsylvania*...	Cracking coil......	53	10	380	150†	0	0	0.120	3.5	1.113	.....
6	Mexico.........	Steam............	50	16	225	150†	10.5	7.5	0.180	11.5	1.040	99.9†
7	Mexico.........	Steam............	54	17	248	150†	....	7.25	0.160	9.0	1.031	99.9†
8	Mexico.........	Steam............	53	14	215	150†	....	6.75	.....	....	1.040	99.9†
9	Mid-Continent..	....	55	21	261	126	5.5	5.0	0.074	5.5	1.014	99†
10	Mid-Continent..	....	52	19	221	150†	5.25	4.5	0.111	5.0	1.005	99†
11	Mid-Continent..	....	48	14	215	100.0	....	4.75	0.193	5.75	1.018	99†
12	Mid-Continent..	....	60	23	226	150†	....	6.25	0.133	6.5	1.010	99†
13	Wyoming.......	....	52	16	225	133	....	5.75	0.1572	5.75	1.029	99†
14	Arkansas.......	Vacuum and steam	49	18	234	150†	5.5	4.75	0.162	5.0	1.027	99†
15	Arkansas.......	Vacuum and steam; oxidized........	56	28	185	62	5.75	5.5	0.053	6.0	1.016	99†
16	Mexico.........	Oxidized.........	56	31	123	4	3.5	0	0.070	3.5	1.017	99†
17	Texas..........	Steam............	52	14	235	150†	....	5.0	0.1975	5.0	1.009	99†
18	Texas blend....	Partly oxidized....	51	22	202	92	6.5	....	0.096	6.0	1.011	99†
19	Colombian.....	Flash-vacuum oxidized..........	52	15	219	150	5.75	5.0	0.137	5.0	1.005	99†
20	Venezuela......	Steam...........	54	16	243	150†	....	6.75	0.186	9.0	1.030	99†
21	Bermudez......	South American flux............	53	17	290	58	....	7.5	0.240	10.0	1.061	97.7
22	Blend..........	Steam and cracking	52	16	204	150†	7.75	6.0	0.127	6.5	1.056	99†
23	Trinidad.......	South American flux............	54	18	251	62	....	5.25	0.2235	8.0	1.257	69.2
24	Trinidad.......	11° API† Mexican flux............	53	..	...	....	....	....	.....	....	.....	71.9

* Cracked kerosene residuum. †American Petroleum Institute. ‡ Test described in *Journal of Industrial and Engineering Chemistry*, Vol. 6, No. 12, p. 976.

tional information as source and methods of refining, in as complete form as such data could be obtained from the producers.

In procuring samples of representative products, asphalt of three ranges of penetration were requested: 40–50, 50–60, and 60–70. Although these penetrations represent the grades commonly used in paving construction, it was considered desirable, after much work had been done, to include some softer materials, and these were secured in some cases.

Specimens 4, 16, and 24, Table 1, were three special cements prepared in the laboratory. For Specimen 4, a vertical-oven gas-house tar was reduced to grade by steam distillation. The crude tar showed the following characteristics:

Water content (percentage by weight)	1.3
Specific gravity (at 25° C.)	1.098
Viscosity (in seconds, Saybolt Furol) at 50° C.	21
Viscosity (in seconds, Saybolt Furol) at 40° C.	37
Viscosity (in degrees, Engler, specific) at 40° C.	8.7
Percentage soluble in carbon disulphide	98.2
Distillation (percentages by weight) to:	
170° C.	0.72
235° C.	14.12
270° C.	23.34
300° C.	32.61
Softening point of residue	106° F

For Specimen 16, a regular Mexican flux (gravity, 11°, American Petroleum Institute) was blown to grade in the laboratory blowing-still. This material had a penetration of about 200 before blowing. For Specimen 24, a refined lake asphalt from the Island of Trinidad was fluxed to grade with the same Mexican flux used in manufacturing the oxidized Mexican cement. Tests were made for cementing value, with contained mineral present.

Supplementary comments referring to Table 1 should also be made regarding Specimens 5, 15, 19, 21, 22, and 23, as follows: Specimen 5 was a synthetic asphalt derived from residual, cracked kerosene; Specimen 15 was run to a penetration of 150 to 200 and then blown to grade; Specimen 19 was a flash-vacuum residual of 100 penetration, blown to grade; in the case of Specimens 21 and 23, tests for cementing value were made with contained mineral present; and Specimen 22, identified in Table 1 as a "blend," was probably a blend of steam-refined Venezuelan, and cracked domestic asphalt.

Preparation of Mixtures

Sand-filler aggregate was thoroughly mixed dry and heated to 350° F; then it was mixed thoroughly with hot asphalt cement at the same temperature. In the case of the more fluid binders, such as coal tar and the cracked asphalts, lower temperatures were used for both aggregates and binders, depending upon the viscosity of the bitumen. Some were heated to 325°F, some to 300° F, and the tar, to 250° F. In this particular the best field practice was simulated.

During the preliminary experiments, mixtures were prepared in a small, laboratory, power mixer, but the practice was abandoned in favor of careful

hand-mixing for the study proper, due to the fact that too large a batch was required for the mechanical mixing. It was found that, in the case of an open pug-mill and hand-mixing, oxidation was identical. Therefore, accuracy was in no manner affected as compared with actual practice, since open mixers of the pug-mill type are still predominantly characteristic of asphalt paving manufacture despite important advantages inherent in sealed rotary mixers.

Each mixed batch was then weighed into the small batches to be moulded into the set of test cylinders. The small batches were stored in an oven at mixing temperatures during the few moments required for moulding.

Preparation of Test Cylinders

The normal size of compressed cylinders for sheet mixtures has commonly been 2 in. in diameter by approximately 1.5 in. in depth. For ordinary temperatures used in testing for stability, this is quite satisfactory for the capacity of the testing machine, but it was soon discovered that low temperatures would produce shearing strengths in excess of the capacity of the machine when using that size of cylinder. It was also found that results on cylinders 1 in. and 2 in. in diameter agreed for sheet mixtures. Therefore, the smaller diameter was used in these studies so as to provide for shearing strength possibilities in excess of 3 000 lb per sq in., if required, without building a new testing machine.

Cylinders were compressed at mixing temperatures in seamless steel tube moulds, using a double plunger, on a hydraulic press under a vertical load of 5 000 lb per sq in. Pressure was released as soon as the dial registered the required load. The compressed mixture was then cooled before being extruded from the moulds on the press, by means of a plunger and over-sized tube or split mould.

As has previously been described elsewhere,[3] this procedure has become standard laboratory practice after several years of experimenting and checking against field compression of paving mixtures. It has been found, repeatedly, that densities thus obtained in the laboratory agree well with those obtained in the field by adequate compacting with 10-ton rollers. The use of a double plunger assures uniform density throughout the specimen.

Testing Procedure

Density determinations (specific gravity) were made upon compressed cylinders a few hours after their preparation. Customary laboratory routine required that the mixtures be tested the day following their preparation, but there is no reason why they may not be tested as soon as they have been properly cooled and their densities determined.

The testing machine stands in a bath sufficiently large to provide storage for a considerable number of cylinders. Small cylinders, 1 in. to 2 in. in diameter, are maintained in the bath at testing temperature for 1 hr before

[3] "Practical Application of the Shear Test to Bituminous Mixtures," by H. W. Skidmore, *Proceedings*, 7th Annual Asphalt Paving Conference; also, *Roads and Streets*, January, 1929.

they are tested, whereas larger ones are held for 2 hr or more, depending upon their size. It is not necessary to remove them from the bath to place them in the machine.

For all temperatures above 32° F, water was used for the bath, adding sufficient ice to secure a temperature of 41° F. Alcohol and dry ice were used for 32° F, 0° F, and −20° F, and proved to be an excellent bath medium for the low temperatures; accurate temperature control was readily maintained.

When the shearing strength test was developed several years ago, it was found by experiment that, by applying the shearing load on cylinders 2 in. in diameter at the rate of 2 lb per sq in. per sec, the most concordant results were obtained for a wide range of mixture composition and temperatures. For this reason it was adopted as the standard rate, and in order to maintain consistent results for various diameters of test cylinders, the rate must be kept proportional to the diameter, since the load is applied circumferentially; for example, one-half the 2-in. rate was required for cylinders, 1 in. in diameter, and double the 2-in. rate was necessary for 4-in. cylinders. These were the rates of load application used in the studies reported herein.

The dynamometer of the testing machine is equipped with a maximum load indicator. In the present studies, values are the average of three test cylinders of each mixture at each temperature. In the application of the stability test at normal air temperature and above, maximum variation in well designed mixtures has been found to be within 5% of the average of the group of individual test cylinders. Poorly designed mixtures usually show greater variation, and if badly out of balance, wide differences between minimum and maximum results are common. In studying mixtures at low temperatures the same general rule seems to apply, except that with highly susceptible bitumens, such as tars and cracked asphalts, even well designed mixtures show erratic results at 0° F and below. In fact, if the curve for a given mixture tends to reverse its direction as the temperature drops, the spread between minimum and maximum becomes much wider as the temperature becomes progressively lower beyond the approximate point of reversal of direction.

Test Results

Results obtained in the use of a common mineral composition are plotted in Fig. 2(*a*), with Fig. 2(*b*) an enlargement of horizontal scales for the lower temperatures. The principal value of this general curve is to demonstrate graphically the spread from maximum to minimum values for the several binders (of common consistency range) studied, and it reveals nicely the characteristic trends of the widely divergent types of cement, with respect to source and refining methods.

The common mixture was composed approximately as follows: Bitumen, 10%; filler, 18%; and sand, 72 per cent. Pro rata variations were made to compensate for differences in the specific gravity and bitumen content of the binder, in order to maintain a constant mixture with reference to pure bitumen, filler, and sand.

As a sidelight upon the accuracy of the shear test in detecting characteristic differences between bitumens at low temperatures, attention is called to the fact that points on the curves for two Mexican cements of practically the same consistency and the same refining process (Specimens 7 and 8, Fig. 2),

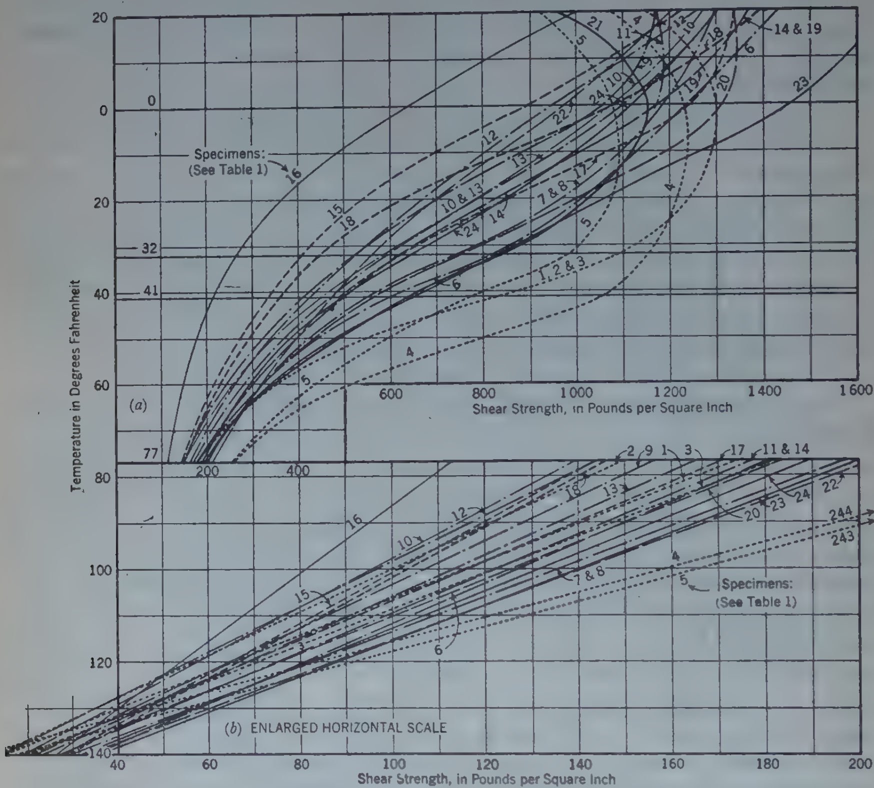

FIG. 2.—SPREAD OF TEST RESULTS FROM MAXIMUM TO MINIMUM VALUES.

agreed so closely that one curve serves for both, and the third Mexican cement, of slightly lower penetration (Specimen 6), falls close to the other two; likewise, the Californian cements from three different refineries (Specimens 1, 2, and 3) fall upon a single curve.

Bituminous binders most sensitive to great extremes of temperature are strongest at moderate temperatures, of the order of 20° F to 90° F, while being characteristically weaker at summer sun heat and severe winter cold, of zero, or below. This is most certainly borne out in practice.

Oxidation tends to smooth out the curve for a given cement and, in doing this, stability (or strength) is reduced at all temperatures, especially at low and moderate temperatures. Past experience has demonstrated repeatedly that highly oxidized asphalts are poor paving cements, particularly in climates in the temperate and frigid zones. Such binders have caused severe cracking of pavements in these localities. Likewise, asphalts which were not oxidized

during the process of manufacture, but which underwent severe oxidation while in thin films on hot mineral aggregate (in the mixer), have cracked badly in pavements which have undergone very low temperatures. Furthermore, the addition of certain salts to the paving mixture for the purpose of oxidizing or hardening the binder, has caused excessive cracking of such compositions. Every student of bituminous pavements has seen these facts demonstrated repeatedly.

This delayed effect was especially noticeable some five or six years after the introduction of the first so-called high filler mixtures (about 1922). At that time, the necessity had not been generally recognized for providing ample dry-mixing periods before introducing the asphalt and thus reducing the temperature of the hot sand (which had to be hotter because of increased filler content), by contact with cold mineral filler, to a degree not dangerous to the asphalt. Most pug-mills revolve at about 75 rpm. Consequently, freshly coated mineral is agitated severely and the asphalt (in thin films) is exposed to air rapidly, during a period of 15 to 60 sec, depending upon the enlightment of the specification writer and enforcer. If one is inclined to doubt the effect of rapid agitation of asphalt under these conditions, let him perform the following simple experiment: Weigh out 50 grams of asphalt into a tin and place it upon a hot-plate, heating it to, say, 400° F and maintaining it at that temperature for about 2 hr. Then determine its penetration and ductility. Repeat the process with a fresh sample of the same asphalt, but this time stir it for 15 min; then determine its penetration and ductility. In the first instance, it shows little if any alteration from its original characteristics, whereas in the second case it has hardened considerably and its ductility has been drastically curtailed.

Many supposedly experienced technologists still fail to take cognizance of these extremely important facts; poorly informed or ill-advised engineers continue to write specifications requiring the introduction of the bituminous binder without adequate (if any) dry-mixing of aggregates or with long wet mixing periods of 1 min, or more; and few plant operators and their employers recognize this important and inescapable result of exposing thin films of bitumen to temperatures in excess of 300° F to 400° F (depending upon the cement) in the presence of free air. If any engineer feels that he must require long mixing time to be perfectly safe, let him apply such precaution to the dry-mixing of aggregates and, to be really safe, require only 15 to 30 sec of wet mixing in any type of mixer, such as a pug-mill, to which free air has access.

Even a hasty inspection of Fig. 2 will disclose the unusual performance of fluxed Trinidad (with South American flux) cement through the low temperature range. This disclosure quite naturally indicated further study to the investigators. Steam-reduced Mexican cement (Specimens 6, 7, and 8, Fig. 2) seemed to come nearest to duplicating the performance of fluxed Trinidad cement, taking into consideration the shape of curve and values throughout the temperature range. Fig. 3(*a*) is introduced to demonstrate the effect of increasing the filler content in the case of Mexican cement, as well as the

effect of retaining the same filler content but using a slightly softer cement. The composition of the mixture is shown in Table 2.

The filler was increased under the assumption that the self-contained mineral in the Trinidad cement might possess some special value as a mineral filler, and softer asphalt was tried because the Trinidad product does not oxidize as readily as the Mexican cement. The slightly softer Mexican cement (Curve *B*, Fig. 3(*a*)) produced an excellent and very smooth curve

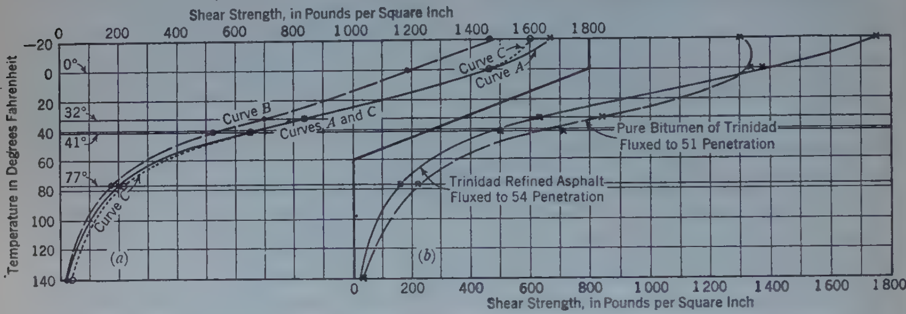

Fig. 3.—Comparison of Design Values, Mexican and Trinidad Cements.

TABLE 2.—Mixture Composition; Curves *A*, *B*, and *C*, Fig. 3(*a*)

Material	Curve *A*	Curve *B*	Curve *C*
54-penetration, Trinidad asphalt cement; South American flux	14.5	....	....
Pure bitumen	10.0	....	....
51-penetration, Mexican asphalt cement; Panuco	....	....	9.6
64-penetration, Mexican asphalt, cement; Panuco	....	9.9	....
Filler; limestone dust	13.5	18.0	22.6
Filler; Trinidad mineral	4.5	....	....
Sand; identical grading	72.0	72.1	67.8

only slightly above the Trinidad curve (Curve *A*) throughout the temperature range; whereas the higher filler with the same consistency of cement (Curve *C*, Fig. 3(*a*)), practically duplicated the results of the Trinidad product. This is simply an illustration of intelligent design of composition in the light of the materials to be used.

From these studies it seems clear that the mineral in Trinidad asphalt is an efficient filler, but that this value can be duplicated readily by proper design when using another cement. Additional indication of the filler value of Trinidad mineral is apparent from the examination of Fig. 3(*b*), in which a South American flux was used in both cements plotted. The relatively pure bitumen of the Trinidad refined asphalt was recovered by an excellent method described[4] in 1933 by Mr. Gene Abson. This asphalt, in its almost mineral-free condition, was fluxed to the consistency shown by the addition of South American (Trinidad) flux; it showed 1.041 specific gravity at 77° F, and was 95.72% soluble in carbon disulphide.

[4] "Methods and Apparatus for the Recovery of Asphalt," by Gene Abson, *Proceedings*, Am. Soc. for Testing Materials, 1933, Pt. II, p. 704.

This investigation gives proof that the presence of the mineral in the Trinidad cement is of value in the pavement to the extent indicated herein. It is important to agitate the fluxed Trinidad cement adequately in the melting kettles, or in the tank car, as it is drawn for use in the mixture. If it is necessary (as has often been the case) to remove several inches of sludge from the kettle at more or less regular intervals, the filler value of the product has been largely dissipated.

In recent years, practical experience has shown, without question, the desirability of using softer bitumen in hot-mix compositions. Stability against displacement at summer temperatures can be secured so easily by suitable mineral content, that the very slight increased stability afforded by ten points of lower penetration becomes insignificant, especially in view of the danger attending the use of harder asphalts when they are likely to be subjected to more or less severe oxidation in the pug-mill mixer commonly used. This study shows conclusively that in climates where comparatively low winter temperatures prevail, bitumens of relatively soft consistency should be used. Asphalts of 70 to 80 penetration have been used successfully in hot-mix pavements in the North Central States to withstand trunk-line traffic during the summer and the sub-zero temperatures of severe winters. (For many years 90-penetration asphalt has been used in hot-mix pavements at Calgary, Alberta, Canada, with remarkable freedom from cracking.) When they are well designed, such pavements have been practically free from contraction cracks and have not been displaced during hot weather.

Further proof of the effectiveness of soft asphalts at low temperatures is shown in Fig. 4, the mixture composition being: Asphalt cement, 9.9%

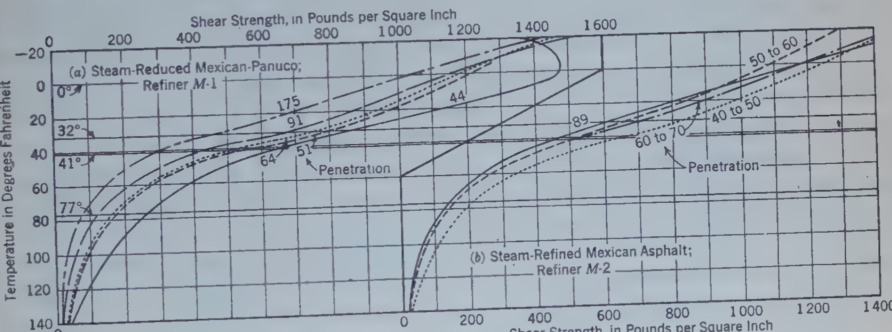

FIG. 4.—EFFECTIVENESS OF SOFT ASPHALTS AT LOW TEMPERATURES.

(9.8% for 91-penetration and 175-penetration); limestone dust, 18.0%; and, sand, 72 per cent. The only variable was the consistency of the asphalt, which was the product of one refiner in Fig. 4 (*a*) and of another in Fig. 4(*b*), using the same crude (Mexican) and the same refining process supposedly for all grades. The reversal of the curve for the 44-penetration cement (supplied by the refiner) is a rather conclusive indication that in the case of this harder grade the refiner varied the manufacture, either by altered processing of the residuum or by blending it with another material. The striking result of

the 175-penetration material undoubtedly will be a surprise to many who have always thought in terms of asphalts with 40 to 60 penetration; but when one takes into consideration the more or less satisfactory performance of some cold-lay mixtures and some rock asphalts, it seems more logical. There is no doubt that, with proper design of mixture, 100-penetration cement may be used successfully in sheet asphalt mixtures in almost any climate, and although there is no need for such a soft material in tropical or semi-tropical regions, it would be highly desirable in all sections subject to temperatures of 0° F, or below. The use of soft bitumens in such sections would probably be found the most important forward step in recent years.

Effect of Varying Mixture Composition

This study has disclosed two important facts not heretofore thoroughly appreciated: First, that there is an optimum proportioning of ingredients that will produce the greatest strength of mixture throughout the entire temperature range from sub-zero to summer sun temperature; and, second, that for best resistance to low temperatures, mixtures should contain slightly more bitumen than will just fill mineral voids, as determined in compacted, dry aggregate. To the present time, technologists have been of the opinion that mixtures should carry slightly less bitumen than will fill the voids, as determined in the dry mineral.

In Fig. 5(*a*) will be seen the results obtained in four designs of mixture using the same materials in all, and ranging from low filler content to high, with bitumen filling the voids in dry aggregate. The mixture composition of materials in Fig. 5 is listed in Table 3. It seems quite certain that too much filler can be used with a given sand or coarse aggregate and a definite guide in this respect is indicated in Fig. 5(*a*). It will be seen that Mixture *D* is inferior to Mixture *C* throughout the temperature range, so that low temperature results, in this case, are not necessary for intelligent selection. Higher bitumen, a greater compaction of mixture, might tend to prevent Curve *D* from reversing itself, and might also increase its strength at all temperatures. There is positive danger of bitumen films being too thin. Only so much compaction is available with practicable construction equipment and safe working temperatures, and although increased filler may continue to lower voids in the mineral, a certain point is reached at which the mixture becomes less compressible, and, consequently, instead of increasing the strength and density of the finished pavement, additional filler actually decreases these important properties.

Increasing the bitumen beyond that required to fill voids in the dry mineral is certainly beneficial at low temperatures, whereas decreasing it has the opposite effect. In Fig. 5(*b*), Mixture *B* of Fig. 5(*a*) was made with both plus and minus 1% bitumen content (equivalent to 10% of the normal bitumen content) with the results shown. Decreased bitumen tended to decrease the stability very slightly at high temperatures and drastically reduced the strength at temperatures of from +20° F to −20° F. This tendency is reliable proof of the danger of using mixtures with less bitumen than will fill the voids; and it offers an excellent explanation of cold-weather

cracking in dry mixtures. Reasonable excess of bitumen, on the other hand, only slightly reduced the stability at maximum pavement temperature and substantially increased the strength at low temperatures. Obviously, in warm climates, this particular phenomenon has no significance.

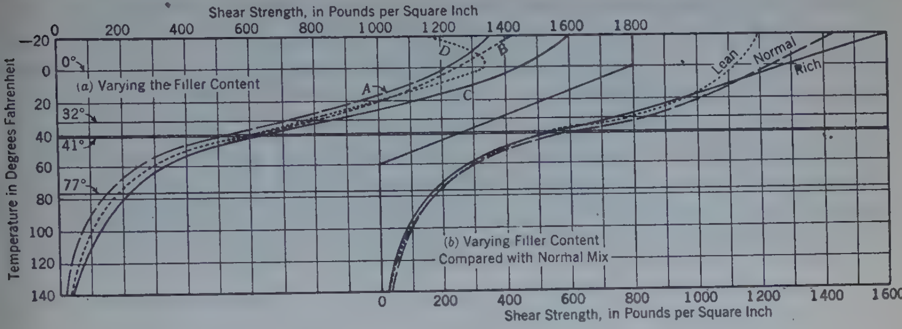

FIG. 5.—DESIGN OF ASPHALT MIXTURES.

TABLE 3.—MIXTURE COMPOSITION (ALL PERCENTAGES), DESIGNS IN FIG. 5

Description	(a) Varying the Filler Content; Fig. 5(a)				(b) Varying the Filler Content Compared with Normal Mix		
	Mixture *A*	Mixture *B*	Mixture *C*	Mixture *D*	Lean mix	Normal mix	Rich mix
(1)	(2)	(3)	(4)	(5)	(6)	(7)	(8)
Mexican asphalt cement *	12.0	9.9	9.6	8.4	8.9	9.9	10.9
Limestone dust	10.6	18.0	22.6	27.5	18.2	18.0	17.8
Graded sand	77.4	72.1	67.8	64.1	72.9	72.1	71.3
Total	100.0	100.0	100.0	100.0	100.0	100.0	100.0
Voids in the compressed mix	3.1	4.0	2.6	4.4	0†	0†	0†

* 51-penetration. † Normal bitumen fills the voids in the mineral.

In Fig. 6, eight distinctly different asphalt cements of the same grade, as determined by the penetration test at 77° F, are compared as to penetration

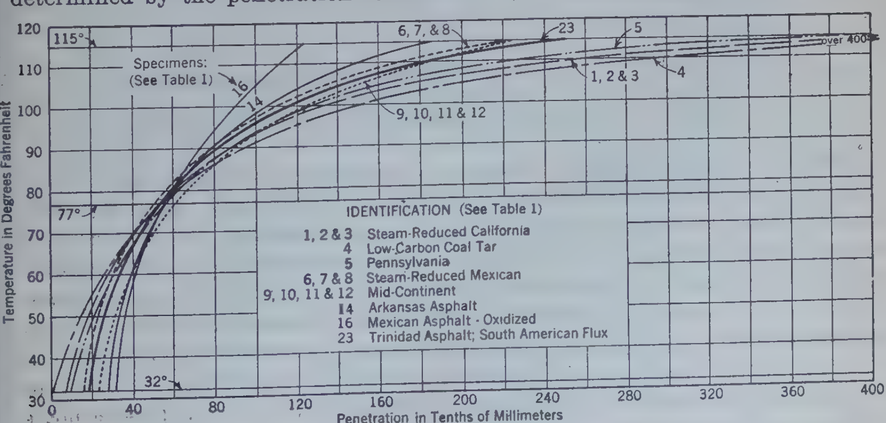

FIG. 6.—CONSISTENCY-TEMPERATURE RELATION.

at the other two standard temperatures, in order to show the wide differences in susceptibility as measured by this test. Such a test, as usually interpreted, can be very misleading. The ratio of penetrations at the several temperatures, when specified with a maximum limit only (as is usually the case) is no guaranty of performance in the pavement. In stipulating requirements for a high-grade paving cement, penetration susceptibility should be omitted in favor of a minimum low-temperature ductility requirement (in the absence of a better test at this time) in all regions where low temperature performance is critical. Specifications containing maximum penetration ratios may invite over-oxidation of what may be a reasonably good asphalt, as a measure of safety on the part of the refiner. Rigid requirements as to low temperature ductility have the opposite effect, since in nearly all cases oxidation will decrease ductility at the lower temperatures. Fig. 7 shows the relative char-

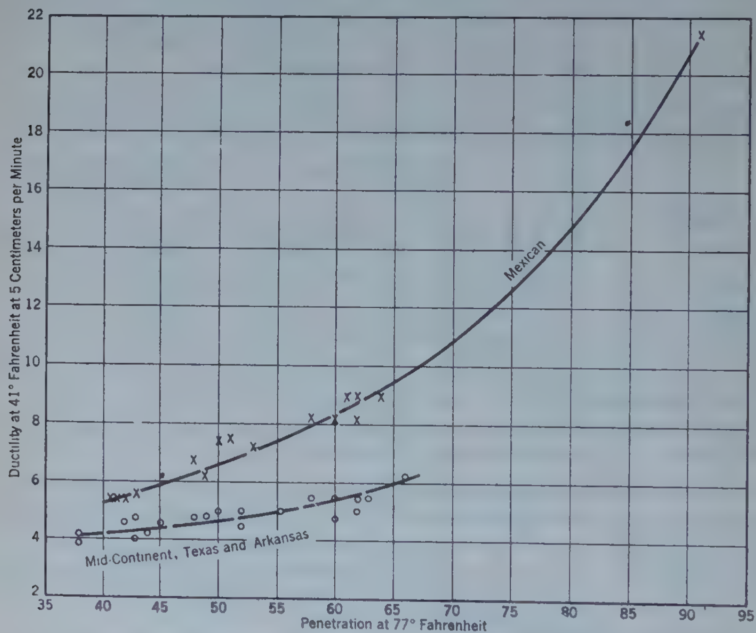

FIG. 7.—RELATION BETWEEN LOW-TEMPERATURE DUCTILITY AND PENETRATION.

acteristics of typical cements common to the market in the Central, West-Central, North and South-Central, and Southwestern States, with respect to ductility at 5° C. These studies are convincing in the light of the fact that, in general, cements of relatively high ductility (normal speed) at low temperatures likewise impart superior strength to mixtures at the lower temperatures. In climates where low temperature performance is important, such a requirement should be specified until a better test upon the asphalt is available.

Ductility as a specified requirement, when the test is conducted at 77° F, or above, means nothing for at least two important reasons: (1) This is not a critical temperature in any bituminous pavement; and (2) all binders possess

ample ductility at such temperatures. Although this test may have some value in comparing a variety of cements, it is practically worthless in a pavement specification.

In an effort to translate shear strengths of bituminous pavement mixtures into comparative values familiar to engineers in general,[5] standard Portland cement mortar cylinders were subjected to the same test over the same range in temperatures. In offering these data, it is recognized that standard mortar is not concrete of the composition used in pavements, but such mortar is generally used as an indicator of concrete strength, and its values are well known from the vast amount of published data available. On the other hand, almost no data are available with respect to bituminous concrete mixtures, and, therefore, the average engineer has a limited understanding of the strength of such compositions, especially at low temperatures. Consequently, a comparison, limited as this one is, seems sufficiently valuable from the standpoint of engineering knowledge in general, to be included in this record as a means of evaluating previously unknown values in terms of well known ones.

Even a brief analysis of Fig. 8 will convince any engineer that bituminous and Portland cement concrete structures are not directly comparable. Portland

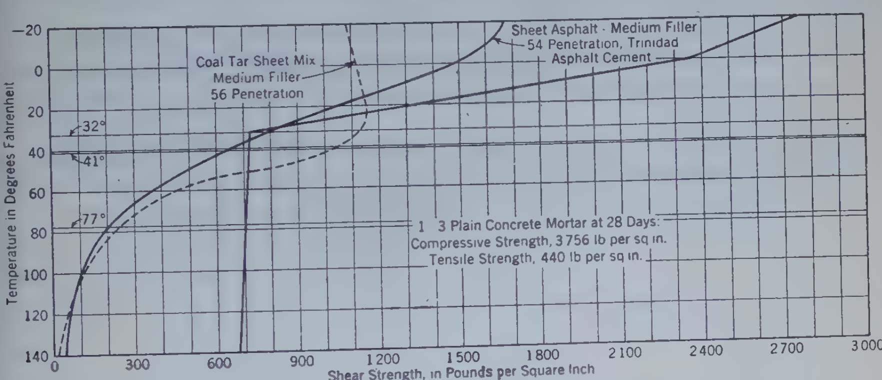

FIG. 8.

cement concrete has a non-ductile binder as a cementing medium in contrast with a ductile binder in a bituminous mixture, of otherwise quite similar composition. Plastic flow is much more pronounced in bituminous compositions than in Portland cement concrete mixtures. Furthermore, the strength of a bituminous mixture is much more a function of temperature than is the case of Portland cement concrete, except at temperatures below freezing. Plastic flow is definitely related to ductility. Contraction forces in bituminous concrete mixtures are obviously absorbed by the ductility of the binder in addition to being resisted by the tensile strength of the structure, whereas in Portland cement concrete these forces are resisted by tensile strength. Patently, the modulus of elasticity will be much higher in the case of Portland cement concrete than in that of bituminous concrete.

[5] A. S. T. M. standard mortar cylinders using standard Ottawa sand, with strengths as shown on Fig. 8.

Summary

The studies described herein have revealed some facts that were previously unknown and have confirmed others that were suspected as a result of experience and observation, as follows:

(1) The inherent characteristics and quantity of the bitumen in the mixture are much more important at low temperatures than at normal and higher temperatures in the pavement;

(2) There is an optimum proportioning of the several ingredients of the paving mixture that will insure the best performance over the entire range of temperatures;

(3) In regions where low temperatures obtain, the adoption of considerably softer bitumens than have been used commonly, will constitute one of the most important advances in the direction of better pavements;

(4) Ample bitumen content is essential; relatively rich mixtures are much safer than lean ones (bitumen slightly in excess of the void content of the mineral aggregate improves low temperature performance without impairing stability at high temperatures);

(5) Mineral filler in excess of the optimum for a given binder and coarse aggregate should not be used; and,

(6) The ductility of the binder at the lower temperatures appears to be an important characteristic. The test for ductility probably should be made at the standard rate of 5 cm per min, and a temperature of 4° or 5° C is about as low as may be used.

(7) At least in so far as resistance to shear is concerned, Portland cement concrete and bituminous concrete are not similar structures due to the fact that their cementing mediums are of decidedly different character.

AMERICAN SOCIETY OF CIVIL ENGINEERS

Founded November 5, 1852

PAPERS

FAILURE THEORIES OF MATERIALS SUBJECTED TO COMBINED STRESSES

By Joseph Marin,[1] Jun. Am. Soc. C. E.

Synopsis

Several theories have been devised and tests made to determine the laws of failure of materials subjected to combined stresses. The main purpose of this paper is to extend the correlation of such theories and test results, representing them by a common set of co-ordinate axes. Without such a correlation, some test results on combined stresses have been interpreted incorrectly. In addition, some new theories are given. The graphical representation used is that of Mr. B. P. Haigh[2] and H. M. Westergaard,[3] M. Am. Soc. C. E.

Notation.—The symbols in this paper are summarized in the Appendix. An effort has been made to conform essentially with "Symbols for Mechanics, Structural Engineering, and Testing Materials,"[4] compiled by a Committee of the American Standards Association, with Society representation, and approved by the Association in 1932.

Theories of Failure

The theories represented will be limited, for the present, to bi-axial stresses, isotropic materials, and gradually applied loads. The assumptions, limitations, and inconsistencies in each particular theory have been treated. The term, "failure," is subject to a variety of definitions. It implies a limiting value of change in shape, stress, sliding, energy, or a combination of these factors, a point of failure being determined experimentally by a stress-strain curve.

Classification.—An element in a stressed member can be conceived as failing when a stress, deformation, sliding, or a combination of these three fac-

Note.—Discussion on this paper will be closed in November, 1935, *Proceedings*.

[1] Ann Arbor, Mich.

[2] "The Strain-Energy Function and the Elastic Limit," by B. P. Haigh, British Assoc. for the Advancement of Science, 1919.

[3] "The Resistance of Ductile Materials to Combined Stresses in Two or Three Directions Perpendicular to One Another," by H. M. Westergaard, M. Am. Soc. C. E., *Journal*, Franklin Inst., May, 1920.

[4] A.S.A.—*Z10a*—1932.

tors, reaches a limiting value. Based on these physical concepts, theories of failure are classified, as follows:

(*a*) General Stress Theories.—

(1) Maximum Stress Theory (Rankine).
(2) Maximum Normal-Stress Theory.
(3) Maximum Stress-Normal Stress Theory.

(*b*) Deformation Theories.—

(4) Maximum Strain Theory (St. Venant).
(5) Maximum Distortion Theory.
(6) Maximum Strain-Distortion Theory.

(*c*) Shear Stress Theories.—

(7) Maximum Shear Theory (Coulomb and Guest).
(8) Internal Friction Theory (Special Cases of Coulomb's Theory).
(9) General Shear Theory (Special Cases of Mohr's Theory).

(*d*) Energy Theories.—

(10) Maximum Strain-Energy Theory (Beltrami and Haigh).
(11) Maximum Shear Strain-Energy Theory (von Mises, Hencky, and Huber).
(12) Maximum Strain-Shear Strain-Energy Theory.
(13) Maximum Volume-Energy Theory.

(*e*) Miscellaneous Theories.—

(14) Wehage's Theory.
(15) Maximum Change-in-Volume Theory.
(16) Maximum Shear-Strain Theory (Becker).

It is possible that combinations of the aforementioned theories, depending on the signs of the principal stress, may be the true ones. Another approach to the problem is to consider the material as non-isotropic. Such a procedure has been followed by Brandtzaeg.[5]

For simplicity, the theories will be represented for the case of bi-axial stresses. In most cases they are easily extended to the case of tri-axial stress. In such cases, instead of a graphical representation in one plane, the theory is represented by a surface symmetrical about three planes at right angles. For brevity, the assumptions and limitations involved will be omitted.

Let s_1 and s_2 be the principal stresses at failure in a material subjected to bi-axial stress; s_t, the stress at failure in simple tension; and s_c, the stress at failure in simple compression. The theories are represented graphically by diagrams with co-ordinates, x and y, in which $+x = \frac{s_1}{s_t}$ and $+y = \frac{s_2}{s_t}$. The remaining quadrants are explained by the illustrations.

[5] "Failure of Materials Composed of Non-Isotropic Elements," by A. Brandtzaeg, Assoc. M. Am. Soc. C. E., Det Klg Norske Videnskabers, *Selskake Skrifter*, 1927, No. 2, Trondhjem, Norway.

General Stress Theories

(1) *Maximum Stress Theory* (*Rankine*).—In Rankine's maximum stress theory, failure is defined as the condition of a material when one of the principal stresses equals the stress, at failure, in simple tension or compression. In other words, failure has occurred when $s_1 = s_t$; $s_2 = s_t$; $s_1 = s_c$; or, $s_2 = s_c$. Referring to Fig. 1, for the case, $s_c = s_t$, a material is defined as having failed when: $x = +1$; $y = +1$; $x = -\frac{s_c}{s_t}$; or $y = -\frac{s_c}{s_t}$. A more complete treatment of Theory (1) (and of Theories (4), (7), and (10), to follow), has been written by Professor S. Timoshenko.[6]

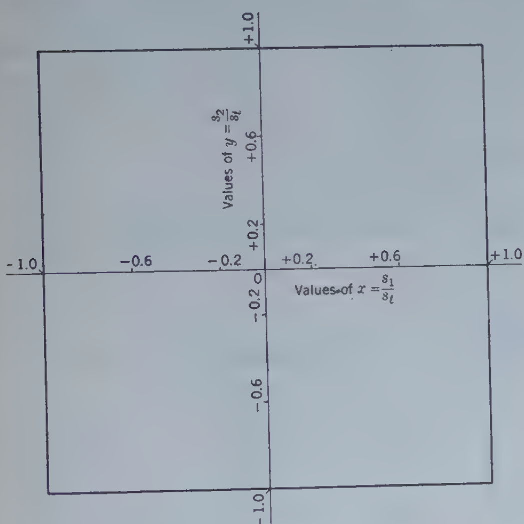

Fig. 1.—Rankine's Maximum Stress Theory.

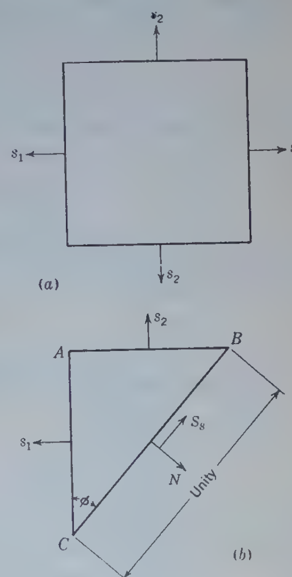

Fig. 2.

(2) *Maximum Normal-Stress Theory.*—Experimental evidence shows that materials do not fracture in a direction perpendicular to the greatest principal stress as required by the maximum stress theory. Consider the fracture to occur at right angles to some intermediate direction, and that the material in question has failed because the normal stress on this plane has reached a limiting value. Furthermore, let this limiting stress be composed of two parts: A normal component, N, of the principal stresses; and a normal component due to internal friction. Assuming the normal component due to friction to be proportional to the shearing stress, s_8, its value is $s_8 f$, in which f equals a coefficient of internal friction. Fig. 2 represents the forces, s_8 and N, acting on the plane of fracture, BC. Hence, the limiting normal stress, s, is:

$$s = N + s_8 f \quad \text{.........................(1)}$$

[6] "Strength of Materials," by S. Timoshenko, Pt. II.

Substituting values of N and s_s in terms of the stresses, s_1 and s_2, and differentiating s with respect to ϕ, $\tan 2\phi = -f$ gives the condition for the maximum value of s. With $\tan 2\phi = -f$, the maximum or limiting value of s is expressed by:

$$s = \frac{s_1 + s_2}{2} + \frac{s_1 - s_2}{2} \sqrt{1 + f^2} \quad \text{(2)}$$

For the case of simple tension: $s_2 = 0$; $s_1 = s_t$; and,

$$s = \frac{s_t}{2}\left(1 + \sqrt{1 + f^2}\right) \quad \text{(3)}$$

Combining Equations (2) and (3):

$$s_1 + \frac{s_2\left(1 - \sqrt{1 + f^2}\right)}{1 + \sqrt{1 + f^2}} = s_t \quad \text{(4)}$$

or, when s_1 and s_2 are positive, and $s_1 > s_2$:

$$x + \frac{y\left(1 - \sqrt{1 + f^2}\right)}{1 + \sqrt{1 + f^2}} = 1 \quad \text{(5)}$$

Fig. 3 represents Equation (5) for values of f = 0.0, 0.3, and 1.0, in the four quadrants.

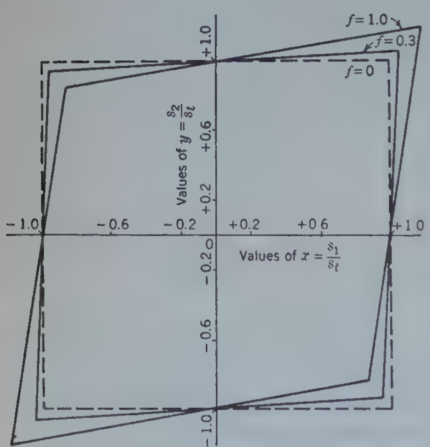

FIG. 3.—MAXIMUM NORMAL STRESS THEORY.

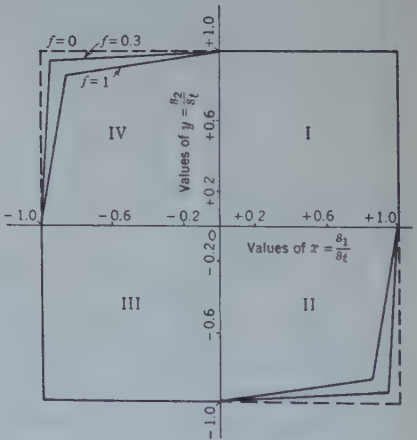

FIG. 4.—MAXIMUM STRESS-NORMAL STRESS THEORY.

(*3*) *Maximum Stress-Normal Stress Theory.*—Consider that the limiting stress is governed by either general stress or normal stress theories, depending on the signs of the principal stresses. Then, the limiting equations are:

For $x = \pm 1$,

$$x + \frac{y\left(1 - \sqrt{1 + f^2}\right)}{1 + \sqrt{1 + f^2}} = 1 \quad \text{(6a)}$$

and, for $y = \pm 1$,

$$y + \frac{x\,(1 - \sqrt{1 + f^2})}{1 + \sqrt{1 + f^2}} = 1 \quad\text{.................}(6b)$$

Fig. 4 represents Equations (6) for values of $f = 0$, 0.3, and 1.0, and for $s_c = s_t$, in Quadrants II and IV.

Deformation Theories

(4) *Maximum Strain Theory (St. Venant).*—In the maximum strain theory failure is assumed to occur when the elongation or contraction in the direction of one principal stress reaches a limiting value equal to the deformation at failure in simple tension. Expressed algebraically, this is equivalent to stating that failure occurs when:

$$x - \sigma y = \pm 1 \quad\text{........................}(7a)$$

or,

$$y - \sigma x = \pm 1 \quad\text{........................}(7b)$$

in which σ = Poisson's ratio. Fig. 5 represents Equations (7) for $s_c = s_t$ and $\sigma = 0.25$ and 0.35.

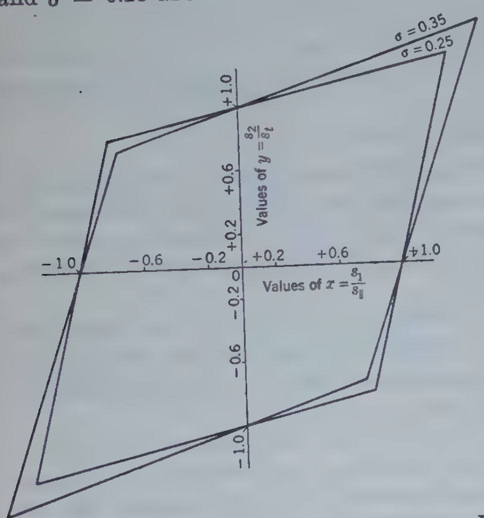

FIG. 5.—ST. VENANT'S MAXIMUM STRAIN THEORY.

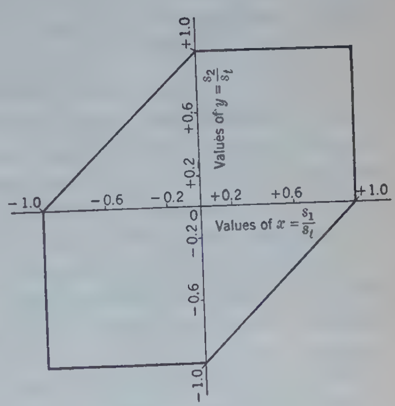

FIG. 6.—MAXIMUM DISTORTION THEORY.

(5) *Maximum Distortion Theory.*—A distortion theory is based on the assumption that a limiting angular deformation or shear distortion is the factor that produces failure. By equating the angular distortion in the case of bi-axial stresses to that for the case of simple tension, the following limiting equations are obtained: $x = \pm 1$; $x - y = \pm 1$; $y = \pm 1$; or $y - x = \pm 1$ (see Fig. 6). As might be expected, this theory reduces to the maximum shear theory (Theory (7)), the discussion of which follows.

(6) *Maximum Strain-Distortion Theory.*—Consider failure as being governed by a limiting elongation, contraction, or angular distortion, equal to the values in simple tension, but depending on the signs of s_1 and s_2. Then the equations defining failure are (see Fig. 7): $x - \sigma y = \pm 1$; $x - y = \pm 1$; $y - \sigma x = \pm 1$; or, $y - x = \pm 1$.

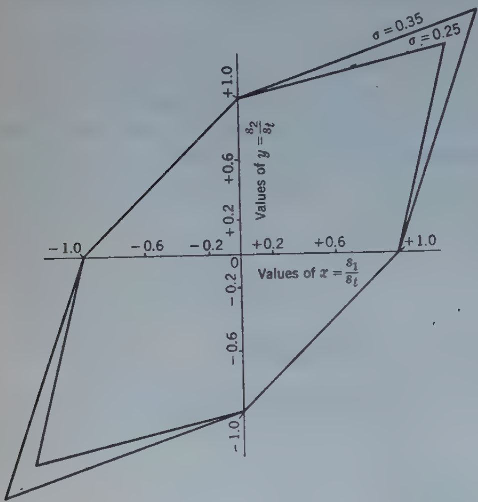

FIG. 7.—MAXIMUM STRAIN-DISTORTION THEORY.

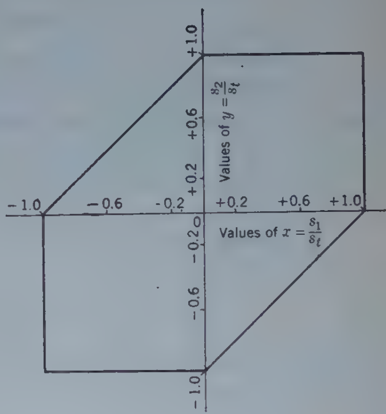

FIG. 8.—COULOMB AND GUEST'S MAXIMUM SHEAR THEORY.

SHEAR STRESS THEORIES

Shear theories are based on the assumption that failure results along some plane as a result of shear stress on the plane having reached a value equal to the limiting value of the shear stress in simple tension. Several theories are rooted in this concept, by defining the direction of the plane of the limiting shear or the value of the shear stress.

(7) *Maximum Shear Theory (Coulomb and Guest).*—In this theory, the plane of sliding or limiting shear is considered to be the plane of theoretical maximum shear, and may be expressed algebraically as follows (see Fig. 8): $x = \pm 1$; $y = \pm 1$; $x - y = \pm 1$; or, $y - x = \pm 1$.

(8) *Internal Friction Theory (Special Cases of Coulomb's Theory).*—Assume the plane of failure or sliding to be at an angle different from that of the theoretical maximum shear. For example, in Fig. 2, consider that the resistance to sliding, or the limiting stress, s_L, on the limiting plane, *BC*, is equal to the sum of a shearing stress, s_S, which is due to s_1 and s_2, and a frictional force proportional to the normal stress, *N*, equal to fN. Then:

$$s_L = s_S + fN \qquad (8)$$

Coulomb showed that, by substituting values of s_1 and s_2 for s_L and N:

For $s_1 \neq s_2$,

$$s_S = \frac{1}{2 \cos \alpha} [s_1 - s_2 + (s_1 + s_2) \sin \alpha] \qquad (9)$$

and, for $s_1 = s_2 = s_T$,

$$s_s = \frac{s_T}{\cos \alpha} \quad \text{(10)}$$

in which $\alpha = \tan^{-1} f$; and s_T = shear stress in torsion.

Special cases of this theory can be obtained and represented by the co-ordinates used for Theories (1) to (7). Thus, consider,

$$s_T = 0.6\ s_t \quad \text{(11)}$$

Such a value is representative for several steels. From Equation (9):

$$s_1 - s_2 + (s_1 + s_2) \sin \alpha = 2\, s_T \quad \text{(12)}$$

From Equations (11) and (12):

$$s_1 - s_2 + (s_1 + s_2) \sin \alpha = 1.2\ s_t \quad \text{(13)}$$

When $s_2 = 0$, $s_1 = s_t$ and from Equation (13) $\sin \alpha = 0.2$, or $\alpha = 11°\ 30'$. Substituting this value of α in Equation (13) (and, when s_1 is positive, s_2 is negative, and when $s_1 > s_2$.), $s_1 - 0.67\ s_2 = s_t$, or $x - 0.67\ y = 1$.

When s_1 and s_2 are both positive, $x = +1$ and $y = +1$. Considering all quadrants the theory requires that, for failure: $x = +1$; $y = +1$; $x - 0.67y = 1$; or, $y - 0.67x = 1$. Fig. 9 represents this special case of Coulomb's theory for $s_T = 0.6\ s_t$.

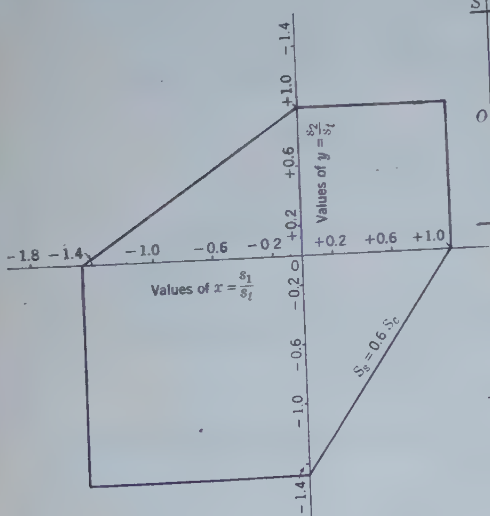

FIG. 9.—INTERNAL FRICTION THEORY, SPECIAL CASES OF COULOMB'S THEORY.

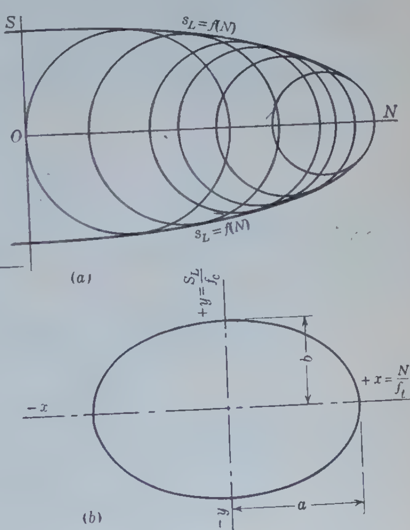

FIG. 10.

(9) *General Shear Theory (Special Cases of Mohr's Theory).*—Assuming that the plane of limiting shear or sliding is dependent in direction on the

relative values of the combined stresses, Mohr stated a general shear theory. It is assumed that the limiting stress, s_L, is equal to a constant stress plus a frictional stress produced by the normal stress, N, on the plane of sliding. The value of s_L is thus a function of N, or,

$$s_L = f(N) \quad \text{.........................} (14)$$

Referring to Fig. 2, in which ϕ defines the direction of sliding, by statics:

$$N = \frac{s_1 + s_2}{2} \times \frac{s_1 - s_2}{2} \cos 2\,\phi \quad \text{..............} (15)$$

and,

$$s_L = \frac{s_1 - s_2}{2} \sin 2\,\phi \quad \text{....................} (16)$$

Mohr represents the values of s_1 and s_2 graphically as shown in Fig. 10(*a*) for different values of s_1 and s_2 as represented by a series of circles. The lines drawn tangent to the circles represent Equation (14) and the co-ordinates of the points of tangency are given by Equations (15) and (16). The envelopes to the circle, therefore, represent the limiting values of N and s_L that define failure.

An empirical correlation between Mohr's theory and other theories is desirable. For this purpose, test results of several experimenters were plotted on the co-ordinate axes as indicated in Fig. 10(*a*), and the average envelopes to the circles were drawn. It was found that the experimental data could best be expressed by the equation of an ellipse. Actual values are given subsequently in Equations (21). Fig. 10(*b*) represents the relation between N and s_L—the envelope to the circles shown in Fig. 10(*a*). Then $N^2 + \frac{a^2}{b^2} s^2_L = a^2\, s^2_t$; or,

$$\frac{x^2}{a^2} + \frac{y^2}{b^2} = 1 \quad \text{......................} (17)$$

in which, $x = \frac{N}{s_t}$; and $y = \frac{s_L}{s_t}$. Substituting Equations (15) and (16) in Equation (17):

$$(y + x)^2 + (y - x)^2 \cos^2 2\,\phi - 2\,(y^2 - x^2) \cos 2\,\phi$$
$$+ \frac{a^2}{b^2} (y - x)^2 \sin^2 2\,\phi = 4\,a^2 \quad \text{.................} (18)$$

For Equation (18) to be consistent for simple tension, let $x = 1$ and $y = 0$. Therefore,

$$1 + \cos^2 2\,\phi + 2 \cos 2\,\phi + \frac{a^2}{b^2} \sin^2 2\,\phi - 4\,a^2 = 0 \quad \text{.......} (19)$$

Assuming $\phi = 45°$ for the case of simple tension, Equation (19) becomes:

$$b^2 = \frac{a^2}{4\,a^2 - 1} \quad \text{......................} (20)$$

From the plotted experimental data and for average limiting values of the envelopes, the values of a and b, consistent with Equation (20) and the test data, are: For $a = 1.30$, $b = 0.54$; and, for $a = 1.00$, $b = 0.58$. Substituting these values in Equation (17):

For $a = 1.30$,

$$N^2 + 5.80\, s^2_L = 1.69\, s^2_t \quad \text{(21a)}$$

and for $a = 1.00$,

$$N^2 + 3.02\, s^2_L = s^2_s \quad \text{(21b)}$$

Substituting the values of N and s_L from Equations (15) and (16) in Equation (12) and assuming that $\phi = 45°$:

For $a = 1.0$,

$$y^2 - x\,y + x^2 - 1 = 0 \quad \text{(22a)}$$

and, for $a = 1.3$,

$$y^2 - 1.41\,x\,y + x^2 - 1 = 0 \quad \text{(22b)}$$

Fig. 11 represents Equations (22) for values of $a = 1.00$ and $a = 1.30$.

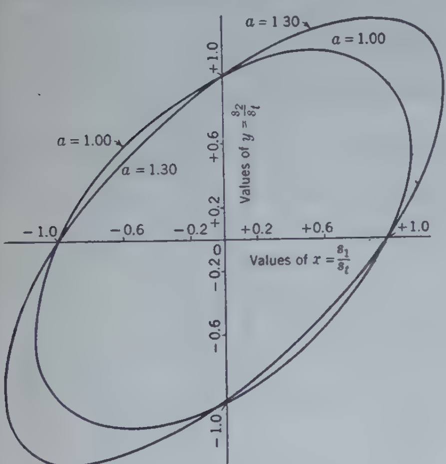

FIG. 11.—GENERAL SHEAR THEORY: SPECIAL CASES OF MOHR'S THEORY.

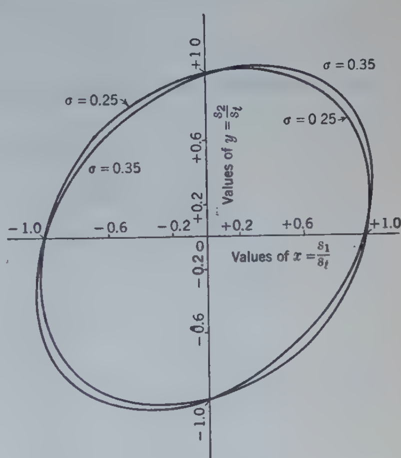

FIG. 12.—MAXIMUM STRAIN-ENERGY THEORY: BELTRAMI AND HAIGH.

ENERGY THEORIES

(10) *Maximum Strain-Energy Theory (Beltrami and Haigh)*.—This theory is based on the assumption that the strain energy at failure for combined stresses equals the value of the energy at failure in the case of simple tension. In other words, failure occurs when,

$$x^2 + y^2 - 2\,\sigma\,x\,y = 1 \quad \text{(23)}$$

Fig. 12 shows Equation (23) for $\sigma = 0.25$ and 0.35.

(11) *Maximum Shear Strain-Energy Theory (von Mises, Hencky, and Huber).*—Assuming that the energy due to shear distortion at failure for combined stress equals the value of shear energy of distortion for simple tension, the theory of von Mises, Hencky, and Huber reduces to $x^2 - x y + y^2 = 1$. This was obtained by subtracting from the total strain energy the energy due to change in volume, which yielded the resulting energy due to change in shape. An independent and shorter derivation follows.

Let ξ = energy of distortion on an element subjected to the principal stresses, s_1 and s_2; then:

$$\xi = \frac{s_s \gamma}{2} = \frac{s_s^2}{2\,E_s} \qquad (24)$$

in which, s_s = shearing stress; γ = angular distortion, and E_s = modulus of elasticity in shear.

For the case of the combined stresses, s_1 and s_2:

$$\xi = \frac{s_1^2}{2\,E_s} - \frac{(s_1 - s_2)^2}{8\,E_s} + \frac{s_1^2}{8\,E_s} + \frac{s_2^2}{8\,E_s} = \frac{1}{4\,E_s}\left(s_1^2 - s_1 s_2 + s_2^2\right) \qquad (25)$$

For simple tension or compression:

$$\xi = \frac{s_t^2}{4\,E_s} \qquad (26)$$

From Equations (25) and (26), $s_1^2 - s_1 s_2 + s_2^2 = s_t^2$; or,

$$x^2 - x y + y^2 = 1 \qquad (27)$$

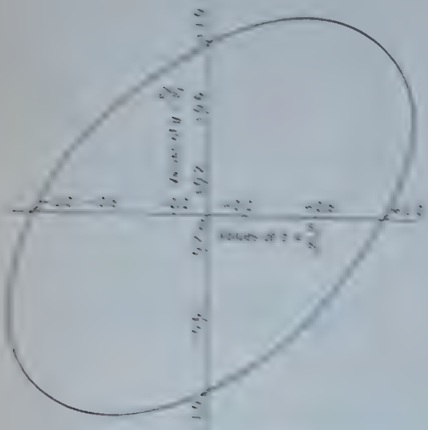

FIG. 13.—MAXIMUM SHEAR STRAIN THEORY (VON MISES, HENCKY, AND HUBER).

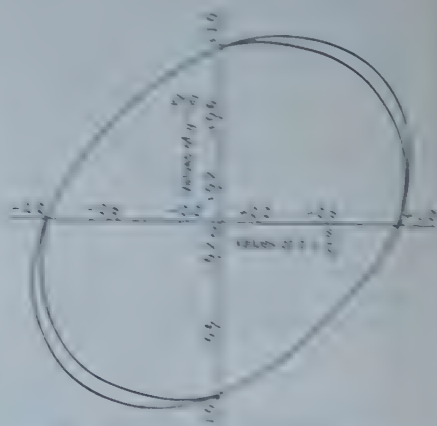

FIG. 14.—MAXIMUM STRAIN-SHEAR STRAIN ENERGY THEORY.

Equation (27) (see Fig. 13) is identical with the special case of Mohr's theory for $a = 1.0$. Theory (11) and other theories have been written by A. Nadai.[7]

[7] "Plasticity," by A. Nadai, 1931.

(12) *Maximum Strain-Shear Strain-Energy Theory.*—Consider that the energy due to either the normal strains or the angular distortions are the limiting factors. The equations defining failure are then expressed as:

$$x^2 + y^2 - 2\,\sigma\,x\,y = 1 \qquad (28a)$$

or,

$$x^2 - x\,y + y^2 = 1 \qquad (28b)$$

The equation which defines failure in Equations (28) depends on the value of σ. Equations (28) are represented in Fig. 14 for $\sigma = 0.25$ and $\sigma = 0.35$.

(13) *Maximum Volume-Energy Theory.*—Let the energy to produce change in volume be the limiting factor. In addition, let the volume energy at failure for simple tension equal the volume energy at failure for combined stress. The energy required to change the volume of an element subjected to the principal stresses, s_1 and s_2, is:

$$\xi = \frac{1}{2}\left(\frac{s_1 + s_2}{3}\right)(\epsilon_1 + \epsilon_2 + \epsilon_3) \qquad (29)$$

in which, ϵ_1, ϵ_2, and ϵ_3 are the principal strains and $\epsilon_1 + \epsilon_2 + \epsilon_3$ = change in volume. Substituting for stresses in terms of strains in Equation (29):

$$\xi = \frac{1}{6\,E}\,(s_1 + s_2)^2\,(1 - 2\sigma) \qquad (30)$$

in which E = Young's modulus. For simple tension: $s_1 = s_t$; $s_2 = 0$; and,

$$\xi = \frac{1}{6\,E}\,(s^2_t)\,(1 - 2\sigma) \qquad (31)$$

From Equations (30) and (31), $s_1 + s_2 = s_t$; and, therefore;

$$x + y = \pm 1 \qquad (32a)$$

and,

$$x - y = \pm 1 \qquad (32b)$$

Equations (32), for $s_c = s_t$, are plotted in Fig. 15.

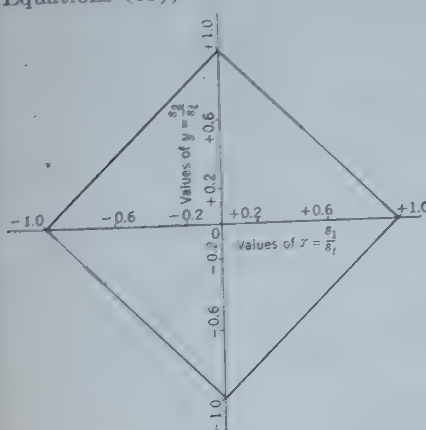

FIG. 15.—MAXIMUM VOLUME ENERGY THEORY.

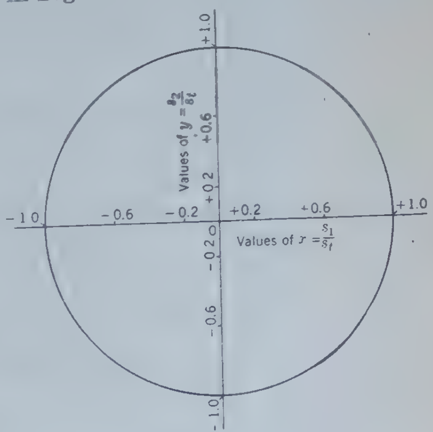

FIG. 16.—WEHAGE'S THEORY.

Miscellaneous Theories

(*14*) *Wehage's Theory.*—This theory is empirical and is based on experiments made with pieces of paper submitted to tension in two directions at right angles. Algebraically, the theory reduces to:

$$x^2 + \frac{a^2\, y^2}{b^2} = 1 \quad \text{.......................(33)}$$

in which a and b are the "yield" point stresses in the two directions. For $a = b$, the theory becomes:

$$x^2 + y^2 = 1 \quad \text{.......................(34)}$$

Equation (34) is represented in Fig. 16 for $a = b$.

(*15*) *Maximum Change in Volume Theory.*—Consider that the volume change is the limiting factor and that the change in volume to the point of failure in simple tension is equal to the change in volume for combined stresses. Let the change in volume $= \Delta V$. For the case of an element subjected to the principal stresses, s_1 and s_2:

When s_1 and s_2 are both positive:

$$\Delta V = \epsilon_1 + \epsilon_2 + \epsilon_3 = \frac{1}{E}(1 - 2\sigma)(s_1 + s_2) \quad \text{.........(35)}$$

When s_1 and s_2 are both negative:

$$\Delta V = -\frac{1}{E}(1 - 2\sigma)(s_1 + s_2) \quad \text{...................(36)}$$

When s_1 is positive, s_2 is negative, and $s_1 > s_2$:

$$\Delta V = \frac{1}{E}(1 - 2\sigma)(s_1 - s_2) \quad \text{................(37)}$$

When s_1 is negative, s_2 is positive, and $s_2 > s_1$:

$$\Delta V = \frac{1}{E}(1 - 2\sigma)(s_2 - s_1) \quad \text{...............(38)}$$

When (in the case of simple tension), $s_1 = s_t$, and $s_2 = 0$:

$$\Delta V = \frac{1}{E}(1 - 2\sigma)\, s_t \quad \text{...................(39)}$$

and, when (in the case of simple compression), $s_1 = s_c$, and $s_2 = 0$:

$$\Delta V = \frac{1}{E}(1 - 2\sigma)\, s_c \quad \text{...................(40)}$$

Equating the formulas, (35) to (38), inclusive, to Equation (39), and letting $s_c = s_t$, the following equations are obtained, defining failure as a limiting volume change; thus:

For $s_c = s_t$,

$$x + y = \pm 1 \quad \text{.......................(41a)}$$

and,

$$x - y = \pm 1 \quad \text{(41b)}$$

and, for $s_c \neq s_t$,

$$x + y = \frac{s_c}{s_t} \quad \text{(42a)}$$

and,

$$x - y = \frac{s_c}{s_t} \quad \text{(42b)}$$

Equations (41) and (42) are represented in Fig. 17.

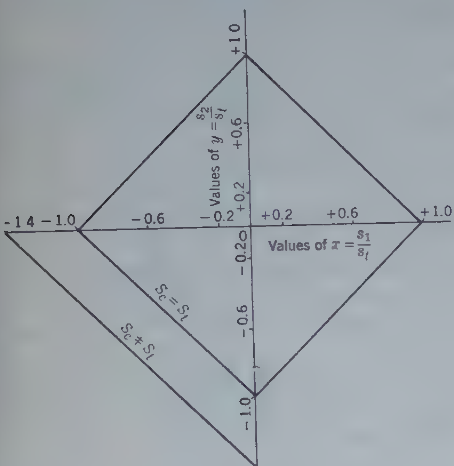

FIG. 17.—MAXIMUM CHANGE IN VOLUME THEORY.

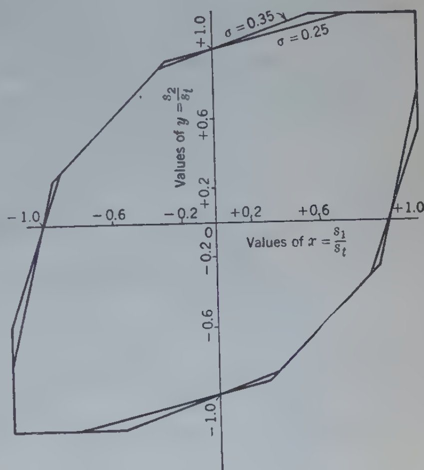

FIG. 18.—BECKER'S MAXIMUM SHEAR-STRAIN THEORY.

(16) *Maximum Shear-Strain Theory (Becker's Theory)*.—Consider that the limiting condition for failure is either a maximum strain or a maximum shear. Then from the formulas of Theory (4) Equations (7), and Theory (7), the conditions defining failure are: $x - \sigma y = \pm 1$; $x - y = 1$; $x = \pm 1$; $y - \sigma x = \pm 1$; $y - x = 1$; and $y = \pm 1$.

Becker introduces an experimental constant in the foregoing equations by assuming that $\frac{s_s}{s_t} = 0.6$ instead of 0.5. Using this value the corresponding formulas become: $x - \sigma y = \pm 1$; $x = \pm 1.2$; $x - y = + 1.2$; $y - \sigma x = \pm 1$; $y = \pm 1.2$; and $y - x = 1.2$. These formulas, for values of $\sigma = 0.25$ and 0.35, are shown graphically in Fig. 18. A number of theories of this type can obviously be obtained by the superposition of others, as seen from Fig. 19.

COMPARISON OF THEORIES

The differences in the dimensions of machine and structural members as a result of designing by the various theories are of interest, if not of importance. The importance is evidently reduced because of the indeterminate factors

involved in the selection of a working stress. The theories are compared graphically in Fig. 19 for the values of the mechanical properties given. From this graphical representation, a numerical comparison can be obtained between the limiting stresses as required by the various theories and the resulting differences in design.

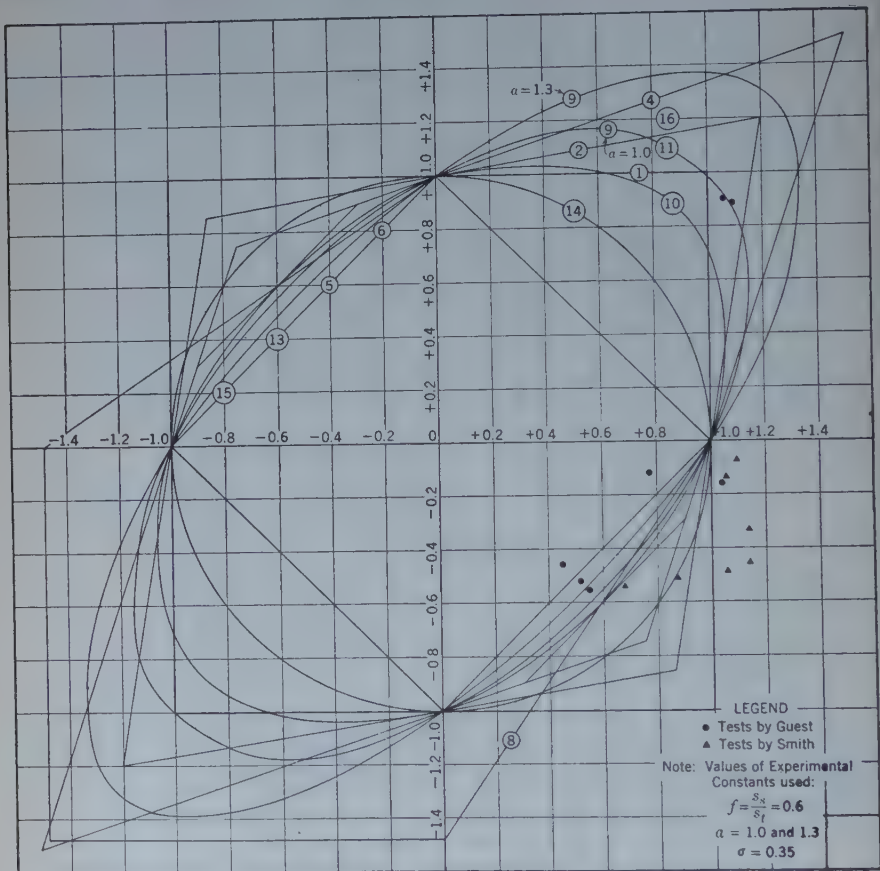

FIG. 19.—COMPARISON OF MEASURED AND THEORETICAL STRENGTH FOR BRASS TUBES.

COMPARISON OF THEORIES AND TESTS

Numerous tests were conducted on specimens of cast iron, steel, copper, and brass, to study the relation between the measured and the theoretical strengths in each case. The specimens were subjected to combined stresses and the results plotted with the corresponding theoretical curve in the manner demonstrated in Fig. 19 for brass tubes. The numerical comparison given in Table 1 is obtained from these plotted results. The percentage values for the discrepancies between the test results and all the theories are approximate. These values for the percentage difference between theoretical and actual

TABLE 1.—Tests to Study Combined Stress

Stress ratio, $\frac{x}{y}$ (1)	Type of specimen (2)	Method of loading (3)	Criterion of failure (4)	Number of tests (5)	Average Percentage Difference Between Tests and Theories: Maximum (6)	Average Percentage Difference Between Tests and Theories: Minimum (7)	Theories that were most consistent with tests (8)
		(a) Combined Tension and Tension in Steel					
>1.0	Tube	Axial tension with torsion and axial tension with pressure	Initial yield point	25	37	4	(1) and (10)
		Axial tension with internal pressure	Elastic limit	3	20	6	(11) and (1)
		Axial tension with internal pressure	Johnson's yield point	7	30	0	(4) and (16)
<1.0	Tube	Tension and torsion and tension and pressure	Initial yield point	12	24	0	(1) and (10)
		(b) Combined Tension and Compression in Steel					
>1.0	Tube	Tension and torsion and tension and pressure	Initial yield point	22	11	3	(11) and (8)
		Tension with torsion and compression with torsion	Proportional limit	14	27	2	(8), (4), and (9)
		Tension with torsion and compression with torsion	Yield point	19	26	1	(7) and (9)
		Bending and torsion	Intersection of elasticity and flow	7	40	9	(7) and (9)
		Tension with internal pressure	Elastic limit	4	37	4	(7)
		Internal pressure	Yield point	21	24	2	(10), (2), and (9)
		Axial tension with internal pressure	Johnson's yield point	4	16	0	(16) and (10)
<1.0	Tube	Tension with torsion and tension with pressure	Initial yield point	1	26	4	(2) and (10)
		Tension with torsion and compression with torsion	Yield point	2	44	1	(4) and (9)
		Tension with internal pressure	Elastic limit	5	29	2	(2) and (9)
=1.0	Tube	Tension with torsion and tension with pressure	Initial yield point	11	55	1	(9)
		Compression with torsion	Proportional limit	3	44	0	(2) and (16)
		Bending with torsion	Intersection of elasticity and flow	2	63	9	(8)
		Tension with internal pressure	Elastic limit	10	44	0	(16) and (8)
		Axial tension with internal pressure	Elastic limit	12	46	0	(9)
		Torsion	"Primitive" elastic limit	3	37	2	(10)
>1.0	Solid rods	Tension with torsion	Initial yield point	2	21	1	(2) and (9)
		Tension with torsion	Proportional limit	14	25	4	(1)
		Tension with torsion and compression with torsion	Yield point	9	26	1	(2), (8), and (10)
		Bending with torsion	Intersection of elasticity and flow	16	20	2	(4), (9), and (2)
<1.0	Solid rods	Tension with torsion and compression and torsion	Yield point	3	32	2	(9), (2) and (8)
		(c) Combined Tension and Compression in Cast Iron					
>1.0	Tube	Internal pressure	Yield point	8	38	2	(1)
<1.0	Solid rods	Bending with torsion	Rupture point	12	12	1	(4)
		Bending with torsion	Rupture point	16	13	1	(4)
		Bending with torsion	Rupture point	21	12	3	(4)
		Bending with torsion	Rupture point	23	14	1	(4)
		(d) Combined Tension and Tension in Copper					
>1.0	Tube	Tension with torsion, tension with pressure, and torsion with pressure	Initial yield point	3	14	1	(9) and (16)
<1.0	Tube	Tension with torsion, tension with pressure, and torsion with pressure	Initial yield point	2	21	5	(9) and (1)

TABLE 1.—(*Continued*).

Stress ratio, $\frac{x}{y}$ (1)	Type of specimen (2)	Method of loading (3)	Criterion of failure (4)	Number of tests (5)	Average Percentage Difference Between Tests and Theories: Maximum (6)	Minimum (7)	Theories that were most consistent with tests (8)
(e) Combined Tension and Compression in Copper							
>1.0	Tube.....	Bending with torsion..........	Intersection of elasticity and flow..	8	27	8	(4) and (9)
		Tension with torsion and tension with pressure.............	Initial yield point.	3	21	0	(9) and (4)
(f) Combined Tension and Tension in Brass							
>1.0	Tube.....	Tension with torsion, tension with pressure, and torsion with pressure....................	Initial yield point..	2	22	2	(9)
(g) Combined Tension and Compression in Brass							
>1.0	Tube.....	Tension with torsion..........	Yield point.......	7	24	2	(1) and (2)
		Tension with torsion, and tension with pressure..........	Initial yield point..	5	37	0	(9) and (4)

stresses were obtained by arithmetical averages. The values in Column (8), Table 1, are based on these results.

A study of the test data and test procedure shows that in some cases the discrepancies between theories and tests may be due to inaccurate test data. Computations were made showing that the errors in the stresses, due to errors in measurement or errors in the values of experimental constants used, may be appreciable. Another source of error is in the computation of the stresses, s_1 and s_2, from the applied loads and the dimensions of the member.

Conclusion

The foregoing comparison shows that no one theory now in use agrees exactly with test results. The precisely correct theory of failure is probably a combination of a number of these theories, depending upon the ratio, $\frac{s_1}{s_2}$. Fig. 19 indicates a number of such cases. Furthermore, there may be several theories equally well supported for one material and the correct theories may vary with the material. Obviously, an ultimate solution will depend on the results of further study in this field.

Acknowledgment

This paper is based in part on a research[8] sponsored by the Engineering Experiment Station, University of Illinois, and the Chicago Bridge and Iron Works. The study was made under the direction of Wilbur M. Wilson, M. Am. Soc. C. E.

[8] Presented as a thesis to the University of Illinois in 1930 in partial fulfillment of the requirements for the degree of Master of Science in Enginering.

APPENDIX

NOTATION

The following symbols, adopted for use in this paper, are offered as a guide to discussers:

a = major axis of an ellipse; also, a = major yield point stress.
b = breadth; minor axis of an ellipse; also, b = minor yield point stress.
c = a subscript denoting "compression."
f = coefficient of internal friction.
s = unit stress in general; s_L = limiting normal stress; s_1 and s_2 = principal stresses at failure; s_t = stress at failure in simple tension; s_c = stress at failure in simple compression; s_s = unit shearing stress; and s_T = shear stress in torsion.
t = a subscript denoting "simple tension."
x = variable distances measured parallel to the X-axis.
y = deflection; variable distances measured parallel to the Y-axis.
E = modulus of elasticity; Young's modulus; E_s = modulus of elasticity in shear.
L = length; as a subscript, L, denotes "limiting."
M = moment of force.
N = normal component of principal unit stress.
T = a subscript denoting "shearing torsion."
V = volume; ΔV = change in volume.
α = $\tan^{-1} f$.
Δ = "change in."
ξ = energy of distortion on an element subjected to the principal stresses, s_1 and s_2.
σ = Poisson's ratio.
ϕ = angle between planes of stress.

AMERICAN SOCIETY OF CIVIL ENGINEERS

Founded November 5, 1852

DISCUSSIONS

EFFECT OF SECONDARY STRESSES UPON ULTIMATE STRENGTH

Discussion

BY MESSRS. LAMOTTE GROVER, AND A. A. EREMIN

LAMOTTE GROVER,[32] ASSOC. M. AM. SOC. C. E. (by letter).[32a]—The practical application of the results of secondary stress analysis to the design of bridge members is discussed in this paper. This subject is most timely in view of the recent tendency toward the use of more comprehensive design methods in order to effect the most favorable distribution of material.

The increased demand for comparatively shallow deck truss construction resulting from higher standards in grade and alignment for both highway and railway structures, together with the trend away from movable spans to the use of fixed spans which require shallow deck construction in many cases, results in types of design in which the effect of secondary stresses is quite appreciable.

With the rapidly increasing use of structural welding, advantage is being taken of the better economy and reliability thus afforded for making rigid joints in which behavior can be predicted with more certainty. The effect of large gusset-plates upon the stiffness and stress distribution in members is a feature that can not be evaluated closely. These large gusset-plates are either reduced in size or eliminated entirely in properly designed welded connections, thereby reducing some of the annoying uncertainties that exist with riveted construction. Such developments challenge the designer to keep in pace by devoting more attention to such refinements as statically indeterminate stress analysis and the investigation of secondary stresses, and they also make it possible for the interpretation of such analysis to be evaluated more accurately and, therefore, better justified.

NOTE.—The paper by John I. Parcel, M. Am. Soc. C. E., and Eldred B. Murer, Jun. Am. Soc. C. E. was published in November, 1934, *Proceedings*. Discussion on this paper has appeared in *Proceedings*, as follows: January, 1935, by Messrs. C. H. Sandberg and J. D. Gedo; and March, 1935, by Messrs. L. E. Grinter, L. T. Evans, and F. E. Fahy.

[32] Bridge Engr., Dept. of Design, State Highway Comm., Topeka, Kans.

[32a] Received by the Secretary March 9, 1935.

Certain other problems of the structural engineer, such as residual stresses caused either by rolling steel shapes or by welding, are inherently self-limiting and these stresses will be better understood as a result of the studies described in this paper. One of the ways in which structural welding will have an influence upon behavior under secondary stress is that welded cover-plates will be virtually fixed along their edges. This will contribute further toward minimizing the tendency for relatively thin plates to fail locally by buckling. Several limitations of the study have been acknowledged by the authors and these might be extended to include a number of others that would indicate the need for further and broader studies in this field.

Further experiments should be made to determine the effect of heavy gusset-plates and the stress concentrations that they cause at the ends of members in double curvature, where the secondary stresses are most serious. Studies might well be made to demonstrate the effect of elaborate provisions which have been made during the construction of some of the larger bridges for the purpose of relieving secondary stresses.

Another condition that would be worthy of investigation is that of an occasional severe strain accompanied by plastic flow, with intermittent strains of lesser magnitude and of a frequency that approaches that which is recognized to be dangerous from the standpoint of "fatigue" failure. It is quite possible to obtain a sufficient number of repeated or alternating stresses to cause apprehension in this regard, if the life and service of modern bridge structures are to be as great as is estimated by many.

The authors have mentioned the possibility of unfavorable effect upon riveted or welded joints due to repeated or alternating stresses, but it should be emphasized that the effect of such stresses might be very severe upon the members themselves, especially in those connected with heavy gusset-plates and bent into double curvature as a result of secondary stresses; and likewise the effect of suddenly applied loads in causing combined stresses of serious magnitude before the metal has had time to creep and permit the adjustment of the stresses over the section by plastic flow. These remarks are especially pertinent in the case of smaller, lighter bridges.

It should also be stressed that the authors' "Summary and Conclusions" pertain exclusively to structures for which an occasional severe overload may be anticipated. They pertain to the stresses that would be caused by such an occasional load as might be expected in the case of a highway structure. Perhaps the results of the studies and experiments are less pertinent in the case of railroad bridges where the loads are subject to more careful control and are of at least daily occurrence.

No explanation is given as to the reason for the inward "dishing" of cover-plates as a result of local buckling, except the general tendency of the bending of a compression member as a whole. It might be considered questionable whether this tendency is decided enough to justify relying upon it, especially if other influences such as rust due to neglect in maintenance, tend to cause outward "dishing."

A. A. Eremin,[33] Assoc. M. Am. Soc. C. E. (by letter).[33a]—The analysis of secondary stresses at the yield point in a steel truss has considerable economic importance. The authors state that the ultimate strength of a steel truss is not affected by the secondary stresses at the yield point. This is true in respect to a truss in which the number of members, n, and number of joints, N, satisfy the equation,[34]

$$n = 2N - 3 \qquad (18)$$

If n is less than $2N - 3$, the fiber stresses at the yield point in the joints will permit excessive displacements and evidently will influence the ultimate strength of the truss. This may occur in a Vierendeel truss in which the secondary stresses at the yield point will affect the ultimate strength of the truss.

If n is greater than $2N - 3$, the secondary fiber stresses at joints as well as the axial stresses in some members of a steel truss, may reach the yield point without materially affecting the ultimate strength of the truss.

The secondary stresses at the yield point may also influence the distribution of the axial stresses in the truss members when the stiffness of the members or the eccentricity of the joints is considered in computing the axial stresses.[35] A method of computing axial stresses, taking the stiffness of the members into consideration, has been presented by Charles A. Ellis, M. Am. Soc. C. E.

The authors are to be congratulated for their valuable contribution to the theory and practice of diagnosing the stresses at the yield point.

---

[33] Associate Bridge Designing Engr., California Highway Div., Sacramento, Calif.

[33a] Received by the Secretary April 1, 1935.

[34] "Structural Engineering," by the late George Fillmore Swain, Past-President and Hon. M. Am. Soc. C. E., p. 81.

[35] "Williot Equations for Statically Indeterminate Structures in Combination with Moment Equations in Terms of Angular Displacement," by Charles A. Ellis, M. Am. Soc. C. E., *Proceedings*, Am. Soc. C. E., January, 1934, p. 73.

AMERICAN SOCIETY OF CIVIL ENGINEERS

Founded November 5, 1852

DISCUSSIONS

RATIONAL DESIGN OF STEEL COLUMNS

Discussion

By Messrs. R. G. Sturm and Marshall Holt, F. E. Turneaure, N. J. Durant, E. C. Hartmann, and Edward Godfrey

R. G. Sturm,[42] Assoc. M. Am. Soc. C. E., and Marshall Holt,[43] Jun. Am. Soc. C. E. (by letter).[43a]—Some of the fundamental principles of instability are applied, in this paper, to the design of steel columns, assuming that when the maximum stresses reach the yield strength the column becomes unstable.

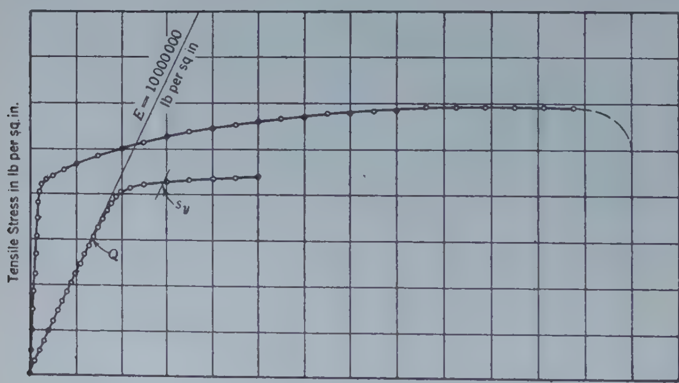

Fig. 23.—Typical Stress-Strain Curves for a Non-Ferrous Metal.

The stress-strain curves of most non-ferrous metals differ from those shown in Fig. 1 by virtue of the fact that they depart gradually from the extended initial modulus line. A typical stress-strain curve for aluminum

Note.—The paper by D. H. Young, Jun. Am. Soc. C. E., was published in December, 1934, *Proceedings*. Discussion on this paper has appeared in *Proceedings*, as follows: March, 1935, by Messrs. William R. Osgood, Alfred S. Niles, J. F. Baker, and K. L. DeBlois; and May, 1935, by Marvin A. Gray, Esq.

[42] Research Structural Engr. Physicist, Aluminum Research Laboratories, New Kensington, Pa.

[43] Research Engr., Aluminum Research Laboratories, Arnold, Pa.

[43a] Received by the Secretary February 25, 1935.

alloys, for example, is shown in Fig. 23. In applying these principles of instability, this stress-strain curve was idealized as one in which the value of the tangent modulus decreases as a straight line from the initial value at the upper limit of the elastic range to a value, λE, at the yield strength (0.2%), and from this decreased value along another straight line to zero at the modulus of failure. (The elastic range of the material may be determined by any standard method because reasonable variations in the actual value will not materially change the computed column strength.) Following the principles proposed by Engesser,[44] the critical load on a perfectly straight column was taken as the value given by Euler's formula, using the value of the reduced tangent modulus corresponding to the average stress in the column at buckling. A relation between the critical stress and the slenderness ratio thus obtained is shown in Fig. 24.

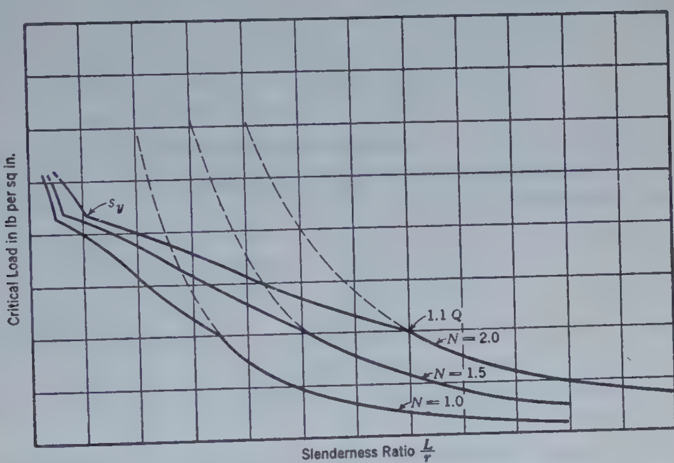

FIG. 24.—RELATION BETWEEN SLENDERNESS RATIO AND BUCKLING LOADS OF STRAIGHT COLUMNS (MADE FROM NON-FERROUS METALS).

In the case of imperfect or eccentrically loaded columns in which the member deflects appreciably, the principles used by the author are the same as those established by T. Claxton Fidler[45] in 1887, namely, that the imperfections and eccentricities in the column can be represented by a sine curve. This leads to Fidler's formula for deflection which is the same as the author's Equation (8). This analysis was advanced still further by Ayrton and Perry[46] and formulas for the stresses in imperfect columns were developed. The formula for maximum stress at the center of an imperfect column is identical with the author's Equation (11).

If the initial eccentricities in the column are small, such that the maximum average stress developed in the column exceeds the elastic range of the

[44] "Die Knickfestigkeit gerader Stäbe," von F. Engesser, *Zentralblatt der Bauverwaltung*, Berlin, 1891.

[45] "Treatise on Bridge Construction," by T. Claxton Fidler.

[46] "On Struts," by Professors W. E. Ayrton, and John Perry, *The Engineer*, December 10 and 24, 1886.

material, the writers found, in their analysis for columns of aluminum alloys, that the value of s_e may be reduced according to the foregoing idealized stress-strain curve. The relations between the reduced value of s_e (say, s'_e) and the average stress in the column, s, are given by the following equations: When f_m exceeds 1.1 times the upper limit of the elastic range of the material, Q, but when s is still less than 1.1 Q, the value of s'_e becomes

$$s'_e = s_e \left[1 - \frac{1}{j}\left(\frac{f_m - Q}{f_u - s}\right)^2\right] \text{.................} (83)$$

in which j is a factor depending upon the form of the member such that: $j = 4$ for solid rectangular sections; $j = 3$ for tubular sections; and $j = 2$ for I and H-sections bending parallel to the web (for bending perpendicular to the web the same as rectangles).

When s is between 1.1 Q and s_y,

$$s'_e = s_e \left[1 - (1 - \lambda)\frac{s - Q}{s_y - Q}\right] \text{................} (84)$$

in which, s_y = the stress at 0.2% permanent set; and λ is a factor that ranges from 0.05 to 0.12 depending on the particular alloy.

When s is greater than s_y,

$$s'_e = \lambda\, s_e \left[1 - \frac{s - s_y}{f_u - s_y}\right] \text{...................} (85)$$

In this way it is possible to extend Equation (11) into the plastic range for aluminum alloys. The maximum fiber stress, f_m, can thus be computed for the plastic range by a simultaneous solution of Equation (11) and Equations (83), (84), and (85).

Fixity of the ends of columns may be considered by re-defining s_e in the more general expression,

$$s_e = \frac{N^2 \pi^2 E}{\left(\frac{L}{r}\right)^2} \text{......................} (86)$$

in which, N is the Eulerian constant for end restraint (that is, $N = 1$ for hinged ends; and $N = 2$ for fixed ends).

It was found that columns fail by bending when the value of f_m reaches the modulus of failure for the material which for non-ferrous metals is practically equal to the tensile strength of the material, except for cases of local buckling.

The writers have used the equivalent of the author's Equation (12) to determine the ultimate load-carrying capacity of a column of aluminum alloys with the following changes: (*a*) s_y is replaced by s_u, the ultimate carrying capacity of the member; (*b*) f_y is replaced by f_u, the tensile strength of the material; and (*c*), s_e is replaced by s'_e. Thus, the ultimate

strength of columns made of materials not exhibiting the definite yield point of mild steel may be computed by the following equation, similar to Equation (12):

$$s_u = \frac{f_u}{1 + \frac{\Delta}{k}\left(\frac{1}{1 - \frac{s_u}{s'_e}}\right)} \quad \text{.................... (87)}$$

It must be understood that Equation (87) applies only to columns that fail as a unit and not to those that fail by local buckling or twisting. In some cases, local buckling can be taken care of by a proper choice of the value of f_u.

These principles and equations can be applied to columns subjected to a combination of axial and transverse loads by treating the transverse load (or moment) as being applied first and considering the deflection produced by this load as an eccentricity of application of the axial load. The amount of stress that can be developed by the action of the axial load (residual stress, f_r), is equal to the modulus of failure, f_u, minus the bending stress, f_b, produced by the transverse loads. A satisfactory agreement was found between the strengths of heat-treated steel and duralumin tubes under combined axial and transverse loads computed in the foregoing manner and obtained from actual test results.[47]

For the aforementioned case of combined axial and transverse loading, Equation (87) becomes,

$$s_u = \frac{f_u - f_b}{1 + \frac{\Delta b}{k}\left(\frac{1}{1 - \frac{s_u}{s'_e}}\right)} \quad \text{.................... (88)}$$

in which, f_b = the stress resulting from the transverse bending; and Δb = the deflection resulting from transverse bending, assuming the initial crookedness to be negligible compared to the deflection.

The equivalent of the author's Equation (13) becomes,

$$s_w = \frac{f_u - f_b}{n + \frac{n\ \Delta b}{k}\left(\frac{1}{1 - \frac{n\ s_w}{s'_e}}\right)} \quad \text{................ (89)}$$

The deflection resulting from the transverse loads, Δb, may be closely approximated by,

$$\Delta b = \frac{f_b\ L^2}{\pi^2\ E'\ c} \quad \text{........................ (90)}$$

[47] "Strength of Tubing Under Combined Axial and Transverse Loading," by L. B. Tuckerman, S. N. Petrenko, and C. D. Johnson, Technical Notes of National Advisory Com. for Aeronautics, No. 307, June, 1929.

in which, E' = a reduced value of E such that,

$$\frac{\pi^2 E'}{\left(\frac{L}{r}\right)^2} = s'_e \quad \ldots\ldots\ldots\ldots\ldots\ldots\ldots\ldots (91)$$

Substituting Equation (91) into Equation (89) and replacing k by its equivalent, $\frac{r^2}{c}$, Equation (89) becomes,

$$s_w = \frac{f_u - f_b}{n + \frac{n f_b}{s'_e}\left(\frac{1}{1 - \frac{n s_w}{s'_e}}\right)} \quad \ldots\ldots\ldots\ldots\ldots\ldots (92)$$

The writers did not use the secant formula to determine the equivalent of the author's Equations (14), (15), and (16), because the expression became quite involved when a reduced effective modulus was necessary.

Under the heading, "Columns in Rigid Frame Construction," the author refers to the elastic action of other members meeting at a joint causing columns to act intermediately between pin-ended and completely fixed-ended conditions. Although he might have intended pin-ended conditions to cover the case of columns with end moments, it should be stated that the other members framing into a joint might throw sufficient initial bending into the column so that the ultimate strength in the assembly might be less than that of a pin-ended column axially loaded (without end moments). An extension of Manderla's original work[48] taking into account the axial stresses in computing secondaries in a truss, leads to the conclusion that continuity in a compression member offers no restraint in itself to end rotation as the load on the member approaches the buckling load. It would be of value if Mr. Young would explain his conception of the end fixation of columns.

F. E. Turneaure,[49] M. Am. Soc. C. E. (by letter).[49a]—The analysis of columns presented by Mr. Young is a valuable contribution. In some respects it differs somewhat from that presented by the Special Committee of the Society on Steel Column Research,[50] while in other ways it is in agreement. In view of the importance of the subject and the comprehensive nature of these two studies, it will be useful to compare them briefly.

Mr. Young is in agreement with the Committee's conclusions in regard to using the yield-point strength as the critical stress to be considered, and that elastic conditions may be assumed for stresses below this point. The variation in yield point and in the form of the stress-strain curve in the vicinity of this point, both below and above, renders a more exact treatment of buckling strength of little practical value for structural columns.

[48] "Die Berechnung der Sekündarspannung welche im einfachen Fachwerke infolge starrer Knotenverbindungen auftreten," *Allgemeine Bauzeitung*, 1880.

[49] Cons. Engr.; Dean, Coll. of Mechanics and Eng., Univ. of Wisconsin, Madison, Wis.

[49a] Received by the Secretary March 27, 1935.

[50] *Transactions*, Am. Soc. C. E., Vol. 89 (1926), p. 1485; Vol. 95 (1931), p. 1152; and Vol. 98 (1933), p. 1376.

As the basis of his fundamental formula Mr. Young has adopted a centrally loaded, curved column and has superimposed upon this column any eccentricity that may occur. From the first, the Special Committee on Steel Column Research used the so-called secant formula, based entirely on eccentricity, and included in the eccentricity the effect of crookedness. The Committee selected this method in order to simplify the analysis of its test results where a definite eccentricity was used, and the final analysis leading to working formulas was made by including the effect of crookedness in the assumed eccentricity. The results of these two methods of procedure are not materially different. Analyses of crookedness made by the Committee and reported in its second progress report[51] indicate a much lower value for crookedness coefficient than Mr. Young has used. From its studies the Committee adopted a crookedness value, in terms of eccentric ratio, of $\frac{ec}{r^2} = 0.001 \frac{L}{r}$. This compares with a value of about $0.003 \frac{L}{r}$, which Mr. Young generally utilizes $\left(\Delta = \frac{L}{400}\right)$. This is a relatively high value and much larger than appears to be justified by the studies of the Committee.

A column in a modern riveted truss is substantially a member of a rigid frame and, therefore, is subject to the secondary stresses, or end deformation moments, that occur in such frames. Mr. Young suggests that these secondary stresses be calculated and the column formula modified accordingly for each member. In its study of working formulas the Committee carefully considered this matter and suggested that for ordinary design purposes it would be reasonable to assume an eccentric ratio, $\frac{ec}{r^2} = 0.25$, for all columns and to assume a free length (between points of inflection) of 75% of the full column length in applying the theoretical formula. A column in a rigid frame having 25% secondary stress at each end, and in such a direction as to bend the member in single curvature, acts nearly like an eccentrically loaded, pivoted-end column of one-half the length and with an eccentric ratio of 0.25.

The Committee felt justified, therefore, in using a column length of three-fourths the full length for a practical working formula. The application of these ideas resulted in a secant formula representing the ultimate strength of the column, based on yield-point strength. Any desired factor of safety could then be applied to this ultimate strength formula. The working formula that was suggested was a parabolic curve coinciding substantially with the resulting secant curve within the usual working limits of $\frac{L}{r} = 140$

[51] *Transactions*, Am. Soc. C. E., Vol. 95 (1931), p. 1152.

to 150. This working formula, adopted recently by the American Railway Engineering Association, is:

$$s = 15\,000 - \frac{1}{4}\left(\frac{L}{r}\right)^2 \ldots\ldots\ldots\ldots\ldots\ldots\ldots (93)$$

Pin-ended columns are not frictionless, but the amount of secondary moment at the ends due to truss deformation is limited. If frictionless, the eccentricity of load would be limited by the effect of crookedness and other incidental column defects; if frictional resistance is sufficiently large, such columns act as riveted members. As a reasonable estimate, the Committee adopted the same eccentric ratio of 0.25 as for riveted columns, but increased the free length to 85% of the full length, leading to the parabolic working formula,

$$s = 15\,000 - \frac{1}{3}\left(\frac{L}{r}\right)^2 \ldots\ldots\ldots\ldots\ldots\ldots\ldots (94)$$

For large and important structures, the writer endorses, fully, Mr. Young's suggestion that secondary stresses be computed and the column formula modified accordingly. The Committee's formula provides for eccentricity acting in the same direction at both ends. However, most columns in a truss will be bent in reverse curvature, resulting in maximum stresses at the ends; and such columns might well be designed at a fixed basic unit strength without reduction for column length. For ordinary practice as covered by general specifications, one would scarcely resort to such a separate calculation, and a single formula is preferable.

The shear analysis presented by Mr. Young appears to be quite complete, and shows clearly the high stresses possible in short members, decreasing to a smaller value with increasing length and then increasing again for long members. In this case, again, the high values assumed for crookedness result in shear values differing somewhat from those corresponding to the column formulas of the Committee. The new shear formula recently adopted by the American Railway Engineering Association was based upon the analyses by Shortridge Hardesty, M. Am. Soc. C. E., using the adopted secant formulas as a basis. This new formula is an empirical one, but is constructed so as to provide reasonably well for both short and long columns, as follows:

$$\frac{V}{P} = \frac{1}{100}\left(\frac{100}{\frac{L}{r} + 10} + \frac{\frac{L}{r}}{100}\right) \ldots\ldots\ldots\ldots\ldots (95)$$

in which, $\frac{V}{P}$ = ratio of shear to direct stress.

It appears to the writer that the paper by Mr. Young and the reports of the Special Committee on Steel Column Research, taken together, present a clear picture of the underlying factors in the rather complex column problem, and suggest rational methods of dealing with the subject.

N. J. DURANT,[52] ASSOC. M. AM. SOC. C. E. (by letter).[52a]—Simple rational formulas for the design of steel columns, which are deduced from elementary analyses, are brought to the attention of the Engineering Profession by this paper. The subject of column analysis is one of the oldest in the broad field of elasticity, but in spite of all the research conducted, the profession has used empirical formulas for years, with the result that, to-day, the engineer has a multiplicity of column formulas at his command, no two of which will give identical results.

These formulas (whether straight lines, parabolas, or of the Rankine-Gordon type), which have been in general use, are merely forms of wasted ingenuity. Usually, the only parameter in them is the slenderness ratio, $\left(\frac{L}{r}\right)$. One of the disadvantages of such formulas (whether or not they conform to test results of a particular material) is, that immediately the designer is confronted with a material with which he is unfamiliar, he feels the necessity for an analysis which will interpret for him the principles as distinct from the incidents upon which experimental results depend.

The chief disadvantage of the approximate formulas, however, lies in the fact that unless the engineer has a rational formula to serve as a standard, he is in complete ignorance regarding their factors of safety, and this alone should be a sufficient reason for their condemnation.

It follows that the engineer must be in doubt regarding the stability of the resulting structures, because it is no criterion that such structures withstand the loads for which they have been designed.

Objections to rational column formulas have been raised because they have been considered too complicated for general use. No formula for columns could be so complicated but that a graph or tabular values of the dependent variable for different values of the argument could not be readily obtained, and this is all the average designer needs. His subsequent uses of the formula, therefore, would involve no additional work beyond that entailed by the use of an approximate formula.

Furthermore, in the case of an investigation, whether of failure of a column or for other reasons, the investigator would arrive at precisely the same formulas as did Mr. Young for similarly imposed conditions.

A rational formula for columns cannot be condemned because it is complicated; neither can a straight-line formula be defended on the basis of its simplicity. Simplicity is a desideratum to be aimed at in any formula, whatever its purpose, but if all the essential variants are absent, the formula ceases to be of general value.

A formula for the design of columns should be one of general utility and if it has a theoretical basis, then by a variation of the fundamental elastic constants it would apply to any material which obeys Hooke's law and which has a compressive or tensile stress-strain curve. Moreover, if the factor of safety in the column formula is equal to that of the material in tension, the resulting structure will have, within narrow limits, a uniform strength.

[52] Designer, Bridge Dept., Rendel, Palmer & Tritton, Westminster, London, England.
[52a] Received by the Secretary March 29, 1935.

The only actual uncertainty in a rational column formula is the value which should be assigned to the length of the column. If the ends were fixed in position and direction this value would be determinate, but such a condition is unattainable.

All members of a frame are subjected to varying degrees of constraint which make the effective length indeterminate, but the true effective length, of course, must be less than the geometric length. If the geometric length were inserted in the formula, the designed column would have a strength greater than that calculated, provided, of course, the material was in no way impaired and that the secondary moments were properly assessed. The value of the constraints will be less, in general, for increases in the yield stress, but no analytical law can be formulated to deal with this phenomenon.

Moreover, the more slender a member is compared with those to which it is attached, the shorter will be its effective length. This statement, although obvious, serves in some measure to fix the effective length of a column. For instance, the web members of a truss are almost invariably of more slender proportions than the chords and, in consequence, their effective lengths are less than their geometric lengths. In general, the chords receive little restraint from the web members and probably their effective lengths are their geometric lengths, approximately.

Throughout his paper the author has used the equation,

$$E\,I\,\frac{d^2y}{dx^2} = -\,M \qquad (96)$$

which is sufficiently accurate for columns of solid cross-section.

For built-up columns, the form is of importance and it would be necessary in a rigorous investigation to use the more general equation:

$$E\,I\,\frac{d^2y}{dx^2} = -\,M + k\,\frac{E\,I}{A\,G}\,\frac{d^2M}{dx^2} \qquad (97)$$

in which k is a constant depending on the distribution and form of the area of the cross-section, and G is the modulus of rigidity.

However, considering the variation in the elastic constants and the diversity of column forms, Equation (97) would not be expedient for general use.

To avoid the anomalies in design created by the approximate formulas, it is to be hoped that a rational formula for column design will soon be incorporated in all specifications for the design of structures.

So much research work has been done on structures, particularly in America, that it appears strange that the march of progress should be marred by adherence to traditional standards, many of which, have no scientific significance.

E. C. Hartmann,[53] Jun. Am. Soc. C. E. (by letter).[53a]—The various factors involved in the rational design of steel columns have been treated in a comprehensive manner by the author, but the writer is inclined to wonder how much of the paper is likely to be absorbed in usable form by those actively

---

[53] Research Engr., Aluminum Co. of America, New Kensington, Pa.

[53a] Received by the Secretary April 27, 1935.

engaged in column design. What most designers want is something reasonably accurate and not too complex, which will take into account the principal variables and will fit neatly into the ordinary design specifications. In the case of a column subjected to eccentric load, or to a side load, for example, the designer would like to know what allowable stress to use on the extreme fiber. Knowing this, he is perfectly competent to proceed with his design in the usual manner, selecting a member on which the combined stress (bending plus direct stress) does not exceed the allowable.

A simple formula for determining the allowable stress for all types of compression members, which incorporates practically all the principles in the author's paper, has been derived by the writer and his associates. For the sake of simplicity the derivation presented herein will be made for steel columns using the same basic assumption as that adopted by the author, namely, that the yield-point stress is the limit of usefulness. It will then be shown how the derivation may be extended to include materials such as the structural alloys of aluminum which have no pronounced yield point and, hence, have a range of useful stress above this point.

Fig. 25 demonstrates a very general case of a pin-ended column having an initial crookedness, Δ, loaded eccentrically at a distance, e, and resisting a side load as well as the column load. The dotted line represents the deflected position of the member under load.

Let the column load, P, and the side load, W, be the design loads for which a factor of safety, n, is to be provided. If the column is properly designed, the fiber stress from combined bending and direct stress should just reach the yield point if P is increased to $n\ P$, and W to $n\ W$, simultaneously. Therefore, the following equation represents the condition at failure:

$$\frac{n\,P}{A} + \frac{n\,P\,e\,c}{I} + \frac{n\,P\,\Delta\,c}{I} + \frac{n\,P\,D\,c}{I} + \frac{n\,M\,c}{I} = f_y \ldots (98)$$

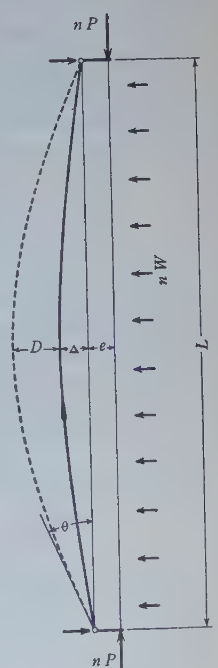

FIG. 25.

in which, in addition to the notation of the paper, D = the total deflection which accompanies the yield-point stress, caused by all loads combined, in inches; and M = the maximum bending moment produced by transverse loads, in pounds. It will be recognized that Equation (98) is simply a summation of the five component parts of the extreme fiber stress, based on the well-known fundamental equation for combined stress:

$$f = \frac{P}{A} + \frac{M\,c}{I}.$$

Transposing the fourth term in Equation (98) to the right-hand side and dividing through by the factor of safety, n:

$$\frac{P}{A} + \frac{P\,e\,c}{I} + \frac{P\,\Delta\,c}{I} + \frac{M\,c}{I} = \frac{f_y}{n} - \frac{P\,D\,c}{I} \ldots\ldots\ldots\ldots (99)$$

The term, $\frac{f_y}{n}$, in Equation (99), may be replaced by f_b, the design stress for the member treated as a beam, which gives:

$$\frac{P}{A} + \frac{P\,e\,c}{I} + \frac{P\,\Delta\,c}{I} + \frac{M\,c}{I} = f_b - \frac{P\,D\,c}{I} \quad \text{.........(100)}$$

Since P and W are design loads (ultimate loads divided by the factor of safety, n), and since M is the moment produced by the design load, W, the terms on the left-hand side of Equation (100) represent the ordinary design calculations for combined stress on the extreme fiber of the member. The equation states that if this calculated stress is equal to the terms on the right, a factor of safety of n is provided against failure (yield-point stress). Therefore, the terms on the right constitute the allowable design stress, f_w; thus:

$$f_w = f_b - \frac{P\,D\,c}{I} \quad \text{.....................(101)}$$

in which f_w = the allowable combined stress, in pounds per square inch, on the extreme fiber at the center of the unsupported length of any member subjected to combined bending and direct stress (includes eccentrically loaded columns); and f_b = the allowable stress, in pounds per square inch, for the member treated as a beam.

The only term in Equation (101) that is unknown is D, the total deflection accompanying the yield-point stress. This deflection may be expressed as the sum of the effects of the various loads, but a simpler and more direct solution is to express it directly in terms of the known total fiber stress, as follows:

$$D = \frac{\left(f_y - \frac{n\,P}{A}\right) L^2}{\pi^2\,E\,c} \quad \text{...................(102)}$$

Equation (102) is readily derived by the use of the well-known moment-area theorem which states that the deflection at the center of a span is the bending moment at the center produced by the moment diagram, divided by EI, considered as a load.

The total bending stress at the center is $f_y - \frac{n\,P}{A}$ and, if M' is the total moment causing this stress:

$$\frac{M'\,c}{I} = \left(f_y - \frac{n\,P}{A}\right) \quad \text{....................(103)}$$

Therefore, in this case, the center ordinate of the moment diagram, divided by $E\,I$, is:

$$\frac{M'}{E\,I} = \frac{\left(f_y - \frac{n\,P}{A}\right)}{E\,c} \quad \text{.....................(104)}$$

The constant, π^2, in Equation (102) results from assuming that the curve of moments is a sine curve and in this respect Equation (102) is an approxi-

mation. Other curves might be assumed; for example, a parabolic moment curve gives a constant, 9.6, instead of π^2.

Let s_e = the critical stress, in pounds per square inch, for the member treated as an Euler column, representing the Euler value, $\frac{\pi^2 E r^2}{L^2}$, as in the author's paper. Transposing terms:

$$\frac{L^2}{\pi^2 E} = \frac{r^2}{s_e} \qquad (105)$$

Substituting Equation (105) in Equation (102) gives the following:

$$D = \frac{\left(f_y - \frac{n P}{A}\right)}{s_e} \frac{r^2}{c} \qquad (106)$$

The term, f_y, may be replaced by $n f_b$, which gives:

$$D = \frac{\left(f_b - \frac{P}{A}\right)}{\frac{1}{n} s_e} \frac{r^2}{c} \qquad (107)$$

Substituting Equation (107) in Equation (101) and replacing I by $A r^2$:

$$f_w = f_b - \frac{P}{A} \frac{\left(f_b - \frac{P}{A}\right)}{\frac{1}{n} s_e} \qquad (108)$$

The derivation of Equation (108) for end conditions other than pinned is relatively simple and leads to the same formula. The method preferred by the writer is to evaluate the end condition in terms of the equivalent length of pin-end column—that is, in terms of the length between the points of contra-flexure of the member. Thus, a fixed-end column acts the same as a pin-end column of one-half its length. Since the line of action of the column load, P, must follow the straight line joining the points of contraflexure, the derivation is simply a repetition of the foregoing, except that the effective length, $z L$, is substituted for L and the effective initial crookedness, $z \Delta$, is substituted for Δ. The Euler value, s_e, becomes $\frac{\pi^2 E r^2}{(z L)^2}$. The value of z for completely fixed ends is 0.5. For round or pin ends, it is 1.0, of course, whereas for the general run of framed ends many designers use 0.75 as a representative average value.

As previously pointed out, the derivation of Equation (108) is based on the line of reasoning adopted by the author in dealing with steel. For aluminum alloys and other materials which do not display the abrupt yield-point characteristic of steel, it is necessary to introduce into the derivation a suitably reduced modulus of elasticity, E_a, when the value of $\frac{n P}{A}$ exceeds the elastic

range. A similar correction should be made even in the case of steel, because the limit of the elastic range is slightly below the yield-point stress. This matter is not as important in steel as in most other materials.

If applied to a column that is eccentrically loaded, the method described herein gives the same result as that in the author's paper. Furthermore, it has the additional advantage that it applies to columns transversely loaded; in fact, it allows any member under combined bending and direct compression to be designed on the same basis as an ordinary beam, with no departure from conventional procedure. In order to clarify the method of using Equation (108) a simple example may be cited, using current standard specifications[54] as a basis for design. Let the problem be to determine whether a 12-in., 65-lb Carnegie beam section, unbraced, on a 15-ft simple span (pin ends) is safe under the combined action of an end load of 200 000 lb and a distributed transverse load of 20 000 lb, acting in the plane of the web. The following are the calculations:

(1) $\frac{P}{A} = \frac{200\,000}{19.11} = 10\,500$ lb per sq in.; $\frac{L}{r}$ (Axis 2–2) $= \frac{15 \times 12}{3.02} = 59.6$; and, the allowable axial compression $= 15\,000 - \frac{1}{3}\,\overline{59.6^2} = 13\,800$ lb per sq in. Consequently, the member is safe for the column load alone.

(2) The bending stress (Axis 1–1) $= \frac{20\,000 \times 15 \times 12}{8 \times 88} = 5\,100$ lb per sq in.; $\frac{L}{b} = \frac{15 \times 12}{12} = 15$; and $f_b = 18\,000 - 5 \times \overline{15^2} = 16\,900$ lb per sq in. Therefore, the member is safe for transverse load alone.

(3) The combined fiber stress (Axis 1–1) $= 10\,500 + 5\,100 = 15\,600$ lb per sq in.; $\frac{L}{r}$ (Axis 1–1) $= \frac{15 \times 12}{5.28} = 34$; s_e (Axis 1–1) $= \frac{\pi^2 E}{34^2} = 248\,000$ lb per sq in.; $n = \frac{33\,000}{18\,000} = 1.83$; $\frac{1}{n}\,s_e = 135\,000$ lb per sq in.; and f_w (Axis 1-1) $= 16\,900 - 10\,500\,\frac{(16\,900 - 10\,500)}{135\,000} = 16\,400$ lb per sq in., which proves the member safe for combined load.

In the foregoing examples it should be noted that, for checking the strength of the member under column load alone, the smallest radius of gyration is used (Axis 2–2), whereas for checking combined stress conditions the radius of gyration is taken about the axis normal to the plane of the transverse bending loads (Axis 1–1).

In using Equation (108) the end conditions for the transverse loading should be consistent with those for the column loading. Thus, in the foregoing example, if the member were assumed to have riveted ends, the value of s_e would have been computed for $z = 0.75$,[55] and, therefore, in computing the bending stress from the transverse load the effective span should be reduced to 0.75×15.

[54] Specifications for Steel Railway Bridges (1934), Am. Ry. Eng. Assoc.

[55] *Loc cit.*, Appendix A.

Certain parts of the foregoing derivation can be used in arriving at a formula for estimating the maximum shear on compression members. Assuming the deflected member in Fig. 25 to take the form of a sine curve, it can readily be shown that the maximum slope of the member is:

$$\tan\,\theta = \frac{\pi\,(D + \Delta)}{L} \quad \ldots\ldots\ldots\ldots\ldots\ldots\ldots (109)$$

The total shear on the member is:

$$n\,V = n\,B + n\,P\,\sin\,\theta \quad \ldots\ldots\ldots\ldots\ldots\ldots (110)$$

in which B is the shear force, in pounds, produced by the transverse load, W. Neglecting the difference between $\tan\,\theta$ and $\sin\,\theta$ and dividing through by the factor of safety, n, gives the following equation:

$$V = B + \frac{\pi\,P\,(D + \Delta)}{L} \quad \ldots\ldots\ldots\ldots\ldots\ldots (111)$$

in which V = the total shear force, in pounds, for which the column should be designed (shear at failure divided by factor of safety). Substituting the value of D from Equation (107),

$$V = B + \frac{\pi\,P}{L}\left[\frac{\left(f_b - \dfrac{P}{A}\right)}{\dfrac{1}{n}\,s_e}\,\frac{r^2}{c} + \Delta\right] \quad \ldots\ldots\ldots\ldots (112)$$

Equation (112) is for pin-ended members only ($z = 1$). It may be generalized as to end conditions by using $z\,L$ instead of L, and $z\,\Delta$ instead of Δ, in accordance with the foregoing discussion of end conditions; thus:

$$V = B + \frac{\pi\,P}{z\,L}\left[\frac{\left(f_b - \dfrac{P}{A}\right)}{\dfrac{1}{n}\,s_e}\,\frac{r^2}{c} + z\,\Delta\right] \quad \ldots\ldots\ldots\ldots (113)$$

in which V = the maximum total shear force, in pounds, for which compression members must be designed in order to provide a factor of safety against shear failure consistent with that against column failure. The Euler value, s_e, should be calculated for the effective length, $z\,L$. The shear, B, from transverse loads should also be that for the effective length, $z\,L$.

Equation (113) fits in nicely with Equation (108) since the two have a number of terms in common. It should be emphasized that the radius of gyration, r, should be taken about the axis normal to the plane in which the shearing force, V, is acting. The distance to the extreme fiber, c, should be taken in a direction consistent with r and, in the case of unsymmetrical members having two values of c, the smaller of the two should be taken unless transverse loads or eccentricities are present which throw the larger compression stresses on the other side.

Equation (113) like Equation (108) gives results in agreement with the author's method when applied to a column eccentrically loaded; and has

the additional feature that it applies also to columns transversely loaded. In order to clarify the method of using Equation (113) an example may be given using the same set of conditions as in the foregoing example. The following are the calculations: $B = \frac{20\,000}{2} = 10\,000$ lb; $\frac{\pi}{L} = 0.0174$;

$$\frac{f_b - \frac{P}{A}}{\frac{1}{n}\, s_e} = \frac{16\,900 - 10\,500}{135\,000} = 0.0474;\ \frac{r^2}{c} = \frac{5.28^2}{6.06} = 4.6;\ \Delta = 0;\ \text{and, } V$$

$= 10\,000 + 0.0174\,P\ [0.0474 \times 4.6 + 0] = 10\,000 + 0.0038\,P = 10\,760$ lb.

The shear produced by column action in this member is less than 1% of the end load, and is a small fraction of the total shear. If the initial crookedness had been assumed equal to $\frac{L}{400}$, or 0.45 in., the resulting shear from column action would be increased to 0.0116 P, and the total shear would be 12 300 lb. In either case, of course, the column selected has ample web section.

In his handling of the shear problem, the author has apparently overlooked the factor of safety. His v_y, which is defined as "the average shearing stress when the load, P, is at its yield-point value," is used in Fig. 16 for direct comparison with values taken from the American Railway Engineering Association specifications. He should have used v_w, or $\frac{v_y}{n}$, following the same logic by which s_w in his Equation (13) is arrived at from s_y in his Equation (12). This would have had the effect of dropping all his curves in Figs. 16 and 18 considerably. The writer wonders if the selection of an average design shear of 600 lb per sq in. would not have been affected by this correction. There is little in the paper to justify a blanket value of 600 lb per sq in. under any circumstances.

The author has pointed out the effect of shearing distortions on latticed or battened members. In the writer's derivations these distortions affect only the magnitude of the deflection, D. In Equations (102 and (107) it is assumed that shearing deformations are negligible. Actually, under the effect of transverse loads, the shearing deflection in a latticed member often runs as high as the bending deflection. Some account of this might be taken in Equations (108) and (113), possibly by inserting a suitable factor by which the term, $\left(f_b - \frac{P}{A}\right)$, is multiplied when latticed or battened columns are under consideration. This is a matter worthy of further study.

The writer would like to emphasize the importance of the term, D, the total deflection of the member, in the foregoing derivations. This deflection is that which occurs just at the point of failure, or just as the extreme fiber reaches the yield-point stress. Dividing through the various equations by the factor of safety, n, does not affect the magnitude of D, so that in the formula for work-

ing stress, f_w (Equation (101)), D is still the deflection corresponding to the yield-point stress. The significance of this to the designer is simply that, in estimating the degree of fixation of the ends of a member (magnitude of effective length, $z\,L$), the conformation of the member should be visualized with respect to conditions just before failure. Many a member which is practically fixed-ended ($z = 0.5$) at low loads may be practically pin-ended ($z = 1.0$) at or near failure, and should be so considered in design.

The writer advocates the use of Equations (108) and (113) in actual design instead of such generalities as $\Delta = \frac{L}{400}$ and average shear stress = 600 lb per sq in., advocated in the author's summary. The designer should be allowed some latitude to evaluate such variables as crookedness, end conditions, and eccentricity of loading in the light of his own peculiar design conditions. Most designers will quickly simplify the application of Equations (108) and (113) by preparing charts and other "short-cuts" for the routine problems, saving the formulas themselves for the unusual cases that always arise.

EDWARD GODFREY,[56] M. AM. SOC. C. E. (by letter).[56a]—The idea that a column is imperfect, that it is not perfectly straight, and that imperfection (lack of straightness) is directly proportional to the length of the column, is a rational assumption. Mr. Young's attack on the problem of the column is in the right direction. A perfect column formula, except for slender columns, is not possible, because a perfect column is an impossibility. The imperfection of a column that is easiest to detect, in columns otherwise carefully made, is lack of straightness. In 1909, the writer pointed out[57] that by visual inspection one can detect deviation from a straight line of about $\frac{1}{400}$ of the length of a structural member. This is the ratio suggested by Mr. Young. The writer chose $\frac{1}{300}$ as the ratio for a rational column formula to allow for eccentric end application of the load.

Mr. Young finds an expression for the total extreme fiber stress which includes the bending stress due to the bow of the column. His design curve for a rectangular section in that column, as shown in Figs. 9 and 10, is almost a straight line for values of $\frac{L}{r}$ up to 120 and for a bow in the column equal to $\frac{1}{400}$ of the length. It is evident that a somewhat larger assumed bow in the column would give a still closer approach to a straight line.

In the writer's solution, using an average value of the radius of gyration as one-third the depth of section, and an assumed bow in the column

---

[56] Structural Engr., Pittsburgh, Pa.

[56a] Received by the Secretary June 4, 1935.

[57] *Railroad Age-Gazette*, July 2, 1909; see, also "Steel Designing," by Edward Godfrey; and *The Structural Engineer* (London), September, 1932.

of $\frac{1}{300}$, the curve of allowed unit stress was found to be a straight line up to $\frac{L}{r}$ equal to about 110. This agreed with the commonly used straight-line formula, $16\,000 - 70\,\frac{L}{r}$. The deviation from this straight line is very slight for slenderness ratios of 150 or less. At $\frac{L}{r} = 150$ the curve strikes the Euler curve with a factor of safety of 2.

It is significant that this is just about the upper limit of structurally permissible columns. Thus, a completely rational formula, too cumbersome to use in practice, however, based on no other supposition than a bow or imperfection that would reject a column subject to ordinary inspection, agrees almost exactly with the common, well-tried, straight-line formula that never laid claim to any except experimental, empirical backing.

The writer recommended that columns be divided into two distinct classes (structurally permissible columns and slender columns), and that design stresses in these two classes be based on entirely different considerations, not forgetting, of course, the zone where the two classes overlap. The unit stress to be used in the first class was based solely on the extreme fiber stress in a bowed column, subject to an endwise load, and that unit stress was shown to be theoretically determinate by the use of a formula of the type, $16\,000 - 70\,\frac{L}{r}$. The unit stress in slender columns was recommended to be on the basis of a factor of safety, say, about 2, based on the ultimate load as shown by the Euler formula. There is no need of a factor of safety greater than 2 in slender columns, because the steel is in no manner distressed in a slender column (even in one having a decided bow) until the ultimate load is nearly reached.

There need be no confusion in the two classes of columns. Specifications for structures need give no recognition to slender columns, except to exclude their use. All structural columns can be designed safely on the same straight-line formula, because there is extra safety in the range approaching slender columns; this is of advantage, because the weight of members and other considerations make it desirable. Slender columns and formulas for them should be reserved for such work as transmission towers, airplanes, etc.

The writer is not familiar with present practice among Continental engineers, but in former years they used the Euler formula with a factor of safety of 5. This is an extravagant waste in slender columns, where the Euler load is of real significance. The Euler load has no meaning whatever in structurally permissible columns.

AMERICAN SOCIETY OF CIVIL ENGINEERS

Founded November 5, 1852

DISCUSSIONS

A DIRECT METHOD OF MOMENT DISTRIBUTION

Discussion

BY W. P. LI, JUN. AM. SOC. C. E.

W. P. LI,[42] JUN. AM. SOC. C. E. (by letter).[42a]—The difference between the original Cross method of moment distribution and the Lin modification may be visualized readily by the following formularized method of procedure:

Assuming an end of a member as being $\dfrac{\text{in a natural condition of restraint}}{\text{fixed}}$, when the joint at that end is released, the unbalanced fixed-end moment is distributed among the members in proportion to the $\dfrac{\text{modified } (K_m)}{\text{direct } (K)}$ stiffness (that is, the $\dfrac{\text{inter-related}}{\text{separate, } \frac{I}{L}\text{,}}$ stiffness). (Note that, in the modified method, for unbalanced "carried-over" moments the distribution is only among the connecting members.) The moment thus distributed, is carried over to the other ends of the members in accordance with $\dfrac{\text{a modified}}{\text{the Cross}}$ carry-over factor. For beams of uniform cross-section the carry-over factor in the Cross method is −0.5.

In the foregoing, compound rule, the inserts in the "numerator" refer to the modified method and those in the "denominator" to the Cross method. It is evident that the modified method is not entirely direct in its application since it requires two steps instead of one for the solution of the problem. The first step, that of computing the modified stiffness and the modified carry-over factor, is usually lengthy, especially when the R-value must be assumed at the beginning, as for the closed frames. Thus, it seems that the modified method is only a variant of the original method. One can scarcely claim that the modified method is more direct than the original;

NOTE.—The paper by T. Y. Lin, Jun. Am. Soc. C. E., was published in December, 1934, *Proceedings*. Discussion on this paper has appeared in *Proceedings*, as follows: March, 1935, by Messrs. L. E. Grinter, W. H. Huang, Felix H. Spitzer, Harold E. Wessman, Egor P. Popoff, and L. T. Evans; and May, 1935, by Messrs. C. S. Salter, Leon Blog, Austin H. Reeves, E. J. Bednarski, John T. Howell, and I. Oesterblom.

[42] Harbor Engr., Kwangtung River Conservancy Comm., Canton China.

[42a] Received by the Secretary April 8, 1935.

ordinarily, the reverse is true. A closed frame such as that in Example 4 of the paper and in the truss in Fig. 23, and in Fig. 24, can be solved more easily and directly by the original method. It is difficult to assume a closed R-value for one of the truss members, say, AB (Fig. 23), and check it along two different paths, $ABCDA$ and $ABDA$.

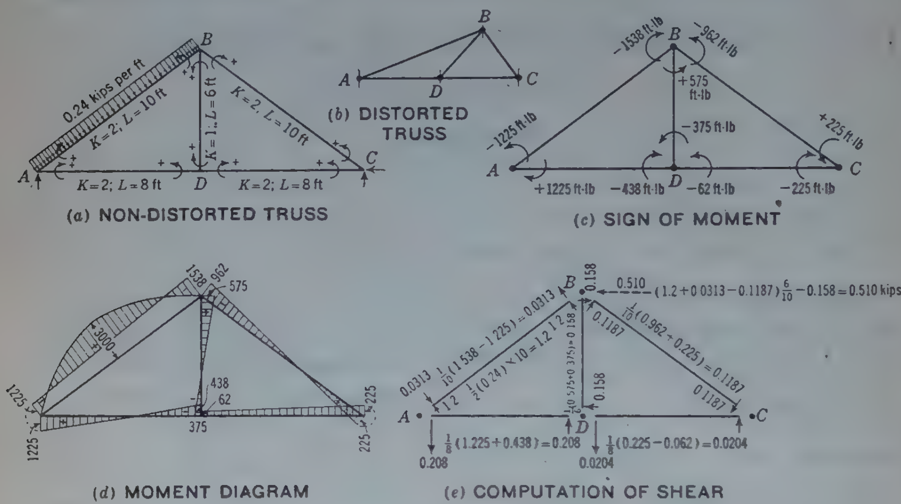

FIG. 23

Adopting Professor Cross' sign convention, the conventional left and right for each joint can be easily seen from the distorted form of the truss, as in Fig. 23(b). The computation may be arranged as shown in Table 4.

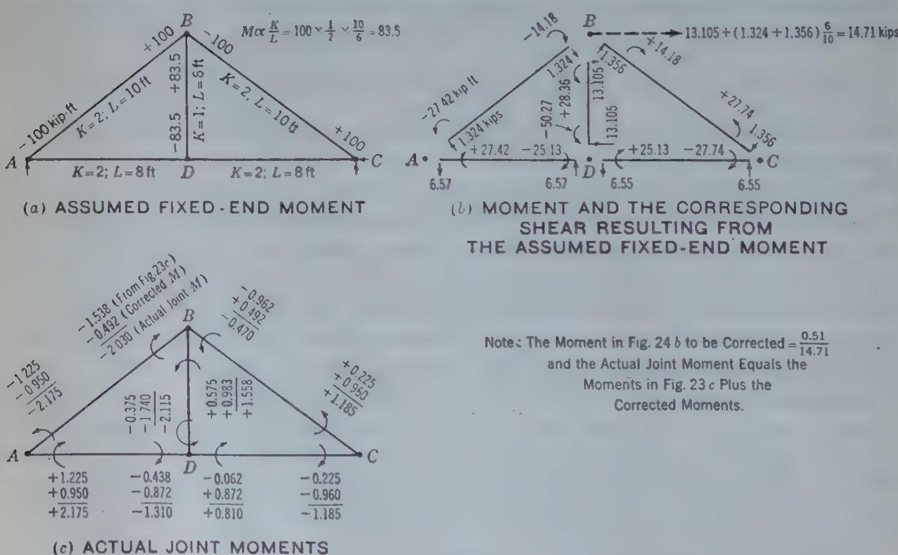

FIG. 24.

An attempt to solve these problems by the Lin method would demonstrate the fact that the Cross method has distinct advantages for this case.

Since the truss in Fig. 23(*a*) is unsymmetrically loaded with wind pressure, Joint *B* will undergo side-sway if subjected to wind pressure alone;

TABLE 4.—MOMENT DISTRIBUTION

Joint	A			B			D			C		
Left, or right	L	R		L		R	L	R		L	R	
(a) For Problem in Fig. 23.												
Relative stiffness factor	....	2	2	2	1	2	2	1	2	2	2	....
Distribution factor	....	0.5	0.5	0.4	0.2	0.4	4	0.2	0.4	0.5	0.5	....
Moment	....	*AD*	*AB*	*BA*	*BD*	*BC*	*DA*	*DB*	*DC*	*CD*	*CB*	....
Fixed-end moment	....	......	−2.0	−2.0	......	......	......	......	......	......	......	....
Distribution:												
From Joint *A*	....	+1.0	+1.0	−0.50	......	......	−0.50	......	......	......	......	....
From Joint *B*	....	......	−0.50	+1.0	+0.50	−1.0	......	−0.25	......	......	+0.50	....
From Joint *D*	....	−0.05	......	......	+0.025	......	+0.10	−0.05	−0.10	+0.05	......	....
From Joint *C*	....	......	......	......	......	+0.138	......	......	+0.138	−0.275	−0.275	....
From Joint *A*	....	+0.275	+0.275	−0.138	......	......	−0.138	......	......	......	......	....
From Joint *B*	....	......	......	+0.10	+0.05	−0.10	...... +0.10	−0.025 −0.05	...... −0.10	...... +0.05	+0.05	....
From Joint *D*	....	......	......	......	......	......	......	......	......	−0.05	−0.05	....
From Joint *C*	....	......	......	......	......	......	......	......	......			
Final moment	....	+1.225	−1.225	−1.538	+0.575	−0.962	−0.438	−0.375	−0.062	−0.225	+0.225	....
(b) For Assumed Fixed-End Moments in Fig. 24(a)												
Moment	....	*AD*	*AB*	*BA*	*BD*	*BC*	*DA*	*DB*	*DC*	*CD*	*CB*	....
Distribution factor	....	0.5	0.5	0.4	0.2	0.4	0.4	0.2	0.4	0.5	0.5	....
Assumed fixed-end moment	....	......	−100	+100	+83.5	−100	......	−83.5	......	......	+100	....
Distribution:												
From Joint *A*	....	+50	+50	−25	......	......	−25	......	......	......	......	....
From Joint *B*	....	......	+51.7	−103.4	−51.7	+103.4	......	+25.8	......	......	−51.7	....
From Joint *D*	....	+6.54	......	......	−3.27	......	−13.08	+6.54	+13.08	−6.54	......	....
From Joint *C*	....	......	......	......	......	+10.44	......	......	+10.44	−20.88	−20.88	....
From Joint *A*	....	−29.12	−29.12	+14.56	......	......	+14.56	......	......	......	......	....
From Joint *B*	....	......	......	−0.34	−0.17	+0.34	......	+0.085	......	......	−0.17	....
From Joint *D*	....	......	......	......	......	......	−1.614	+0.807	+1.614	−0.807	......	....
From Joint *C*	....	......	......	......	......	......	......	......	......	+0.488	+0.488	....
Final moment	....	+27.42	−27.42	−14.18	+28.36	+14.18	−25.13	−50.27	+25.13	−27.74	+27.74	....

however, Joint *D* is held against side-sway by the horizontal member, *ADC*, which is twice as stiff as Member *BD*. The shear correction for the side-sway of Joint *B* can be computed as follows: (1) Find the horizontal force to be applied at Joint *B* in order to hold it against side-sway; (2) assume a system of convenient fixed-end moments and find the final moment and the corresponding horizontal shear at Joint *B*; (3) by proportioning the force and the shear thus computed, find the moments to be corrected at the joints due to side-sway; and (4), combine the corrected moments with the moments obtained by simple moment distribution (as in Fig. 23(*c*)) to obtain the actual joint moments.

DISCUSSIONS

ELASTIC PROPERTIES OF RIVETED CONNECTIONS

Discussion

BY E. MIRABELLI, M. AM. SOC. C. E.

E. MIRABELLI,[20] M. AM. SOC. C. E. (by letter).[20a]—In Table 3 the author intimates that the carrying capacity of beams under gravity loading may be increased by as much as 95% by making use of the end restraint provided by the connections. This percentage approaches, very closely, the theoretical maximum of 100% which would occur with a perfectly balanced design when, under full working load, the connections yield just enough to make the bending moment at mid-span equal to the restraining moment at the connections. Such percentages may lead to unwarranted optimistic conclusions regarding the extent to which economy is possible in an actual design. The possibility of extremely large savings from utilizing resistance of connections is doubtful for an ordinary building frame, for the following reasons:

(1) The elasticity of the connections differs from that of the remainder of the beam and, as a result, the stresses developed in the beam are not proportional to the applied load. The bending moment at mid-span increases more rapidly than the loading, whereas the bending moment at the end increases less rapidly than the loading. The variation for Specimen 10 (see Table 3) is shown by the calculated curves in Fig. 38. Because of this characteristic, the factor of safety based on unit stresses is larger than that based on loading. For example, if the factor of safety is 2 measured to the yield point for the beam of Fig. 38, the resisting moment at the yield-point stress is twice that at the working stress. As indicated by the broken lines, the applied load at the yield point is less than twice the working load. The factor of safety based on loading for the case shown is only 1.78, whereas the stress intensities indicate a factor of 2.00. The importance of dealing with applied loads rather than with unit stresses may be appreciated

NOTE.—The paper by J. Charles Rathbun, M. Am. Soc. C. E., was published in January, 1935, *Proceedings*. Discussion on this paper has appeared in *Proceedings*, as follows: February, 1935, by Ralph E. Goodwin, Assoc. M. Am. Soc. C. E.; and May, 1935, by Messrs. Harold C. Rowan, Walter Scholtz, J. F. Baker, L. E. Grinter, and C. R. Young and K. B. Jackson.

[20] Asst. Prof., Structural Eng., Mass. Inst. Tech., Cambridge, Mass.

[20a] Received by the Secretary May 2, 1935.

if an extreme case is considered in which the increase in moment is so rapid that an increase of, say, 5% in loading beyond the working load causes the bending stress to be doubled.

The percentages of permissible excess loading shown in Column (19) of Table 3 were computed with the factor of safety based on unit stresses. Table 5

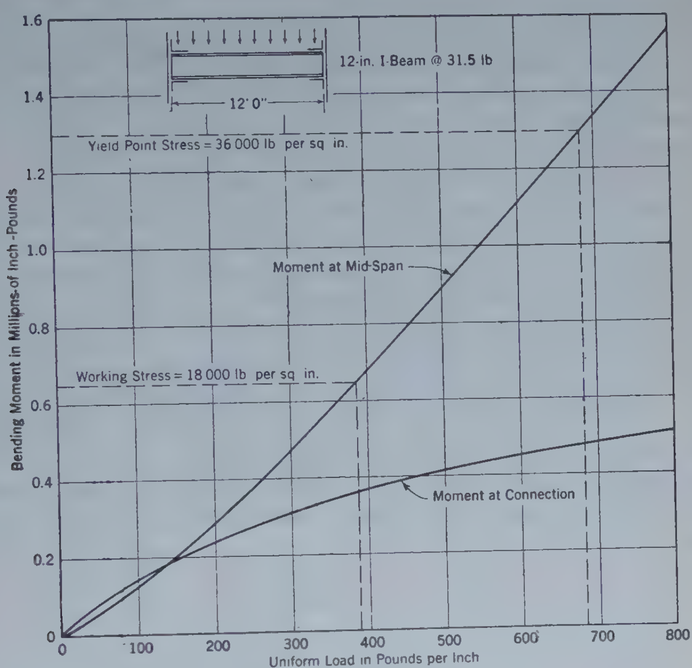

FIG. 38.—RELATION BETWEEN APPLIED LOAD AND BENDING MOMENT

indicates how some of these percentages are reduced if the factor of safety is based on applied loads. The allowable excess load is reduced by an average of about 30 per cent.

TABLE 5.—COMPARISON OF EXCESS (UNIFORM) LOADS DUE TO CONNECTIONS (1 Kip = 1 000 Pounds)

Specimen (see Table 3)	Span length, L, in feet	Load allowed on unrestrained beam, in kips	Load, in Kips, Allowed on Restrained Beam When the Factor of Safety Is Based on:		Percentage Allowable Excess When Factor of Safety Is Based on:		Specimen (see Table 3)	Span length, L, in feet	Load allowed on unrestrained beam, in kips	Load, in Kips, Allowed on Restrained Beam When the Factor of Safety Is Based on:		Percentage Allowable Excess When Factor of Safety Is Based on:	
			Stress	Load	Stress	Load				Stress	Load	Stress	Load
(1)	(2)	(3)	(4)	(5)	(6)	(7)	(1)	(2)	(3)	(4)	(5)	(6)	(7)
2	8	21.3	26.1	24.5	22	15	12	12	36.0	62.4	54.7	73	52
4	12	36.0	41.3	39.9	15	11	15	16	108.1	210.6	184.3	95	71
6	18	59.0	71.8	67.4	22	14	16	22	127.6	248.0	202.0	94	58
8	12	36.0	49.7	44.5	38	24	18	16	108.1	206.0	188.2	91	74
10	12	36.0	56.0	49.2	55	37	..	..	.....	.....	.....	....	....

(2) The author's percentages are based on the use of perfectly rigid supporting columns. Flexibility of the columns has the effect of reducing the allowable excess loading. The greatest effect from this source is likely to be in the upper stories of a building where column sections are relatively small, and the least effect is in the lower stories of a tall building where column sections are large.

(3) Bending moment in the beams of a building frame is reduced at the expense of the columns. Unless the arrangement is such that the end moments in adjacent beams balance each other, the restraining moments are transferred to the columns, and much of the saving in material of beams may be offset by an increase in required material for columns.

(4) Table 3 was compiled for uniform loading which leads to more favorable results than concentrated loading. As an illustration, with a concentrated load at mid-span the percentages for Specimens 10 and 15 in Table 5 are changed from 55 and 95 to 43 and 68, respectively, and Percentages 37 and 71 are changed to 31 and 55, respectively.

(5) From the possible economy in material must be deducted the added cost of the more complex analysis involved in the use of end restraint. The method of analysis undoubtedly would be simplified through experience, but would always be more costly than the analysis with unrestrained connections.

Regardless of whether or not very large savings can be accomplished, information of the type given in this paper is of great value in providing an essential "missing link" in the precise determination of stresses in building frames.

AMERICAN SOCIETY OF CIVIL ENGINEERS

Founded November 5, 1852

DISCUSSIONS

HYDRAULIC LABORATORY RESULTS AND THEIR VERIFICATION IN NATURE

Discussion

BY MESSRS. J. C. STEVENS, AND PAUL W. THOMPSON

J. C. STEVENS,[17] M. AM. SOC. C. E. (by letter).[17a]—"Man marks when he hits but fails to mark when he misses." The author has given some excellent examples confirming the behavior of open river models by prototype performances. It is truly remarkable that the small-scale models and distortions between horizontal and vertical dimensions which it was necessary to adopt, should show such excellent similitude of behavior, and this is all the more remarkable when one realizes that the model sands could not have differed greatly from the prototype sands. To reduce sizes of model sands to simulate prototype sands is impossible, of course. If it were done the model material would be colloidal.

It would have been most instructive if the author could have drawn from his magic bag an example or two in which prototype performance failed to conform to model behavior, and explained the "why" of the failure. It is vitally important to be able to recognize the limitations of models and to stay within those limits. Failures are the most potent means of defining those limitations.

The writer, therefore, offers the following negative "verification" with the belief that it will be just as instructive as the author's positive ones.

Field tests of three of the seven Leaburg siphons were made by the writer, and the results have been fully described.[18] Three models of Siphon No. 7, to scales of 1:20, 1:15, and 2:15, had been made and tested independently, and a study of the published[19] results will reveal the following points of dissimilarity between model and prototype performances:

1.—It was impossible to simulate the cavitation effects found in the prototype. Velocities practically corresponding to a head of 1 atmosphere were

NOTE.—The paper by Herbert D. Vogel, Assoc. M. Am. Soc. C. E., was published in January, 1935, *Proceedings*. Discussion on this paper has appeared in *Proceedings*, as follows: May, 1935, by Messrs. W. F. Heavey, Chilton A. Wright, Paul S. Reinecke, Morrough P. O'Brien, and John A. Jameson, Jr.

[17] Cons. Hydr. Engr. (Stevens & Koon), Portland, Ore.

[17a] Received by the Secretary April 30, 1935.

[18] "On the Behavior of Siphons," by J. C. Stevens, M. Am. Soc. C. E., *Transactions*, Am. Soc. C. E., Vol. 99 (1934), p. 986.

[19] *Transactions*, Am. Soc. C. E. Vol. 99 (1934), p. 1008; also, *Engineering News-Record*, August 18, 1932, p. 187.

found in the Leaburg siphons near the summits. The live stream passing around the summit curves would swing from one side of the barrel to the other, leaving the intermediate spaces filled with pronounced eddies at high negative pressures.

In the model the live stream completely filled the barrel of the three models, and no effect of cavitation was detected.

2.—The coefficients of discharge for the models were higher than for the prototype. Based on the outlet area of the siphon the coefficients of flow, $C = \frac{Q}{A\sqrt{2gH}}$, were:

Models	Coefficient of Flow	Percentage Error of Model
Prototype, No. 7 Siphon..........	0.63	....
1:20 model	0.68	+ 8.0
1:15 model	0.69	+ 9.5
2:15 model	0.71	+12.7

The models showed consistently higher discharges than the prototype, and the larger the model the greater the error. This is believed to be due to the eddy losses in the prototype as a result of cavitation that did not exist in the model.

3.—The depth of flow on the crest of the siphon summit necessary for priming was much less in the prototype than in the model. At first, this was attributed to air leakage around the priming gates of the prototype. In the models, as the fore-bay rose air was compressed in the summit which precluded the possibility of obtaining sufficient depth of flow over the crest to prime quickly.

A small air outlet at the summit of the 2:15 model was provided to simulate the air leakage at the summit of the prototype which improved somewhat the sensitiveness to priming of the model. The question arose: If the leakage around the primer of the prototype were stopped would it require a greater depth of flow to prime? In order to test this, the priming gates of all three siphons were later sealed tightly and tested for priming head. The siphons became more sensitive and primed with less depth of flow than before sealing the gates, as the following will show:

Head Required to Prime, in Feet	Siphon No. 7	Siphon No. 6
Primer unsealed	0.41	0.34
After sealing primer..................	0.19	0.20

The explanation of why the siphon models failed in these important particulars to predict prototype performances probably lies in the fact that the tests were based on the Froudian similitude for gravity forces, whereas friction forces, including eddies and impact, have effects of nearly equal magnitude in producing the phenomenon of flow through them. These friction forces become of great importance in the prototype on account of the high velocities, but are of lesser moment in model performance because of the relatively low velocities that obtain in them.

PAUL W. THOMPSON,[20] JUN. AM. SOC. C. E. (by letter).[20a]—The author "hits a nail on the head" when he refers to the infrequency of the cases in which actual recorded data from a prototype have checked data previously secured from a small-scale model of that prototype. His paper presents the results of what is probably the most extensive, and successful, attempt yet made to confirm model results by actual data from the prototype.

It appears that the illustrations of the paper offer almost conclusive proof to the proposition that small-scale models are capable of yielding dependable qualitative data, even in the cases of problems involving erosion and transportation of débris by rivers. It might even appear from the illustrations that quantitative results have been obtained from the models; however, such appearance is probably coincidental rather than real. There are a few stubborn facts, each of which seems to preclude the possibility of any precise quantitative interpretation of data derived from small-scale models, at least in so far as problems in erosion and transportation of débris are concerned.

To begin with, he who would study problems involving the transportation of débris in natural rivers is confronted by a phenomenon about which little is known. It would not appear to be possible to simulate exactly a phenomenon when the phenomenon itself is imperfectly understood.

The troubles of the experimenter are not confined to the difficulty of attempting to simulate characteristics about which he knows little. Frequently, he finds himself unable to simulate those factors about which he does know something. Thus, most of the models described by the author were built to a horizontal scale of 1 to 1 000 and to a vertical scale of 1 to 100. Such distortion of linear dimensions was necessary and, as the results of the experiments show, was justified. However, there is no question but that distortion affects the behavior in a model. Just what the effects may be seems to be beyond accurate determination at the present time; but it does appear unreasonable to believe that a model which is geometrically similar to a river ten times as deep as the one being investigated, can yield precise quantitative results in regard to the latter.

The fact that data from small-scale models are often not quantitatively dependable should cause no one to conclude that model studies are a waste of time and money. That carefully designed models are capable of yielding data which are qualitatively and comparatively dependable is enough to justify the use of such models in almost any problem in hydraulics involving large expenditures of money. Perhaps a time will come when models which produce quantitative results can be built; however, by that time science will probably know all the answers that the models can give. Meanwhile, the Engineering Profession is indebteded to Lieut. Vogel for another convincing presentation of the possibilities of model research.

---

[20] 1st Lieut., Corps of Engrs., U. S. Army; Asst. to Dist. Engr., Omaha Dist., Missouri River Div., Omaha, Nebr. (Formerly Asst. to Director, U. S. Waterways Experiment Station, Vicksburg, Miss.)

[20a] Received by the Secretary May 8, 1935.

AMERICAN SOCIETY OF CIVIL ENGINEERS

Founded November 5, 1852

DISCUSSIONS

STABILIZING CONSTRUCTED MASONRY DAMS BY MEANS OF CEMENT INJECTIONS

Discussion

By Messrs. Oren Reed, F. F. Fergusson, and Joseph Wright

Oren Reed,[3] Assoc. M. Am. Soc. C. E. (by letter).[3a]—A helpful service to those members of the profession who are interested in the design and maintenance of masonry dams, has been rendered by Mr. Cole. Leaky masonry dams are difficult to repair successfully.

An attempt was made to stabilize the Ringedalsvand Dam, in Western Norway, by cement injections but this method was soon abandoned for another. The writer had occasion to inspect this structure in 1930. The first section, built in 1912–1913, was constructed of granite blocks pointed up with 1:2 mortar. This section has a maximum height of 54 ft. From 1914 to 1918, the dam was raised by constructing a concrete structure back of the initial section and incorporated with it to give a maximum height of 112 ft. The body of the dam is constructed of 1:5:6 concrete with about 30% "plums." The up-stream and down-stream faces are of granite. Back of the stone facing on the water side there is a tightening layer of 1:2½:3 concrete. The thickness of this rich concrete, measured from the water face, varies from 3 ft at the crown to 10 ft at the top of the original masonry dam. Immediately behind the rich tightening concrete is a drainage system consisting of a double row of vertical drain pipes on 24-in. centers. These vertical pipes are connected to a horizontal header, which empties into the inspection gallery, whence the water is conducted to the down-stream face of the dam.

An effort was made to inject cement into the tightening layer during the summer of 1927, in two adjacent blocks of the structure, which constituted a length along the crown of 180 ft. In all, thirty-seven grout holes and six observation holes were bored for testing and grouting. They were located about 3 ft from the up-stream face and were bored vertically to depths

Note.—The paper by D. W. Cole, M. Am. Soc. C. E., was published in February, 1935, *Proceedings*. This discussion is printed in *Proceedings* in order that the views expressed may be brought before all members for further discussion.

[3] Asst. Engr., Tennessee Val. Authority, Pickwick Landing Project, Corinth, Miss.

[3a] Received by the Secretary April 22, 1935.

varying from 50.4 ft to 72.8 ft. Near the bottom, the holes were 5.9 ft from the up-stream face and 4.6 ft from the vertical drain pipes. A total of 2 300 ft of ordinary injection holes were bored, together with 390 ft of observation holes.

The first holes were spaced 9.8 ft apart, but the distance was found to be too great and intermediate holes were bored. Pressure tests and observations indicated that the 4.9-ft spacing was still too great, but it was not decreased. The holes were not bored to their full depth at one time, but in stages, depending on the soundness of the concrete. The tightness of each length of hole was tested by water pressure. Cement was injected at a pressure varying at the nozzle from 0 to 294 lb per sq in. A total of 276 600 lb of cement was used, divided into the four groups of holes as shown in Table 4. The part of the dam under treatment had an area of about 11 300 sq ft. Therefore, more than 24 lb of cement was used per sq ft of dam surface.

TABLE 4.—Cementation Record, Ringedalsvand Dam, Norway

Group No.	Cement used, in pounds	Total length of bore holes, in feet	Average use of cement, in pounds per foot
1	70 600	621	113.7
2	29 900	548	54.5
3	126 900	1 126	112.7
4	49 200	390	126.0

For Groups Nos. 1, 2, and 3, Table 4, a mixture of approximately equal parts of cement and water was used, or about 9.9 lb of cement per gal of water. A thin mixture (3.9 lb per gal) was used in Group No. 4. As shown in Table 4, an average of 113.7 lb of cement per ft of hole went into Group No. 1, where the distance between holes was 9.9 ft, whereas only 54.5 lb of cement per ft went into Group No. 2, which was placed midway between the holes of Group No. 1. There was considerable variation, however, between the cement use of the different holes. Injection in five of the six observation holes, which were placed between the holes of Groups Nos. 1 and 2, showed the largest average use of cement—127 lb per ft of hole. A thin mix of 3.6 lb of cement per gal of water, was used for these holes. The injected material had probably spread over a large area, especially up stream to the stone facing and down stream to the drainage system. For the most part, the cement was injected when the lake level was low, but some holes were treated when the water level was at its full height. The leakage water did not seem to indicate a severe loss of cement.

The objective which was set up at the beginning of the work, respecting the clogging of the drainage system, was not attained. The cement paste did not reach the inspection tunnel except in a few places, but the drainage system was put out of operation at several places, as evidenced by the leakage which appeared on the down-stream face of the dam directly back of the injected section. Measurement of the leakage before and after the cement injection showed that about 76% of the leakage was stopped.

The following conclusions were drawn from the cement injection trial at the Ringedalsvand Dam:

(1) The result of the injection was not fully satisfactory. Even if a large part of the leakage was stopped, a relatively large part still remained. Removal of soluble material in the concrete would continue, therefore and it would probably only be a question of time until the injection must be repeated.

(2) Pores, holes, and passages in the concrete were partly filled with a dark organic slime, or had a coating of slime on the wall surfaces. During the injection the cement would mix with the slime, and the slime would possibly hinder or weaken the setting and hardening of the cement. In all cases there would be a film of slime between the concrete surface in the pores and holes, and the injected cement.

(3) For a dam with a drainage system immediately behind the tightening layer, it will be difficult with cement injected in the foregoing manner to prevent partly filling the drainage system. Therefore, leakage will find a way through the lean concrete in the down-stream part of the section, and wash out the soluble portion.

Due to the foregoing disadvantages of the cement-injection method, it was not continued and other solutions were studied for the repair of the dam. The adopted method of reconstruction, begun in 1929, consisted of building a concrete flat-slab dam $6\frac{1}{2}$ ft in front of the up-stream face of the old dam and resting against it on struts. The new vertical deck was proportioned to take the full water load so that the only purpose served by the original dam is as a support. This work was completed in 1931.

F. F. FERGUSSON,[4] ASSOC. M. AM. SOC. C. E. (by letter).[4a]—Because it is a record of a difficult work, completed satisfactorily, and because its author has given such precise detail as to the method followed, this paper should prove of great practical value. It is particularly interesting and valuable to engineers in India because it draws attention to weaknesses in a type of construction which is probably peculiar to that country, namely, the use of lime instead of cement mortar or Portland cement concrete, in hydraulic structures.

The widespread use of lime is due to its general occurrence geologically in the form of "kankar", the ease with which it is quarried and prepared, and, consequently, its cheapness as compared with cement. The cost of masonry work in lime mortar in the region around Jodhpur is less than one-half that of masonry in cement mortar and less than one-quarter the cost of massive concrete work; these considerations force the engineer to use the lime prepared locally for almost all work, important or otherwise.

The weakness of lime when used for hydraulic works, such as dams, canal walls, and overflow weirs, is abundantly in evidence in many parts of India, but probably no where more so than in Rajputana, where the surface of the country is littered with masonry walls of all sizes built across stream beds

---

[4] Senior Executive Engr., Dept. of Public Works, Jodhpur Govt., Jodhpur, Rajputana, India.

[4a] Received by the Secretary April 29, 1935.

and depressions for the purpose of arresting the flow of water and storing it for use during the few months immediately succeeding the monsoons, when wheat cultivation is undertaken. At some time or other during their life, a high percentage of these walls or dams have been breached, and the reason puzzled the writer because many of the structures observed were statically stable even with greater overtopping than could have occurred. Eventually, it was traced to the fact that water gains access through joints in the mortar and eventually passes through the wall, leaching out the lime in its passage. This action has been found to be especially drastic in a wall through which the writer had to cut recently in making some modifications. The wall, which is subjected to a pressure due to 25 ft of water, is 5 ft thick at the ground level and is backed by a bank of sand on both sides, the bank on the water side being pitched to protect it from wave action. The rock used in the masonry is a hard rhyolite that splits with smooth faces. It has been found that the lime has poor adherence to this stone and probably this may be said of the trap-rock, of which the dams described in Mr. Cole's paper, are constructed. It is also a well-known fact in Rajputana that the local masons prefer to work with sandstone and not with granite or rhyolite, because they find difficulty in making the lime "stick" to the stones.

The writer has constructed several small dams in sandstone or rhyolite, according to the geological formation of the locality, but in all cases the greatest care has been exercised to grind the lime fine and to use a mixture of 1 part lime to 1 part clean sand, to avoid regular courses in the masonry, and, finally, to rake out the mortar in both the up-stream and down-stream faces, and to point deeply with a mortar consisting of 1 part cement to 2 parts fine clean sand. This procedure has prevented leaks effectively and should form a rigid part of all specifications for this class of work.

The author's reflections on the stability of gravity dams is also of interest, as the writer has in his jurisdiction a 25-ft masonry dam, built about forty years ago, in which the resultant, due to water level with the crest, falls far outside the middle-third. The masonry is so deplorably poor that the dam is emptied through leaks within a few weeks of filling; it has had a 3-ft surcharge over its entire length and yet has shown no sign of failure. Notwithstanding these facts the writer agrees entirely with the author's final paragraph.

JOSEPH WRIGHT,[5] M. AM. SOC. C. E. (by letter).[5a]—This is a most concise and thorough account of a novel and interesting job well done, wherein experience, meticulous care, and a full understanding of the difficulties encountered, and the hazards, involved, were conspicuously essential to the success attained. The profession is much indebted to the author for a full and clear description of the work.

The work on these important Indian dams indicates not only what may be done to save defective dams, but emphasizes more forcibly what must be done to avoid such defects. A dam that permits water to percolate through

[5] U. S. Engr. Office, Nashville, Tenn.

[5a] Received by the Secretary July 17, 1935.

it cannot be classed as a safe, permanent structure, whether built of stone or concrete, and the remedy is to use a dense concrete or mortar well placed, with special care given to construction joints.

The close spacing and total length of drill holes required and the quantity of cement used is staggering, but is not surprising when it is considered that the dams are of uncoursed rubble masonry and that much of the grout would inevitably be lost in the reservoir or through the down-stream face. For a few of the most serious of these leaky holes the writer is inclined to think the use of asphalt by the "Christians'" process would have saved many tons of cement which found its way out of the dam section, and would have facilitated the cementation process.

Since no dimensions are given upon the dam sections shown, the author's comments concerning their refusal to fail as would be expected in accordance with accepted principles of instability, cannot be verified. The sections do seem light; and although the writer can agree fully that dam builders "should take no chances on the soundness of their materials, or the competency of their workmanship and field direction", he cannot agree that any chances should be taken in the provision for uplift. If all dams were founded upon basalt, or granite, one might reduce the allowance for uplift with safety. Dams fail more often by sliding upon strata beneath their bases; and where the foundation rock is stratified and horizontally bedded, it is believed that designers err more often in the other direction. In his closing discussion, it is hoped that the author will supply dimensions of dam sections, and will show the resultants of forces acting upon their bases.

On the whole, this paper is a model for a concise, clear-cut, detailed review of a completed job, and is most valuable for the data presented.

AMERICAN SOCIETY OF CIVIL ENGINEERS

Founded November 5, 1852

DISCUSSIONS

THE HYDRAULIC JUMP IN TERMS OF DYNAMIC SIMILARITY

Discussion

By Messrs. F. V. A. E. Engel, Baldwin M. Woods, and J. C. Stevens

F. V. A. E. Engel,[29] Esq. (by letter).[29a]—The investigations reported in this paper are of particular interest to the writer and they are a valuable contribution to the application of a dimensionless presentation of hydraulic test results in open-channel flow. In these days the application of the Reynolds number is a common occurrence in analyzing the frictional coefficient in closed conduits, the discharge coefficient of orifices and Venturi tubes, etc. Nevertheless, few papers deal with the specific problems of open-channel flow on that basis.

Several pages of the paper refer to "Theoretical Premises," which involve the Reynolds, Froude, and Boussinesq numbers. The remarks concerning the Reynolds number are quite consistent with the usual conception of that expression in hydraulic engineering, but the writer would like to suggest some modification of the sections on the Froude and Boussinesq numbers, especially as he feels himself responsible for introducing a term which has been called the "Boussinesq" number.

The kinetic flow factor, known as the Froude number, was applied for the first time in a similar form by Th. Rehbock in 1919 for the calculation of the head losses for water flow through bridge piers. This factor (see Equation (2)) is given as twice the ratio of the kinetic energy head to the potential energy head contained in each pound of liquid flowing at the depth, d. The velocity, V, is the mean velocity obtained by dividing the rate of flow through the cross-section of the stream. This expression certainly is very convenient and may also be sufficient in some cases; but Coriolis, de Saint Venant, and others have shown that it is often necessary to use a value which takes into

Note.—The paper by Boris A. Bakhmeteff, M. Am. Soc. C. E., and Arthur E. Matzke, Jun. Am. Soc. C. E., was published in February, 1935, *Proceedings*. Discussion on this paper has appeared in *Proceedings*, as follows: March, 1935 by Hunter Rouse, Esq.; and May, 1935, by Messrs. Sherman W. Woodward, Robert E. Kennedy, L. Standish Hall, and Morrough P. O'Brien.

[29] Director of Research, Electroflo Meters Co., Ltd., London, England.

[29a] Received by the Secretary April 24, 1935.

account the velocity distribution over the cross-section. For such conditions the kinetic energy is greater than the kinetic energy based on the mean velocity,[30] and, therefore, Equation (2) becomes:

$$\epsilon = \epsilon_p + \epsilon_k = d + \frac{\alpha V^2}{2g} \qquad (38)$$

in which α is greater than unity.

Equation (12), therefore, would become:

$$\lambda = 2 \frac{\epsilon_k}{\epsilon_p} = \frac{\alpha V^2}{g d} \qquad (39)$$

This expression, including α, would certainly be rather tedious to evaluate, and the reason for presenting it is mainly to show that the relations given by the authors are not quite as simple as they would indicate. They point out that "the hydraulic radius is related inherently with friction effect." In turn, the friction effect influences the velocity distribution and also the new term, α, in Equations (38) and (39). It seems quite reasonable to combine α and d in Equation (39) in such a manner that it becomes:

$$\lambda = \frac{V^2}{g \dfrac{d}{\alpha}}$$

and to replace the ratio, $\frac{d}{\alpha}$ (which has the dimensions of a length, but also takes into account the velocity distribution), by r', the hydraulic mean radius, obtaining Equation (18), the dimensionless quantity which has been called the Boussinesq number.

The writer has made extensive use of both the Froude and Boussinesq numbers in his present investigations on flow through side-contracted open channels (Venturi flumes).[31] The Froude number characterized a type of flow which is known as "free discharge." For a given rate of flow "free discharge" is defined as that condition under which the up-stream depth is unaffected, whatever the down-stream conditions may be.

The occurrence of a hydraulic jump could not always be determined by a "critical" Froude number. Rehbock[32] and other investigators also found that the "critical depth" had not yet been reached by the water level in the narrowest section of the contraction in spite of the appearance of surface rollers, which are commonly attributed to the presence of a hydraulic jump. Rehbock regarded this "partial change to rapid flow" ("Teilweiser Fliesswechsel") as being due to an uneven velocity distribution. In some section of the water stream, there is a sufficiently high velocity to produce a state of rapid flow.

The writer has analyzed[33] the expression which Professor Rehbock used to determine the first occurrence of a hydraulic jump. Rehbock's relation is

[30] "Elemente der Technischen Hydromechanik," by R. v. Mises, Leipzig and Berlin, 1914, pp. 153–155.

[31] "Non-Uniform Flow of Water: Problems and Phenomena in Open Channels with Side Contractions," by F. V. A. E. Engel, *The Engineer*, Vol. 155 (1933), pp. 392 to 394; 429 to 430; and 456 to 457; and "The Venturi Flume," *The Engineer*, Vol. 158 (1934), pp. 104 to 107; and 131 to 133.

[32] *Zentralblatt der Bauverwaltung*, Vol. 39 (1919) pp. 197 to 200.

[33] "Venturi-Kanalmesser: Die messtechnischen Eigenschaften in Abhängigkeit von den Strömungsarten," by F. V. A. E. Engel, *Archiv für technisches Messen*, No. 45, March, 1935.

a function of the Froude number and for that reason is not satisfactory to determine the change from streaming flow to rapid flow. The "critical" Boussinesq number was found to be more reliable over a wide range of flow to characterize the change from one type to another.[33]

The attacks on the Boussinesq number seem to the writer to be relatively unfounded. Three different applications have proved the usefulness of this number. The practical engineer must judge the merits of a new expression, especially with regard to the extent to which it simplifies the presentation of hydraulic test results, even if the definite theoretical proof is not yet established.

In three cases the application of the Boussinesq number has been found to yield some simplification in presenting the following hydraulic features:

(1) The discharge coefficient of a Venturi flume in the range of rapid flow is a linear function of the Boussinesq number.[31]

(2) The dissipation of energy in the case of a Venturi flume for the "limit of free discharge" can be presented in a simplified way by plotting the ratio of the down-stream depth to the up-stream depth against the Boussinesq number for a section in the throat;[31] and

(3) The change from turbulent or streaming flow to rapid flow is given by a critical Boussinesq number which determines the first occurrence of a hydraulic jump.[33]

It would have been very interesting if the authors had published the different features of the hydraulic jump in cases where the up-stream depth, or the depth at the foot of the hydraulic jump, exceeds the hydraulic mean radius. From Table 1, the writer perceives that the investigators cease their investigations at a point where the depth at the foot of the jump exceeds the value of the hydraulic mean radius. Furthermore, in Fig. 3, some test results in the range of the undulating jump (that is, for values of the kinetic flow factor smaller than 3) would be of general interest.

BALDWIN M. WOODS,[34] ESQ. (by letter).[34a]—As one interested in fluid mechanics, although more especially in aerodynamics, the writer desires to endorse heartily the plan of attack followed in this paper and the presentation of results in generalized, dimensionless form through the aid of the principle of dynamic similarity. From practical considerations alone, the growing interchange of material between countries having differing systems of units, such as the English and the metric, makes it highly important to have results equally useful regardless of the basic system of units. Furthermore, as has been so often noted, the method of dynamic similarity causes one to give careful scrutiny to the variables involved and to the most significant simple combinations of these variables into coefficients or parameters.

There is also much to be said in favor of the tri-dimensional representation of the profile, as given in Fig. 9. Engineers generally need to culti-

[34] Prof. of Mech. Eng., Univ. of California, Berkeley, Calif.

[34a] Received by the Secretary April 29, 1935.

vate familiarity with these three-dimensional presentations and facility in reading them. They are labor-saving devices, much simpler in actual use than the combination of several two-dimensional charts, which are otherwise necessary. The entire Engineering Profession is indebted to the authors for the elegance of treatment resulting from the discrimination exercised in selecting this form of presentation.

J. C. STEVENS,[35] M. AM. SOC. C. E. (by letter).[35a]—In presenting the results of their research on the length of the jump, the authors have made a most valuable contribution to hydraulics. They might have made a more happy choice of symbolism, however. The writer has found the notation, which follows Professor Bakhmeteff's book entitled "Hydraulics of Open Channels,"[36] quite a "hazard" in mastering this paper.

There are only two independent characteristics of the hydraulic jump, the initial depth and the initial velocity. From them are derived the initial energy head, the final depth, final velocity, the final energy head, the lost energy head, and the empirical characteristic—length. If these factors are expressed in terms of any other, a series of ratios is obtained which expresses the characteristics of the jump in dimensionless terms of dynamic similarity.

The authors have chosen the initial energy head as the denominator of their dimensionless terms. Mr. E. S. Crump[37] has expressed the jump characteristics in terms of Belanger's critical depth. Mr. G. A. M. Brown[37] has expressed them in terms of the lost energy head. The writer following Woodward[38] and others has chosen to express them in terms of the initial depth. Thus, the dimensionless terms, in reality, become jump dimensions for a unit initial depth. Viewed in this light, such a jump may for brevity be termed a "unit jump," and a far simpler conception of it is had by thinking of it as such than through any other set of dimensionless terms. There appears to be no advantage in the use of the "kinetic flow factor," λ, over the ratio of initial kinetic to potential energy. This ratio, $k = \frac{V^2_1}{2\,g\,d_1}$ (which equals $\frac{\lambda_1}{2}$), has the limiting value of 0.5 for critical velocity, which expresses the simple criterion for critical flow that, in any shape of channel whatever, the velocity head is one-half the mean depth.

The authors' height of jump, $d_j = d_2 - d_1$, in practical applications is quite inferior to the ratio heretofore used by Woodward and others, namely, $J = \frac{d_2}{d_1}$, particularly when dealing with jumps in channels other than rectangular.

---

[35] Cons. Hydr. Engr. (Stevens & Koon), Portland, Ore.

[35a] Received by the Secretary April 30, 1935.

[36] Eng. Societies Monographs, McGraw-Hill Co., 1932.

[37] "The Standing Wave or Hydraulic Jump," *Publication No. 7*, Central Board of Irrig., Simla, India.

[38] Technical Repts., Pt. III, Miami Conservancy Dist.

The writer suggests the following simplified notation: Let d_1 = initial depth; d_2 = final depth; h_1 = initial velocity head; h_2 = final velocity head; E_1 = initial energy head = $d_1 + h_1$; E_2 = final energy head = $d_2 + h_2$; I = energy lost by impact and eddies = $E_1 - E_2$; and L = length of jump.

Then the following dimensionless terms apply in a "unit jump": $k = \frac{h_1}{d_1}$; $J = \frac{d_2}{d_1}$; $e_1 = \frac{E_1}{d_1}$; $e_2 = \frac{E_2}{d_1}$; $i = \frac{I}{d_1}$; and $l = \frac{L}{d_1}$.

In a rectangular channel, of unit width, the fundamental relationship applies:

$$J^2 + J = 4\,k \quad \text{......(40)}$$

which may be verified from Equation (16) by substituting $2k = \lambda_1$. The jump characteristics may now be expressed in terms of either k, or J, or both. Thus:

$$e_1 = k + 1 \quad \text{......(41)}$$

$$e_2 = J + \frac{k}{J^2} \quad \text{......(42)}$$

and,

$$i = e_1 - e_2 = \frac{(J - 1)^3}{4\,J} \quad \text{......(43)}$$

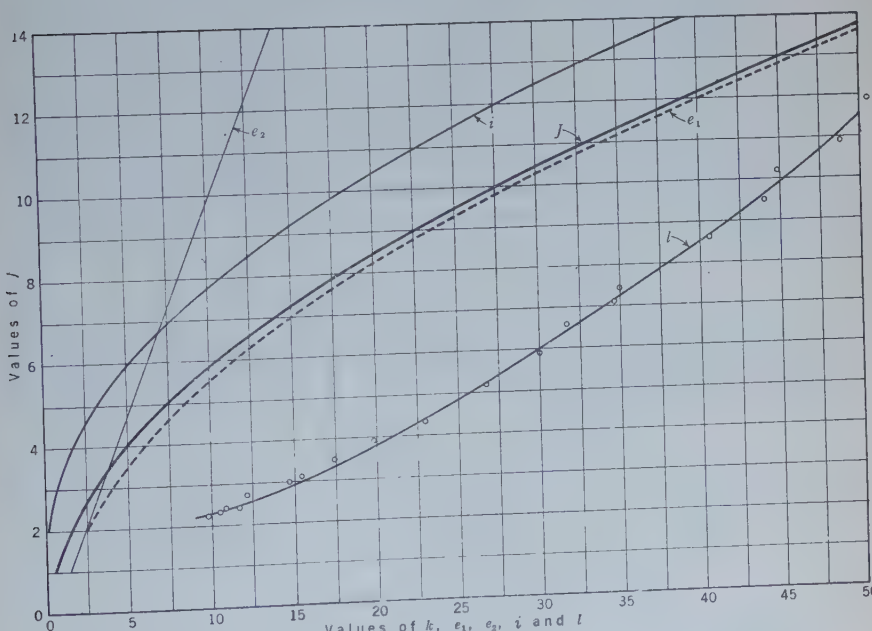

FIG. 10.

Fig. 10 shows the dimensionless characteristics of the unit jump in terms of either k or J. Curve J, as a function of k, is fundamental, and through

it values of e_1, e_2, i, and l are found in terms of either k or J. The length is an empirical ratio obtained by averaging the values in Columns (13) and (14), Table 1.

It is significant to note in Fig. 10 that the characteristic curves are without points of maxima or minima. There is no maximum height of jump. The authors' maxima for d'_2 and d'_j, in Fig. 3, are not physical characteristics of the jump at all, but merely consequences of the terminology in which its characteristics are set forth. As a matter of fact these so-called maxima are for very low jumps: $d'_2 = 0.800$ for $\lambda_1 = 3$ corresponds to $k = \frac{3}{2}$ and $J = 2$, also $d'_j = 0.507$ at $\lambda_1 = 7.674$ corresponds to $k = 3.84$ and $J = 3.45$.

The advantage of the writer's terminology becomes apparent when expressions for the characteristics of the jump are desired for channels other than rectangular. Fig. 10, like Fig. 3, is applicable only to rectangular conduits and to unit widths. The fundamental relationships between J and k, however, may be found for a wide variety of conduits.[39] Once this relationship is found the other characteristics follow logically.

The general dimensionless formula for height of jump in a trapezoidal channel is:

$$J^4 + \left(\frac{5}{t}\,t + 1\right) J^3 + \left(\frac{3}{2}\,t^2 + \frac{5}{2}\,t + 1\right) J^2$$
$$+ \left[\frac{3}{2}\,t^2 + t - 6\,k\,(t + 1)\right] J - 6\,k\,(t + 1)^2 = 0 \quad \ldots\ldots (44)$$

in which $t = \frac{b}{s\,d_1}$; b = bottom width; and s = the side slopes (that is, s on 1); if the two side slopes are different, s is the average of the two. For a rectangular channel $s = 0$, and it can be shown that Equation (44) reduces to Equation (40). For a triangular conduit $b = 0$, and Equation (44) reduces to:

$$J^4 + J^3 + J^2 - 6\,k\,(J + 1) = 0 \quad \ldots\ldots\ldots\ldots\ldots (45)$$

Considering a conduit with a cross-sectional area that may be expressed by the exponential function, $a = K d^n$, in which K is a determinable constant, the height of the jump is given by,

$$\frac{J^n\,(J^{n+1} - 1)}{J^n - 1} = 2\,k\,(n + 1) \quad \ldots\ldots\ldots\ldots\ldots (46)$$

For a parabolic section, $n = \frac{3}{2}$, and Equation (46) becomes,

$$J^4 - (5\,k + 1)\,J^3 + 5\,k = 0 \quad \ldots\ldots\ldots\ldots\ldots (47)$$

[39] "The Hydraulic Jump in Standard Conduits," by J. C. Stevens, M. Am. Soc. C. E., *Civil Engineering*, October, 1933, p. 364; also, discussion by G. H. Hickox, Jun. Am. Soc. C. E., *Loc. cit.*, May, 1934, p. 270. In these papers the ratio, r, is used instead of k. The latter is preferable and avoids the possibility of confusing it with the hydraulic radius.

In channels, the cross-sectional areas of which are segments of circles, a table of hydrostatic pressures is essential. Such a table and an explanation of its use in finding the height of the jump in circular conduits will be found in the writer's paper previously cited herein.[39]

In irregular channels the characteristics of the jump may be found graphically from the energy and momentum-plus-pressure curves as outlines[40] by Julian Hinds, M. Am. Soc. C. E.

All the foregoing expressions are dimensionless and for any given channel, involve only the two simple ratios, k and J, which are sufficient for the complete solution of the hydraulic jump. While the expressions are of many degrees, they are in effect single valued, since for every value of k there is only one value of J that will fulfill the physical conditions, and *vice versa.* Once k is known J is readily found by trial.

The writer questions the significance given to the "zone of undulating jumps" (Fig. 3). Fig. 7 shows a gradual transition from stable to undulating jumps as the ratio of kinetic to potential energy is diminished. Quite properly, the authors refrain from putting these results in terms of the initial energy because of the accelerations involved and the consequent departure from hydrostatic pressures, in the water prism.

In reality is not this "undulating jump" merely a "hang-over" from the oscillations that always accompany critical flow? At critical flow depths may vary considerably without appreciably changing either the energy or momentum-plus-pressure values. As a consequence the surface is in an unstable state and pronounced waves occur. For such conditions there is no jump, and in all the foregoing equations $J = 1$ and $k = \frac{1}{2}$ (the authors' $\lambda = 1$). If, now, the kinetic energy is increased and the potential energy is reduced ever so slightly (as, for example, by closing the sluice-gate) both k and J increase in value and a low jump occurs; but the flow is still barely removed from the critical, and the surface waves persist. These waves gradually fade away, as the ratio of kinetic to potential energy increases, and sensibly disappear for $k = 2$, say ($\lambda_1 = 4$). In reality, are there any valid grounds for stating that "the region near $\lambda_1 = 3$ is a zone of transition?" The range of undulations is for all values of λ_1 less than 4, and the less the value of λ_1 the greater the undulations. The point the writer wishes to bring out is that there appears to be no more reasons for setting up two kinds of jumps[41]—the "undular form" and the "direct form"—than for drawing a distinction between big jumps and little jumps.

The data on length of jumps are particularly interesting. The length expressed in terms of $d_2 - d_1$, varied from about 8 to 4.5, the latter value probably approaching a lower limit for which one may state that the kinetic energy expended can not cause the water to stand on a much steeper slope than 1 on 4. The upper limit, of course, is infinity for critical flow—at which

[40] "The Hydraulic Jump and Critical Depth in Design of Hydraulic Structures," *Engineering News-Record*, November 25, 1920, p. 1034; see, also, the *M*-function, "Hydraulics of Open Channels," by Boris A. Bakhmeteff, M. Am. Soc. C. E., p. 232.

[41] "Hydraulics in Open Channels," by Boris A. Bakhmeteff, M. Am. Soc. C. E., Eng. Societies Monograph, 1932, p. 228.

there is no jump. The writer believes that for the sake of consistency the authors' ratio, $\frac{L}{d_1}$ (Table 1), is to be preferred, and this is the ratio given in Fig. 10.

The length of the jump must be the resultant of two motions: (1) The translatory motion of the prism down stream; and (2) the vertical motion due to the rate of conversion of kinetic to potential energy. The physical phenomena involved in this conversion are but little known. It appears that the greater the initial kinetic energy the more rapidly is this conversion effected; hence, the shorter lengths accompany the expenditure of the greatest amount of kinetic energy.

One practical value of these data is that now something tangible is available by which the length of the apron at the foot of overflow dams, and the spacing of baffles, can be determined rationally. Knowing the fall from forebay to apron, and the discharge, the initial depth on the apron is readily found. The height, and now the length, of the jump may be expressed in terms of this depth.

AMERICAN SOCIETY OF CIVIL ENGINEERS

Founded November 5, 1852

DISCUSSIONS

FRICTIONAL RESISTANCE IN ARTIFICIALLY ROUGHENED PIPES

Discussion

By Messrs. Warren E. Wilson, Richard G. Folsom, and Ralph W. Powell

---

Warren E. Wilson,[15] Jun. Am. Soc. C. E. (by letter).[15a]—A well-planned program of research is indicated by this paper; the author has obtained results which, without doubt, are a valuable addition to the present knowledge of the characteristics of flow in pipes. The writer will make no attempt to evaluate the results, but will endeavor only to comment on the methods used to measure the loss of head in the test section of pipe.

Differential manometers were used with the evident purpose of obtaining large readings when the loss of head was small. If one assumes that the difference in elevation of the menisci in a differential manometer gives a true measure of the actual pressure difference which it is desired to observe, and if one bases his computations on the usual formula:

$$z_m = \frac{w}{w - w_k} H \quad \text{(12)}$$

(in which z_m is the manometer reading; w, the specific gravity of water; w_k, the specific gravity of the gauge liquid; and H, the pressure difference under observation), the value of H which is calculated will generally be in error, as has been demonstrated on a previous occasion.[16]

The magnitude of the error in any manometer reading depends on the liquids and the form of the menisci. The height of rise of a liquid interface in a capillary tube may be computed from the expression,

$$h = \frac{4\,\sigma \cos\theta}{g\,D_t\,(w - w_k)} \quad \text{(13)}$$

in which σ is the surface tension expressed in dynes per centimeter; h, the

---

Note.—The paper by Victor L. Streeter, Jun. Am. Soc. C. E., was published in February, 1935, *Proceedings*. This discussion is printed in *Proceedings* in order that the views expressed may be brought before all members for further discussion.

[15] Research Asst., California Inst. of Technology, Pasadena, Calif.

[15a] Received by the Secretary March 15, 1935.

[16] "Differential Manometers Investigated," *Civil Engineering*, January, 1934, p. 30

height of rise, in centimeters; θ, the angle of contact between meniscus and wall of the tube; g, the gravitational constant; and D_t, the diameter of the tube, in centimeters.

If the menisci form as in Fig. 15(*a*) the error of the reading is zero, providing the angle of contact is the same in the two tubes. If the formation is

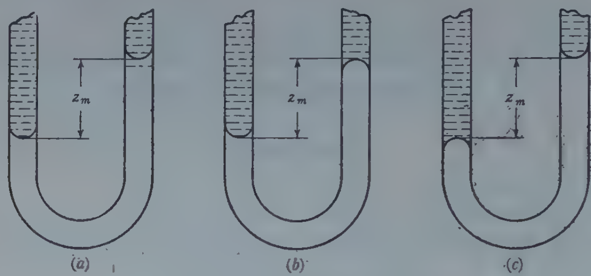

FIG. 15.

as shown in Fig. 15(*b*) the reading, z_m, is smaller than Equation (12) would indicate by an amount not greater than 2 h, in which h is given by Equation (13), since each meniscus has an effect which probably does not exceed that of a single meniscus in a capillary tube. If the formation is as shown in Fig. 15(*c*), the reading, z_m, is larger than Equation (13) would indicate by an amount not greater than 2 h.

As a specific case, consider the manometers used and described by Mr. Streeter. The inside diameter of the tubes was about 6 mm. The liquids were acetylene tetrabromide, and xylene, with surface tension values of approximately 36 to 38 dynes per cm. The specific gravities of the solutions were about 1.3, 1.05, and 2.97. Assuming the specific gravity of water to be unity (that is, neglecting the effect of temperature), the values of h may be computed by means of Equation (13).

The foregoing comments have shown that the error in a reading could vary from zero to 2 h. This error will correspond to an error in the computed head, H, which is H_f and will depend on the multiplication factor of

TABLE 3.—POSSIBLE ERROR IN H_f WHEN COMPUTED FROM z_m BY EQUATION (13)

Specific gravity (1)	Multiplication factor (2)	Height of rise, h, in centimeters (3)	Possible error in z_m, in centimeters (4)	Possible Error in H_f When Computed from z_m, in Equation (13)	
				In centimeters (5)	In feet (6)
1.05	20.0	5.03	10.06	0.503	0.0165
1.30	3.33	0.838	1.68	0.503	0.0165
2.97	0.508	0.128	0.256	0.503	0.0165

the manometer. Table 3 which is based on an assumption of the value of σ as 37 dynes per cm, and of the value of θ as zero, indicates the possible limitations of the manometer.

It is obvious that the possible error in the measurement of the loss in head does not depend on the multiplication factor of the gauge, but on the diameter of the tubes and the surface tension at the interfaces. The possible error may be expressed by Equation (14) when H_e denotes the error in the measurement of H_f which is possible for any given manometer:

$$H_e = \frac{8\,\sigma}{g\,D_t}\text{ (in centimeters)} = 0.000268\,\frac{\sigma}{D_t}\text{ (in feet)} \qquad (14)$$

in which the specific gravity of water is assumed to be 1.0, and θ is assumed to be zero.

It should not be inferred from these statements that Equation (14) will give an exact value for a correction to be applied to the computed loss of head. There are too many important factors which have been neglected to permit such a simple method of correction. For instance, the cleanliness of the tubes controls the magnitude of θ to a great extent. In practice, it is found that the form of the meniscus varies widely and hence the angle is by no means constant.

The writer wishes to emphasize the magnitude of the error that may occur in any one reading of a differential manometer. It is his belief that the water-air manometer is best suited to the type of work described by the author, and will give quite as satisfactory results as a differential manometer using any liquid known to him. It must not be concluded that any serious errors exist in the research reported in this paper. It seems very probable that the wide scattering of the points in Fig. 11 for low values of the Reynolds number, may be at least partly explained by attributing an error to the manometers. For the lowest head observed, 0.0265 ft in Run I, the possible error is 62%, but for all heads of 1.65 ft, or more, the error is less than 1 per cent. However, the writer has found that the variation of the readings from the value predicted by Equation (12) seldom reaches the value given in Equation (14) and probably averages about one-third this value. However, it seems reasonable to believe that, with the ordinary water-air manometer, one can obtain an accuracy of 0.003 ft of water, which is better than what might be expected with the author's manometers even when the values given by Equation (14) are reduced by two-thirds.

RICHARD G. FOLSOM,[17] ESQ. (by letter).[17a]—Valuable experimental data regarding characteristics of rough surfaces are recorded in this paper. The method of expressing roughness in terms of the equivalent sand size is an interesting and practical one, particularly as Nikuradse[14] has obtained excellent results in the application of Equation (10). A further understanding of the frictional resistance requires a study of the mechanism of flow past the roughened surface.

[17] Instr. in Mech. Eng., Univ. of California, Berkeley, Calif.

[17a] Received by the Secretary April 22, 1935.

[14] "Strömungsgesetze in rauhen Röhren," von J. Nikuradse, Verein Deutscher Ingenieur, *Forschungsheft*, No. 361, 1933.

In 1931, the writer conducted a series of tests[18] to investigate the characteristics of ultra-rough surfaces formed on the concentric core of an annular section. Flow pictures of aluminum-bronze particles and friction-factor determinations were made. Three views for different degrees of roughness are presented in Fig. 16, which demonstrates clearly the totally different types of flow existing for various groove dimensions.

Fig. 16(*a*) illustrates conditions when the projections causing roughness are placed relatively close together. A whirl is formed in the grooves which

(*a*) (*b*) (*c*)

FIG. 16.—FLOW PICTURES OF ALUMINUM BRONZE PARTICLES. (ARROWS INDICATE DIRECTION OF FLOW).

prevents the flow of fluid into these spaces; hence, this type of roughness produces only small divergencies from flow over a smooth surface. Fig. 16(*b*) and Fig. 16(*c*) illustrate the flow when the grooves are large enough to allow the

[18] "An Experimental Investigation of the Phenomena Produced by the Highly Turbulent Flow of Water Past a Series of Sharp Obstacles," by R. G. Folsom, presented to California Inst. of Technology in 1932, in partial fulfillment of the requirements for the degree of Doctor of Philosophy.

inflow of fluid behind the whirl. For Fig. 16(*b*), the spacing of projections is a minimum for this type, and hence gives a maximum frictional resistance. Fig. 16(*c*) shows that the same flow conditions occur at wider separations of projections. Motion pictures of these flows show successive formation and sweeping out of the whirls or vortices. Measurements indicated that maximum friction occurred when the depth of the groove was about one-fourth the spacing, this relation holding throughout the investigated range of relative roughnesses (ratio of projection length to length between walls).

These and other photographs indicate that a rough surface produces disturbances which spread throughout a large part of the flowing fluid. Contrary to the author's statement (under heading "Discussion of Results: Roughness III") that, "this indicates that a projection causes greater turbulence than a groove," the disturbance depends on the shape of the groove due to its control of the action of the vortices. The whirl or vortex formed has a diameter of the same order of magnitude as the depth of the groove, but the size and shape of the groove determines when the vortex will pass out into the main flow and dissipate its energy. As the roughness becomes greater, the disturbances increase with a resulting increase in energy dissipation, the latter being measured as a larger frictional drag.

Experiments at the University of California with unsymmetrical projections in an ultra-rough surface indicate that in some cases the frictional drag is very different, depending upon the direction of flow. Thus, the characteristics shown in Runs I and I*a* as being almost independent of the direction of flow cannot be considered as general.

Table 4 contains the author's results in comparison with those given in a British report[19] for wavy or corrugated surfaces. Houghton's experiments

TABLE 4.—COMPARISON OF RESULTS

Experimenter	Wave length, in inches	Ratio of groove depth to wave length	Relative roughness	log 100 f
Streeter, IV	0.043	0.276	0.011	0.58
Streeter, VI	0.087	0.184	0.015	0.68
Houghton	3.0	0.4	0.067	0.60
Houghton	1.0	0.4	0.022	0.48

were conducted in a 3-ft square wind tunnel with air as the fluid. The value of f in Table 4 corresponds approximately to Reynolds' number of 10^6. The relative roughness is the ratio of groove depth to pipe radius, or equivalent dimension. Even if the corrugation shapes and relative roughnesses differ, the author's friction factors appear to be high. In some measure at least, this result is caused by the spiral motion of the water, which is the result of the method of making the artificial roughness.

Although the author presents an excellent brief account of principal investigators in the field, the writer believes the work of Fage[20] should have

[19] "Note on the Velocity Distribution in the Neighborhood of a Corrugated Sheet," by R. Houghton, Tech. Rept., Aero. Research Comm., 1932–33. R and M No. 1466.

[20] "Fluid Flow in Rough Pipes," by A. Fage, Tech. Rept., Aero. Research Comm., 1934, R and M. No. 1585.

been noted. This material includes pressure and friction measurements for a surface composed of pyramids. The ultra-microscopic method is used to study velocity distributions and turbulence. The magnitude of the fluctuating velocities was about 2.5 times those for smooth pipes. The data show an approximate check with von Kármán's generalized velocity representations although the disturbances due to the wall extend further into the flowing fluid with the rough surface.

RALPH W. POWELL,[21] M. AM. SOC. C. E. (by letter)[21a].—Not only is this paper based on an extensive series of experiments, clearly and completely reported, but it is an excellent summary of past work in the same field. Perhaps the most noticeable omissions in the author's references are to the work of Stanton and Pannell[22] and to the extensive collection of data published by Kemler.[23]

In an unpublished study made in 1914[24] the writer offered some suggestions for future experimenters, among which was the following:

"The most fruitful field for experiment seems then to be on rough pipes from $\frac{1}{4}$ in. to 6 in. in diameter. It has been suggested[25] that threading pipes on the inside throughout their length would give a very rough pipe whose roughness could be duplicated at different diameters. The suggestion seems good, although it opens the question, not considered in this thesis, as to what size threads on a $\frac{1}{4}$-in. pipe would correspond to a given size thread on a 6-in. pipe."

As this study applies directly to the subject of this paper, and as the results confirm many of the author's statement's, it is, perhaps, not out of place to offer a brief summary, even at this late date.

The thesis consisted of a study, on the basis of Reynolds' number, of the previously published data on pipe flow that recorded the temperature. The principal part of the data was that published by Saph and Schoder,[7] which it was afterward found had already been studied from the same standpoint by Blasius.[8]

The results of the entire study are condensed into Fig. 17, which gives a plotting of f against R and corresponds to the author's Figs. 2 and 11. The points for the brass pipes studied by Saph and Schoder, represent 831 separate observations on 15 pipes ranging from 1.5 in. to 0.1 in. in diameter and at temperatures from 35.5° F to 84.0° F. These observations were re-arranged in the order of the Reynolds' numbers irrespective of what pipe

[21] Assoc. Prof. of Mechanics, Ohio State Univ., Columbus, Ohio (Temporarily on leave as Hydr. Engr. with the Muskingum Watershed Conservancy Dist., New Philadelphia, Ohio.)

[21a] Received by the Secretary June 26, 1935.

[22] "Similarity of Motion in Relation to the Surface Friction of Fluids," by T. E. Stanton and J. R. Pannell, *Transactions*, Royal Soc., Vol. 214 (1914), pp. 199–224.

[23] "A Study of the Data on the Flow of Fluids in Pipes," by Emory Kemler, *Transactions*, A. S. M. E., Vol. 55, HYD, pp. 7–32 (August 31, 1933).

[24] "The Flow of Water in Straight Pipes," by Ralph W. Powell, presented to Cornell Univ. in 1914 in partial fulfillment of the requirements for the professional degree of Civil Engineer.

[25] *Transactions*, Am. Soc. C. E., Vol. LXXVII (1914), p. 890.

[7] *Loc. cit.*, Vol. LI (1903), p. 253.

[8] "Das Ahnlichkeitsgesetz bei Reigungsvorgängen," von H. Blasius, *Physicalische Zeitschrift*, Vol. 12, p. 1176, 1911; or, *Forschungsarbeiten Ingenieur*, Heft 131.

they were taken on, and averaged in consecutive groups. (The only exception was in the critical region where cases in which stream-line flow seemed to be persisting were kept separate from those in which the flow was clearly turbulent.) Each point up to R = 2 500 represents the average of four or

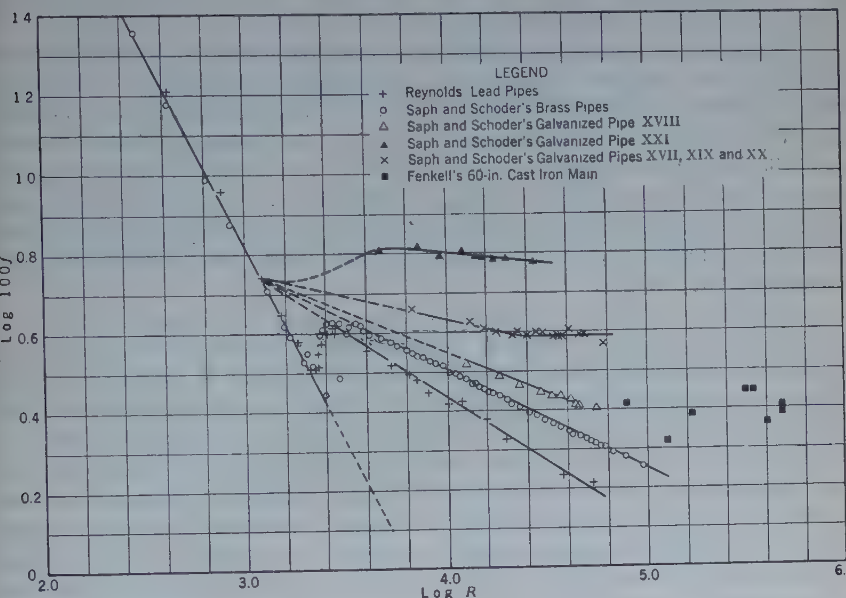

FIG. 17.

five determinations, generally on two or three pipes. For higher values the number in the group increased from six and then to ten; and between R = 4 000 and R = 40 000, it is twenty. One of these groups of twenty taken at random was found to include runs on eight different pipes, ranging in diameter from 1.25 in. to 0.10 in. The largest departure of any of these twenty values from the line that best represented all the runs was 3.6 per cent. The equation of this line was found to be:

$$f = 0.329 \ R^{-0.253} \quad \text{.......................(15)}$$

which agrees very well with Equation (6). As noted by the author, Saph and Schoder did not extend their tests to a value of R quite high enough to show the upward curve in the line, which was discovered later by Stanton and Pannell and confirmed by Nikuradse and others.

The plotting of Reynolds' original experiments on two lead pipes ($\frac{1}{4}$ in. and $\frac{1}{2}$ in. in diameter) was made in the same way, except that each point represents the average of only four runs. These experiments are interesting for two reasons: (a) They show that, compared with lead pipe even "smooth" brass pipe must be considered as having a definite roughness; and (b) they show noticeably larger discrepancies from a smooth line above the critical velocity and from Poiseuille's formula below it, than the experiments of Saph

and Schoder. In this connection the writer stated,[24] in 1914, that "it is worthy of note that Saph and Schoder's experiments prove Reynolds' formula better than those he himself performed and used to derive it." This is all the more noteworthy because Saph and Schoder seem to have taken little "stock" in Reynolds' work, and their results had been in print for a number of years before the agreement was ever investigated.

The five galvanized pipes studied by Saph and Schoder seem to fall into three definite groups as far as roughness is concerned. Pipe XVIII (diameter, 0.85 in.) was not so much rougher than the brass pipes and each point in Fig. 17 is the mean of only two runs. On the other hand, Pipe XXI (diameter, 0.35 in.) was extremely rough and each point in Fig. 17 represents the mean of three runs. The other three pipes (diameters, 1.042, 0.626, and 0.486 in., respectively) fall between the other two and differ very little among themselves. They have been grouped together, each point representing the average of four runs.

In order to check the methods for larger pipes the values for a 60-in. cast-iron main given by George H. Fenkell, M. Am. Soc. C. E.,[26] were reduced by the same method and each point in Fig. 17 represents a single run. Only the mean temperature for all the runs was given, but temperature has little effect in this case, as the curve is nearly horizontal. Perhaps it should be noted that the slope of the curve measures the influence of temperature on the friction head. Below the critical velocity where the slope is one, the resistance varies as the first power of the kinematic viscosity. Above the critical velocity where the slope is, say, one-fourth, the exponent of R in Equation (6) is -0.25, and the resistance varies as the fourth root of the kinematic viscosity; but where the curve is horizontal, f is independent of R and change of temperature has no effect on friction head.

One other point may be noted: All the lines as drawn in Fig. 17 intersect at the point, $\mathsf{R} = 1\,162$ and $f = 0.0551$ ($\log \mathsf{R} = 3.0652$ and $\log 100\,f = 0.7408$). This agrees very well with the intersection of the Blasius line with the stream-line flow line on Fig. 11. Therefore, the lower critical velocity will always be greater than $\mathsf{R} = 1\,162$; as the author states, it is generally about 2 100.

If it were true that all these lines were straight and radiated from a single point, the formula would be,

$$f = 0.0551 \left(\frac{1\,162}{\mathsf{R}}\right)^{2-m} \dots\dots\dots\dots\dots\dots\dots (15)$$

in which m is the exponent of the velocity in the ordinary exponential formula for friction head in pipes, and varies from about 1.67 for lead pipe to 1.80 for wrought-iron or steel pipes in good condition. In fact, this formula holds fairly well for all these pipes except Pipe XXI for the range from $\mathsf{R} = 4\,000$ to $\mathsf{R} = 100\,000$ (and also, of course, below the critical range where $m = 1$); but it does not hold for higher values of R, and, as the author shows, no formula can tell the entire story in the case of very rough pipes. The relationship between f and R is so complicated that only a plotting, such as Fig. 11, will suffice.

[26] *Transactions*, Am. Soc. C. E., Vol. LI (1903), p. 323.

AMERICAN SOCIETY OF CIVIL ENGINEERS

Founded November 5, 1852

DISCUSSIONS

UNDERGROUND CORROSION

Discussion

BY MESSRS. E. P. FETHERSTONHAUGH, JOHN F. SKINNER, AND F. N. SPELLER

E. P. FETHERSTONHAUGH,[15] ESQ. (by letter).[15a]—The gradual accumulation of information on soil corrosion and the growth of knowledge of the subject as a result of studying the data are well described in this paper. The theory of differential aeration as a probable major cause of soil corrosion is apparently supported by many of the observed and recorded facts and, if fully substantiated, may prove of great usefulness in forecasting what is likely to occur under a given set of conditions. It also suggests some important possibilities with regard to the value of protective coatings in prolonging the life of pipe buried in corrosive soils.

In the references in the paper to the observed reduction in the rates of corrosion and the causes of this phenomenon, there seems to be an assumption that special abnormal conditions should be sought to account for the shape of the curves that show decreasing rates of penetration with increasing life. A consideration of an assumed set of ideal conditions would seem to indicate that the decreasing rate of penetration might be regarded as a normal, rather than as an abnormal, phenomenon.

The ideal conditions suggested are that: (*a*) The source of the electromotive force causing the pitting remains constant; (*b*) the resistance of the path of the current through the earth, the pipe, and the pit, remains constant; and (*c*) throughout its growth, the shape of the pit remains constant.

Conditions (*a*) and (*b*) would result in a constant current flowing from the pit to the earth and, therefore, equal weights of metal removed in equal intervals of time. With equal weights or volumes of metal removed in equal intervals of time, the volume of the pit will increase at a constant rate, but since its shape is assumed to remain unchanged, its depth will increase as the cube root of the time. These assumptions suggest a funda-

NOTE.—The paper by K. H. Logan, Esq., was presented at the meeting of the Sanitary Engineering Division, New York, N. Y., on January 18, 1934, and published in March, 1935, *Proceedings*. Discussion on this paper has appeared in *Proceedings*, as follows: April, 1935, by Messrs. Thomas F. Wolfe, and John R. Baylis.

[15] Prof. of Elec. Eng., Univ. of Manitoba, Winnipeg, Man., Canada.

[15a] Received by the Secretary April 5, 1935.

mental law governing the relation between penetration and time which may be expressed by the equation:

$$D = A \sqrt[3]{T} \qquad (1)$$

in which A is a constant, or the depth of the penetration at the end of the first year; T is the time of exposure, in years; and, D is the depth of the pit at the end of T yr.

It could not be expected that observed data from tests in which there are so many possible variables would follow any mathematical curve exactly, but the similarity between the curve plotted from Equation (1) and the graphs plotted from observed data is striking, and even in other graphs of observed data, in which there is a greater departure, their general form seems to be at least characterized by a fundamental law such as that expressed by the formula.

It seems, therefore, that it is not necessary to attribute the decreasing rates of penetration to any varying condition, such as the gradual settlement of back-fill, as a rapid decrease is to be expected when all the aforementioned conditions are constant. The decreasing rates of loss of weight may perhaps require such explanations, but it is interesting to note that this decrease is in many cases comparatively small, which might suggest that the conditions assumed herein do not differ greatly from those which, in some cases, obtain in and around a buried pipe.

The value of this method of approaching this intricate problem lies in the fact that it suggests a normal law for the rate of penetration with which observed results may be compared, in order that the importance of various abnormal or fluctuating influences, such as those suggested by the author, may be more closely evaluated. Equation (1) may also prove of some value in an attempt to calculate from a single set of observations the time in which a pipe might be penetrated if the conditions of exposure remain constant.

JOHN F. SKINNER,[16] M. AM. SOC. C. E. (by letter).[16a]—The information presented by Mr. Logan is interesting in the light of experience with a pipe line (designated Conduits I, II, and III) in Rochester, N. Y. Conduit I, about 28.3 miles long, is still in service although constructed in 1874. The first 10 miles of it, 36 in. in diameter, is made of wrought iron, $\frac{3}{16}$ in. thick. Then follows 3 miles of 24-in. wrought-iron pipe. The remainder of the conduit is cast iron, with a diameter of 24 in. Conduit II was completed in 1894, twenty years later. It consisted of 12 000 ft of 6-ft brick tunnel and a pipe line of which the greater part (nearly 26 miles) was made of riveted steel plate, $\frac{1}{4}$ in., $\frac{5}{16}$ in., and $\frac{3}{8}$ in., in thickness.

At the end of 1913, when the writer prepared a report[17] on the subject, there were 727 holes in Conduit II through approximately 450 of the steel

[16] Cons. Engr., Los Angeles, Calif.

[16a] Received by the Secretary April 22, 1935.

[17] Report on the Steel Plate Pipe Conduit II of the Rochester, (N. Y.), Water-Works, by John F. Skinner, M. Am. Soc. C. E. (Copies of this report may be had from the City Engineer, of Rochester.)

sheets. In the 36-in. section of Conduit I (which was 20 yr older and made of thinner material), there were only 34 holes in 14 sheets. The next leak through the wrought-iron plate occurred on May 29, 1916, after a hiatus of 10 yr; and, to January 1, 1934, there had been a total of 81 holes in 29 sheets of Conduit I, which was then more than 58 yr old.

For several miles these conduits are parallel and only 20 ft apart, so that the soil conditions are practically identical. The first leak due to pitting the wrought-iron plate of the 36-in. Conduit I was discovered on July 12, 1894, after the pipe had been in the ground nearly 19 yr. The first leak through the steel plate of Conduit II was discovered on May 21, 1900, after the pipe had been in the ground nearly 6.5 yr, and the second on October 15, 1900; and 13 holes occurred in 1901 through 10 sheets. scattered over 9.7 miles of conduit. All these leaks were through the $\frac{1}{4}$-in. plate. The first leak through the $\frac{5}{16}$-in. plate was in 1904; and the first through the $\frac{3}{8}$-in. plate was in 1908. By the end of 1913, when the aforementioned report was published, 31 978.7 ft of Conduit II had been excavated, scraped clean, and re-coated on the outside. This painting covered 23.5% of the conduit and included 77.5% of the holes discovered.

During the fall of 1933, a section of the conduit was uncovered upon which many leaks had been repaired since the last re-coating operations. To the time this work was begun, 2 260 holes in the steel pipe had been repaired. Including the foregoing work, a total of 2 532 holes had occurred prior to January 1, 1934.

When re-coating is in progress, a great many incipient leaks are scratched through in the process of scraping, thus anticipating holes which, if undisturbed, would occur in the following year or two. The first 200 ft of pipe re-coated in the fall of 1933 was laid through boulders which had injured the original coating. Along this section the plates showed an unusual amount of pitting, and the holes were more numerous than they were farther along the line where the trench was free from boulders. The coating of California asphalt had apparently given protection, where it was not abraded, for about ten years.

Conduit III was constructed during the World War (1914–1918). About 17.6 miles of this line was a lock-bar steel pipe made of plates $\frac{1}{4}$ in and $\frac{5}{16}$ in. thick with riveted circular seams. A few leaks have occurred, generally where the painting was found to be defective. It has been suggested that the subsequent laying of the steel pipe parallel to the wrought-iron pipe may have had an inhibiting effect upon the corrosion of the wrought iron. The answer to this is that 58% of the holes in the wrought-iron pipe (and 52% of the sheets affected) occurred after the steel pipe was installed. The difference in the pitting of steel and wrought iron, in practically the same location, over a long period, is worthy of serious consideration.

In 1901, Professor F. L. Kortright investigated the causes of pitting in Conduit II. He examined samples of earth from twenty-five test pits along Conduit II, as well as rock from the vicinity, ground-water from the trench excavations, and the contents of pits in the steel, both outside and inside the pipe.

From his analysis, he concluded that the earth surrounding the conduit did not affect it except that, being more porous in some places than in others, it admitted the ground-water more freely to the pipe in the places where it was porous and in this way allowed carbon dioxide and oxygen freer access. He reported that the rock in the vicinity of the pipe had no effect on it; but that the injurious constituents in the water were dissolved oxygen and the carbon dioxide that was brought to the pipe in large quantities by the calcium carbonate, which is loosely combined with it.

Electrical measurements were made between Conduits I and II, and between the conduits and the surrounding earth, but neither current nor difference of potential could be detected.

From the foregoing remarks it will be noted that in nearly identical locations and exposure, the wrought-iron Conduit I resisted the first pitting through a $\frac{3}{16}$-in, plate nearly three times as long as the steel Conduit II and that, in later years, although it is twenty years older and of thinner material, it has developed far less pitting through the plate. Although the comparisons shown in the paper exhibit a marked uniformity of action for different pipe materials under the same exposure, it must be evident that a much longer period, commensurable with the life of such structures, may show very different results, such as have been observed in the different behaviors of different materials in places where one has replaced another and is subject to the same environment.

Mr. Logan is to be commended for the energy, imagination, and enthusiasm he has put into this work. It is hoped that he and his successors will be able to continue their observations over a period sufficiently long to insure reliable conclusions of lasting value.

F. N. SPELLER,[18] ESQ. (by letter).[18a]—The principal work on soil corrosion of metals and the study of protective coatings has been centered at the National Bureau of Standards. Considerable progress has been made in correlation of soil factors with corrosion, but much remains to be done before the practice of pipe-coating underground can be said to be on a sound engineering basis.

It is now probable that an economical and durable coating can be found for use in most of the corrosive soils. In many cases, as Mr. Logan points out, no coating is required. This is particularly true in the eastern part of the United States. In Philadelphia, Pa., the records of the local gas company over the thirty-six years, 1899 to 1935, indicate that small steel service pipes having a thickness of about $\frac{1}{8}$ in. have an average life of forty-seven years with no more than a thin coat of coal-tar paint which probably gave little advantage except to prevent more general distribution of pit-holes.

It seems very unlikely that a low-cost, rust-resisting metal will be found that is sufficiently durable in all corrosive soils, and (as Mr. Logan points out), there is no material difference between the corrosion resistance of the common ferrous metals, therefore, for the present, the work should be con-

[18] Director, Dept. of Metallurgy and Research, National Tube Co., Pittsburgh, Pa.

[18a] Received by the Secretary June 14, 1935.

centrated on improvements in protective coatings. Such coatings should be chemically resistant to soil water, mechanically strong or sufficiently reinforced to resist soil stresses, and thick enough to be durable and prevent contact between the soil and the metal. Reinforced bituminous coatings usually should not be less than $\frac{3}{32}$ in. in thickness.

Portland cement concrete coatings ($\frac{5}{8}$ in. to 1 in. thick) cost from 6 to 10 cents per sq ft, and are highly durable in many soils. They have given 35 to 40 yr of satisfactory protection on oil pipe lines; for instance, on lines crossing low salty marshes, and acid streams in coal-mining districts.

Research work on soil corrosion is of such general interest to tax-payers at large that it seems a portion of the expense of this work should be paid by the Government. Thus far, it has been carried out on this basis by the National Bureau of Standards with the co-operation of the American Petroleum Institute, American Gas Association, and pipe manufacturers, but has been seriously retarded by curtailment of appropriations due to the economy program. The general opinion of those who have followed this investigation is that it should by all means be continued in order to realize on the $300 000 already invested through the Bureau toward the solution of this problem.

AMERICAN SOCIETY OF CIVIL ENGINEERS

Founded November 5, 1852

DISCUSSIONS

THE ADJUSTMENT OF A LEVEL NET

Discussion

By Messrs. Earl F. Church, and W. H. Rayner

Earl F. Church[5] Assoc. M. Am. Soc. C. E. (by letter)[5a].—This interesting paper well deserves the attention of all engineers interested in the practical computations of surveys. It contains a description of two methods for adjusting engineering level nets and one of the most interesting features is that the two methods presented are identical. (The term, "engineering leveling," is used to denote ordinary leveling as distinguished from "geodetic leveling.") The first is the least squares method, the "condition multipliers" being the usual "correlatives." This part of the paper refers to a "converging increment" method of approximation for solving the normal equations to be used instead of the precise Gauss method. The lack of rigidity in the theory is implied by the author in his statement that the method "appears to be applicable to the vast majority of normal equations encountered in practical engineering problems." After all, the real test of any method of solving normal equations lies in obtaining values of the correlatives which satisfy the equations; and this method of approximation will undoubtedly give the desired results in most cases of engineering level nets, as it does in the specific examples shown. Regardless of whether the method possesses any marked advantages over the usual Gauss method, the author is entirely justified in presenting it on account of the fact that, by the identity of the results by the two methods and even of the steps in obtaining the results, it establishes the correctness of the second method.

The second method, called "successive distributions," shows a process of adjusting engineering level nets which is certainly a useful one. Requiring no knowledge of least squares and eliminating the necessity of setting up the normal equations themselves, it is easy to comprehend and easy to apply; and for both these reasons it should appeal to the average surveyor. The

Note.—The paper by George H. Dell, Assoc. M. Am. Soc. C. E., was published in April, 1935, *Proceedings*. This discussion is printed in *Proceedings*, in order that the views expressed may be brought before all members for further discussion.

[5] Associate Prof. of Photogrammetry, Coll. of Applied Science, Syracuse Univ., Syracuse, N. Y.

[5a] Received by the Secretary May 9, 1935.

method appears at first glance to have no relation to least squares and to give results which, although they might render the level net consistent, would bear no relation to the "most probable values" and might even vary with the order arbitrarily chosen for closing the various circuits. This is not the case, however. The identity of the results of the two methods shows the elevations from the second method to be virtually the "most probable values." Furthermore, the identity of the steps in obtaining the results in the two methods establishes the correctness of the second method as virtually a least squares adjustment for cases in which the "converging increments" would solve the normal equations, regardless of the order chosen for closing the circuits in the second method.

The following notes may be of assistance in observing the identity in the successive steps in the two processes. Compare the values shown in Fig. 4 for the method of "successive distribution" with those shown in Table 5 for the solution of the normal equations by "converging increments": On Line 1 of Table 5, 4.85, 1.71, and 5.71 are the values "carried over" in Fig. 4 from Circuit No. I into Circuits Nos. II, III, and IV, respectively; on Line 2 of Table 5, –6.48 is the value in Fig. 4 "carried over" from Circuit No. II to Circuit No. I, and the two blank spaces on Line 2 show that in Fig. 4 there were no values "carried over" from Circuit No. II to either Circuit No. III or Circuit No. IV; on Line 3 of Table 5, –1.82 and 3.04, are the values in Fig. 4 "carried over" from Circuit No. III to Circuits Nos. I and IV, respectively; on Line 4 of Table 5, 2.79 and –1.39 are the values in Fig. 4 "carried over" from Circuit No. IV to Circuits Nos. I and III, respectively; on Line 5 of Table 5, 5.51 is the closure distributed in Circuit No. I, in Fig. 4 the second time; and 1.91, 0.67, and 2.24, on Line 5 of Table 5, are the values in Fig. 4 "carried over" the second time into Circuits Nos. II, III, and IV, respectively. This identity of the steps can be followed throughout.

Undoubtedly, the use of series summations to obtain section corrections in the method of "successive distribution," will generally prove to be a useless refinement. In fact, in the specimen adjustment shown in Fig. 4, the correct values of the section corrections would have been obtained if the additions had been made after the third distribution, and both the fourth distribution and the series summations were actually unnecessary.

This discussion may be summarized somewhat as follows: The second method (that of "successive distribution"), gives a simple and useful means of adjusting engineering level nets. This method is particularly simple in the frequent cases in which one can dispense with the series summations. The desirability of the method depends entirely upon whether the resulting elevations are the "most probable values" regardless of the order of closing the circuits, and that they are approximately the most probable values is proved by the identity with the results from the least squares method. The only remaining question is whether the first method (with which the comparison is made) actually gives "most probable values" when the converging increment approximation is used to solve the normal equations; but it will be observed that it must do so provided the correlatives obtained actually satisfy

the normal equations. Therefore, for any cases in which "converging increments" would solve the normal equations, the second method of "successive distribution" without the normal equations will give correct results.

In presenting to the average surveyor an excellent process for adjusting ordinary engineering level nets, this paper serves a useful purpose and is to be highly commended.

W. H. RAYNER,[6] ASSOC. M. AM. SOC. C. E. (by letter).[6a]—This presentation is an excellent example of that type of study which consists in the application of existing theory to new problems; and an especial reason for commendation is the fact that, for good measure, the author has given two equally good solutions of a complex and important problem.

The simplicity and clarity of treatment are excellent but a statement under "Solution of Normal Equations," needs a brief additional explanation, it seems, to make clear the computation of the "condition multipliers," C_{I}, C_{II}, etc. Referring to Table 5(a), Mr. Dell states that "Line 18 contains the sums of the principal terms (including the quantities in Line 17), and the values of the unknowns (the condition multipliers), are given in Line 19." The value of C_{I}, for Method 1, Example No. 1, is given by the relation, $C_{\text{I}} = \dfrac{\text{Major terms of Circuit No. I}}{\text{Total effective length of Circuit No. I}}$. Hence, $C_{\text{I}} = \dfrac{22.07 \text{ (Line 18)}}{24.5}$ $= 0.901$. Likewise $C_{\text{II}} = \dfrac{-17.65}{19.5} = -0.905$.

Two approximate methods are sometimes used to adjust level nets, and may be designated: (1) The "successive-circuit" method; and (2) the Geological Survey method. The writer was interested to compare both the results and the labor involved in each of these approximate methods with those of Mr. Dell's methods.

Briefly stated, the successive-circuit method consists in adjusting the sides of connected circuits in proportion to the lengths of the sides, beginning with that circuit having the largest error of closure. The second circuit to be adjusted is the one having the second largest error of closure, etc. The method is described in detail, in the more complete surveying textbooks.[7]

The Geological Survey method consists in beginning with a fixed benchmark, from which the nearest junction points of connected circuits are given a preliminary adjustment. The weights assigned to the different elevations of such junction points, as found by the different connecting lines, are inversely proportional to the lengths of the lines. Using the preliminary adjusted values thus found, other junction points are similarly adjusted to include all points within the level net. From such tentative values, a second computation establishes the final elevations of the successive junction points.[8]

---

[6] Asst. Prof, of Civ. Eng., Univ. of Illinois, Urbana, Ill.

[6a] Received by the Secretary June 24, 1935.

[7] "Surveying," by Davis, Foote, and Rayner, Second Edition, p. 174.

[8] The method is described in detail in "Instructions to Topographers of the U. S. Geological Survey."

For purposes of comparison, a net including five circuits comprising nine lines from 5 miles to 30 miles in length, was adjusted by each of the approximate methods and by each of Mr. Dell's methods, with the results shown in Table 11.

TABLE 11.—COMPARISONS OF ADJUSTMENTS OF A LEVEL NET

Point	Dell	Geological Survey		Successive-Circuit	
	Elevation	Elevation	Discrepancy with Dell	Elevation	Discrepancy with Dell
E	650.00	650.00	0.00	649.85	—0.15
B	810.21	810.25	+0.04	810.26	+0.05
A	601.39	601.35	—0.04	601.39	0.00
F	682.65	682.64	—0.01	682.56	—0.09
D	748.17	748.18	+0.01	748.14	—0.03
C	715.29	715 28	—0.01	715.36	+0.07

It is evident that, for this example, the discrepancies between the Geological Survey method and the Dell method are, in the average, about one-third as large as those of the successive-circuit method. Of course, the two Dell methods yielded identical results.

Each of the Dell methods and the Geological Survey method required about an equal amount of labor. However, the writer believes that the layman will find Method 2 the easier to apply. The successive-circuit method is much easier of application than the others; but it is also the least accurate.

It is evident, therefore, that for engineers who meet this problem, Mr. Dell has provided two methods that are mathematically correct and convenient, thus making unnecessary and inexcusable the use of approximate methods.

AMERICAN SOCIETY OF CIVIL ENGINEERS

Founded November 5, 1852

DISCUSSIONS

THE SHEAR-AREA METHOD

Discussion

By Messrs. George E. Large, Samuel T. Carpenter, Roland H. Trathen, A. W. Fischer, J. Charles Rathbun, Harold R. Kepner, and Fred L. Plummer.

George E. Large,[4] Assoc. M. Am. Soc. C. E. (by letter).[4a]—The writer has often noticed that many engineers do not fully understand the relationship of the beam diagrams so often drawn. The slope diagram shown in Fig. 1 is almost a total stranger to them, yet a recognition of it as a member of the family of five curves is necessary to a full understanding of the very useful general relationships about to be mentioned. It so happens that the order of the diagrams, correct in Fig. 1, is also important, especially to the beginner, yet new textbooks are still appearing with cuts faulty in this respect. Instructors have been too facile with their calculus and too sparing with correct and complete sketches showing the geometry of the operations being performed.

It will be demonstrated herein that no new principles or devices are necessary for solving the authors' examples quickly if advantage is taken of a simple geometric relation which exists between the slope and shear diagrams, as well as between the deflection and moment diagrams.

The moment-area principles referred to by the authors are not usually applied to any diagrams except the moment and deflection diagrams. Note the restricted usage required by the usual statement of these principles:

(1) When a member is subjected to flexure, the change in slope of the elastic curve between any two points is equal in magnitude to the area of the $\frac{M}{EI}$ - diagram for the part of the member between the two points.

(2) When a member is subjected to flexure, the ordinate from any point, Q (Fig. 22), on the elastic curve, to a tangent drawn to the elastic curve at any

Note.—The paper by Horace B. Compton, Assoc. M. Am. Soc. C. E., and Clayton O. Dohrenwend, Jun. Am. Soc. C. E., was published in May, 1935, *Proceedings*. This discussion is printed in *Proceedings* in order that the views expressed may be brought before all members for further discussion.

[4] Associate Prof. of Civ. Eng., and Research Engr., Eng. Experiment Station, Ohio State Univ., Columbus, Ohio.

[4a] Received by the Secretary June 6, 1935.

other point, P, is equal in magnitude to the moment of the area of the $\frac{M}{EI}$-diagram between the two points, about Point Q.

The generalized statement of these principles is much more useful because they may then be applied to any of the five beam diagrams, including the slope and shear diagrams so much used by the authors.

General Relationship of Beam Diagrams.—When the five diagrams, or curves, of any beam are arranged in the ascending order shown in Fig. 22,

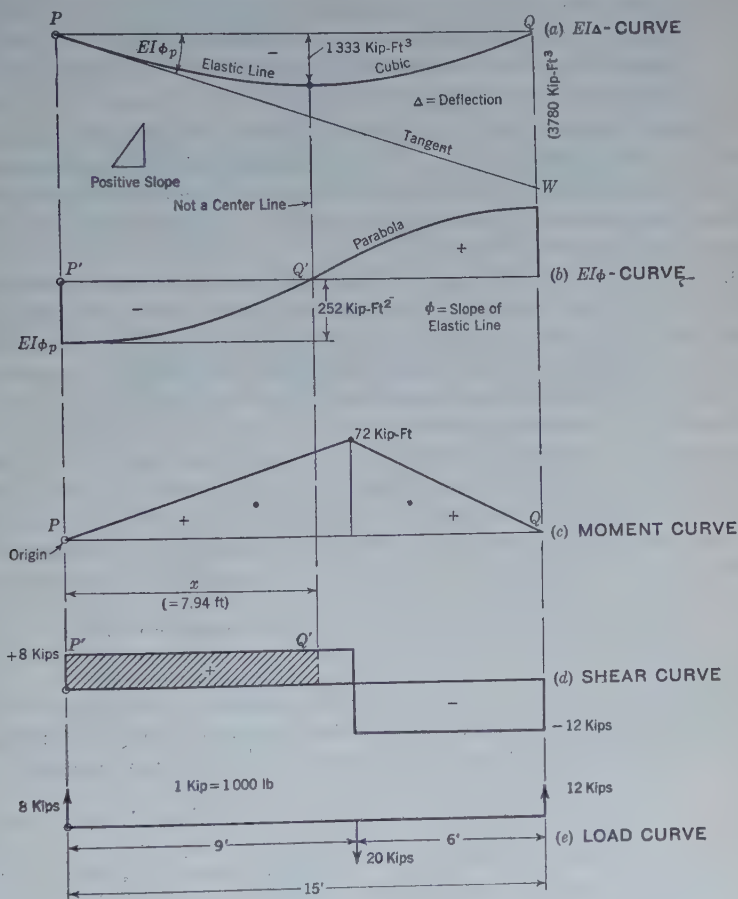

FIG. 22.—COMPLETE BEAM SOLUTION BY MOMENT-AREA PRINCIPLES.

each curve is the integral of the one immediately below it. (The ascending order is somewhat preferable especially if the user thinks of successive integration as an ascending process.) An equation may be written for the lowest curve, successive integrations of which will yield the equations of all the higher curves, including the deflection curve. This procedure has long been used with conspicuous success by C. C. More, M. Am. Soc. C. E., in teaching

structures at the University of Washington, Seattle, Wash. The relationship thus established makes it possible to state the moment-area principles in a more general form, so that their assertions may be utilized to determine all the curves completely. As stated by Professor More they are:

I.—The ordinate at any point on any curve equals the slope at the corresponding point in the next higher curve;

II.—The area between any two ordinates on any curve equals the difference of the corresponding ordinates in the next higher curve; and,

III.—The ordinate from any point (Point Q, Fig. 22) on any curve, to a tangent drawn to the curve at any other point (Point P) is equal in magnitude to the moment of the area of the second lower curve between the two points, about Point Q.

In accordance with the foregoing laws, if the ordinates of one curve are positive and increase from left to right, the slope of the next higher curve will also be positive at that point and will increase from left to right. Corresponding statements may be made for negative ordinates, and for ordinates that decrease from left to right.

These principles enable one to sketch the curves of any beam in their correct relation, one after the other, and to evaluate their maximum points. In Fig. 22, a numerical example of the authors' Case 3 (Fig. 5), the uniform ordinates of the shear curve determine the uniform slopes of the moment curve (Law I). By Law II, the maximum bending moment may be found from the shear curve. The increasing positive ordinates of the left portion of the moment curve call for an increasing positive slope to the $E\,I\,\phi$-curve directly above it (Law I), $E\,I$ being constant. Upon drawing the $E\,I\,\Delta$-curve by inspection it is seen that the slope of the elastic line is negative at the left end, or that the Y-intercept on the $E\,I\,\phi$-curve is negative. The value of this intercept is determined as usual, by applying Law III to the moment and deflection curves;

Thus, $Q\,W = 36 \times 6 \times 4 + 36 \times 9 \times 9 = 3\,780$ kip-ft³; and $E\,I\,\phi_p = \dfrac{3\,780}{15} = 252$ kip-ft².

The point of maximum deflection will be where the $E\,I\,\phi$-curve crosses the X-axis and this point is easily found without resort to any new principles by applying Law III to the slope and shear curves. Taking moments of the shear area about the unknown point, Q': $8\,(x)\left(\dfrac{x}{2}\right) = E\,I\,\phi_P = 252$; and $x = 7.94$ ft. Furthermore, by Law II, the maximum deflection is the area of the $E\,I\,\phi$-diagram: $E\,I\,\Delta_{max.} = \frac{2}{3} \times 252 \times 7.94 = 1\,333$ kip-ft³; and, $\Delta_{max.} = \dfrac{1\,333 \text{ kip-ft}^3}{E\,I}$.

Statically indeterminate beams can also be solved with corresponding facility, as compared to the authors' expressions.[5] The writer cannot refrain from

[5] See Appendix of *Bulletin 66*, Ohio State Univ. Eng. Experiment Station, "The Moment Distribution Method of Structural Analysis Extended to Lateral Loads and Members of Variable Cross-Section" (Revised Edition), by George E. Large, Assoc. M. Am. Soc. C. E., and Clyde T. Morris, M. Am. Soc. C. E.

suggesting that the introduction of an equivalent "mathematical beam" device may easily be a source of confusion, which is quite unnecessary, once the general relationship of all curves is recognized.[5a]

Samuel T. Carpenter,[6] Jun. Am. Soc. C. E. (by letter).[6a]—Moment areas have proved their usefulness and shear areas are no doubt a unique application of moment-area principles. However, the writer doubts if "mathematical beams" are to be preferred to real beams. Engineers have used area moments as a tool, the principles being easily retained and recalled when the need arises; only two laws must be remembered. The shear-area method has at least five relations which must be remembered or reviewed before using. The authors suggest that for a student the "mathematical beam" will aid his knowledge of beam action; the writer would make an exception to this since area moments must necessarily be understood before shear areas could be grasped. It will be granted that teachers of applied mechanics have been lax in the past by not calling to the attention of students the relation of the third, second, and first derivatives of the elastic line, or the shear, moment, and slope curves as depicted in Fig. 1. C. C. More, M. Am. Soc. C. E., has taught those relations successfully at the University of Washington, at Seattle, Wash., without the aid of the "mathematical beam."

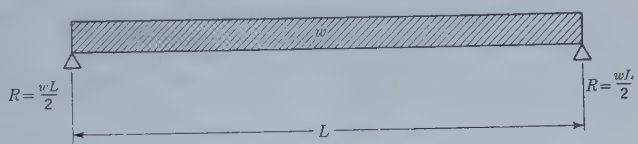

(a) LOAD DIAGRAM

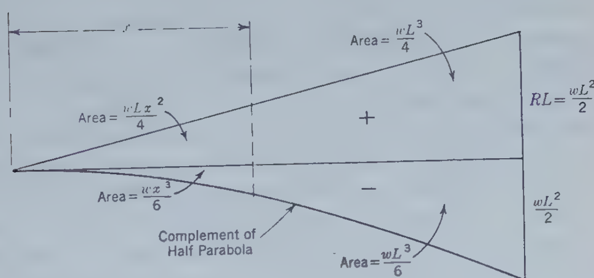

(b) MOMENT DIAGRAM

Fig. 23.

The authors suggest that the shear-area method is particularly adaptable to problems involving a distributed load, stating that the shear areas are used more easily than the curved moment areas. This is true with the moment

[5a] Correction in paper: In Fig. 1, the slope curve (Fig. 1(d)), should have its concave side next to the X-axis and should be horizontal at each end, as in Fig. 22.

[6] Instr., Div. of Eng., Swarthmore Coll., Swarthmore, Pa.

[6a] Received by the Secretary June 7, 1935.

diagrams as ordinarily used. For some time the writer has followed the method suggested by Mr. James E. Boyd[7] for treating uniform loads, which places the parabola involved in a form easier to apply. To illustrate, take the authors' Case 1. Fig. 23 indicates how the moment diagram would be drawn, the diagram being divided into positive and negative areas; the curved negative area is the complement of a half parabola. This is convenient when finding deflections at any point on the beam. The end slopes are: $2\,E\,I\,\phi = \dfrac{w L^3}{4} - \dfrac{w L^3}{6} = \dfrac{w L^3}{12}$; and $\phi = \dfrac{w L^3}{24\,E I}$. The deflection at any point a distance, x from the left end is: $E\,I\,y = \dfrac{w L^3}{24}\,x - \left(\dfrac{w L X^2}{4} \times \dfrac{X}{3} - \dfrac{w X^3}{6} \times \dfrac{X}{4}\right)$; and $y = \dfrac{w X}{24\,E I}\,(L^3 - 2\,L\,X^2 + X^3)$.

This means of building up the moment curves is equally applicable to cases of concentrated loads and continuous beams, the component curves always being easily drawn by starting from the left end and considering all the loading elements.

Roland H. Trathen,[8] Esq. (by letter).[8a]—The "shear-area method," presented by Professor Compton and Mr. Dohrenwend, supplies a new and novel procedure for the solution of the elastic functions of beams. There are many cases, of course, in which the method is not advantageous. This, in itself, in no way detracts from the usefulness of the concept.

The writer looks upon the method as a new tool to facilitate structural analysis. No one method of analysis is universal in scope and simplicity. The methods of "slope deflection", "moment areas", "the column analogy", "moment distribution", "internal work", etc., are all available to the structural engineer. Each of them is peculiarly adapted to the solution of particular problems. The structural engineer who is familiar with all methods is usually able to decide before beginning an analysis, which is likely to prove to be the most expedient.

In presenting, "the shear-area method", to the profession the authors have dealt quite thoroughly with beams. In the space of a few pages they have derived equations for slope and deflection, for a variety of beams, each under several conditions of loading. Such a wealth of beam functions if available for immediate reference may prove to be very useful. The same information may be found in any standard textbook on the strength of materials, but the writer has never been able to find all the given data in such condensed form. Students as well as structural engineers may well look upon the paper as a convenient reference table of slopes and deflections to be used in the solution of more complex problems.

The following simple problems are included to illustrate the usefulness of the paper when applied in this manner. The notation of the original

[7] "Strength of Materials," by James E. Boyd, McGraw-Hill Publishing Co., 1924.
[8] Instructor in Civ. Eng., Rensselaer Polytechnic Inst., Troy, N. Y.
[8a] Received by the Secretary June 26, 1935.

paper is preserved throughout, with the following exceptions: ϕ_{BC} = partial slope at End B of Member BC; and ϕ_{TBC} = total slope at End B of Member BC.

Problem 1,—An L-Frame with Concentrated Load Applied at Mid-Point of Deck.—The structure shown in Fig. 24 is indeterminate to the first degree. In Fig. 25 it has been reduced to a determinate structure by cutting it at

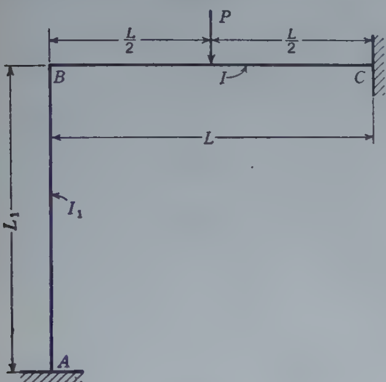

FIG. 24.

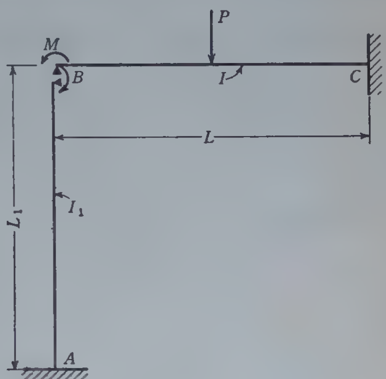

FIG. 25.

Point B. The determination of the moment, M, will be sufficient to make the structure statically determinate. The solution for the unknown moment at Joint B is as follows, using directly the slopes as derived in the paper: By Equation (80), the slope, ϕ_{BC}, due to the concentrated load, P, is $\frac{P L^2}{32 E I}$; by Equation (83), the slope, ϕ_{BC}, due to the bending moment, M, is $-\frac{M L}{4 E I}$; and the total slope, ϕ_{TBC} equals $\frac{P L^2}{32 E I} - \frac{M L}{4 E I}$.

By Equation (83) again, the total slope, ϕ_{TBA}, due to the bending moment $= -\frac{M L_1}{4 E I_1}$. Since $\phi_{TBC} = -\phi_{TBA}$, it follows that $\frac{P L^2}{32 E I} - \frac{M L}{4 E I} = \frac{M L_1}{4 E I_1}$; and,

$$M = \frac{P L^2}{8} \left(\frac{I_1}{L_1 I + L I_1} \right) \quad \text{.................(96)}$$

Problem 2.—Two-Span Continuous Beam with Uniform Load on One Span and Concentrated Load at Center of Other Span.—The structure in

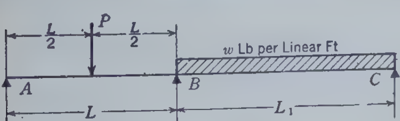

FIG. 26.

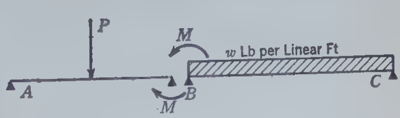

FIG. 27.

Fig. 26 is statically indeterminate to the first degree. The solution for the moment over the support at Point B will make it statically determinate.

The beam is reduced to a simple structure by cutting it as shown in Fig. 27. Then, by Equation (14), the slope, ϕ_{BA}, due to a concentrated load, P, on Span L, is $\frac{P L^2}{16 E I}$; by Equation (33) (when $a = 0$ and $b = L$), the slope, ϕ_{BA}, due to the bending moment, M, on Span L, is $-\frac{M L}{3 E I}$; and, as in Problem 1, the total slope, ϕ_{TBA}, is the sum, or $\frac{P L^2}{16 E I} - \frac{M L}{3 E I}$. Finally, by Equation (8), the slope, ϕ_{BC}, due to a uniform load, w, on Span L_1, is $\frac{w L_1^3}{24 E I}$; by Equation (33) (when $b = 0$ and $a = L$), the slope, ϕ_{BC}, due to a moment, M, on Span L_1, is $-\frac{M L_1}{3 E I}$; and, the total slope, ϕ_{TBC}, is $\frac{w L_1^3}{24 E I} - \frac{M L_1}{3 E I}$. Since $\phi_{TBA} = -\phi_{TBC}$, it follows that: $\frac{P L^2}{16 E I} - \frac{M L}{3 E I} = -\frac{w L_1^3}{24 E I} + \frac{M L_1}{3 E I}$

and,

$$M = \frac{3 P L^2}{16 (L + L_1)} + \frac{w L_1^3}{8 (L + L_1)} \qquad (97)$$

Problem 3.—Continuous Beam of Two Equal Spans, with Concentrated Load at Center of One Span.—The structure in Fig. 28(*a*) is indeterminate

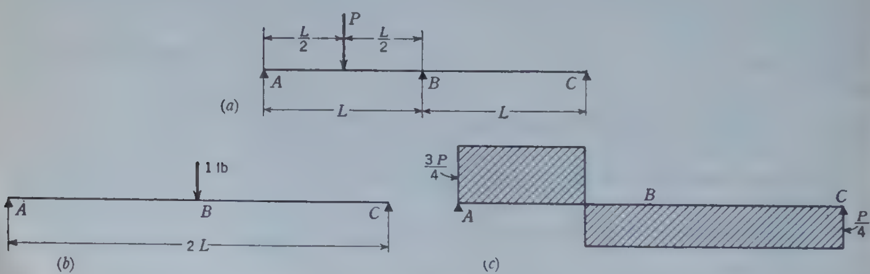

FIG. 28.

to the first degree. In this case the reaction at Point B will be chosen as the redundant. With the reaction at this point known, the structure is statically determinate, as shown in Fig. 28(*b*) and the shear diagram for this case is shown in Fig. 28(*c*). By Equation (17), the deflection, y_B, due to a unit load at Point B, is $\frac{L^3}{6 E I}$; and, by Equation (24), the slope, ϕ_R, due to a concentrated load, P, is,

$$\phi_R = \frac{P a b}{6 E I L}(L + b) = \frac{P \times \frac{3}{2} L \times \frac{1}{2} L}{12 E I L}\left(2 L + \frac{1}{2} L\right) = \frac{5 P L^3}{32 E I} \qquad (98)$$

Then, by Equations (7), and (9) the deflection, y_B, due to a concentrated load, P, is,

$$y_B = \phi_R\, x - \frac{1}{2}\, I_x = \frac{5\, P L^2}{32\, E I} \times L - \frac{1}{2} \times \frac{P}{4} \times L^3 \times \frac{E I}{3}$$

$$= \frac{5\, P L^3}{32\, E I} - \frac{P L^3}{24\, E I} = \frac{11\, P L^3}{96\, E I} \quad \ldots\ldots\ldots\ldots\ldots\ldots (99)$$

and, the reaction is,

$$R_B = \frac{y_B \text{ (due to Load } P)}{y_B \text{ (due to load of unity)}} = \frac{11\, P L^3}{96\, E I} \times \frac{6\, E I}{L^3} = \frac{11\, P}{16} \quad \ldots\ldots (100)$$

A. W. FISCHER,[9] ESQ. (by letter).[9a]—An interesting method of calculating the deflection of beams is offered in this paper, but as stated in the "Conclusions," it is not suggested as the shortest method for solving slopes and

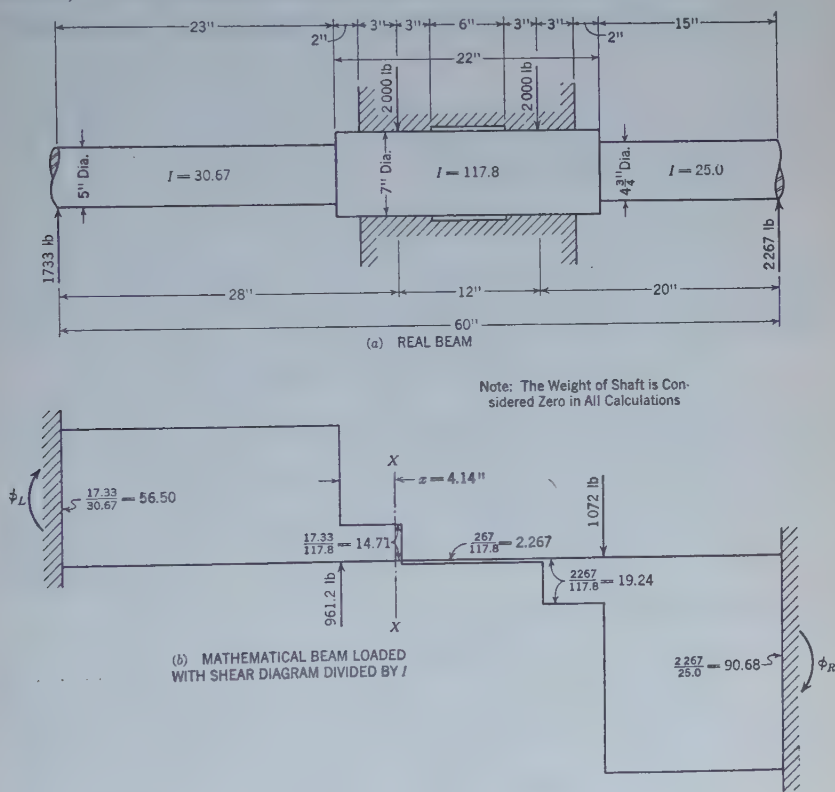

FIG. 29.

deflections for all problems. This is a true statement because there are many problems in which slopes and deflections can be solved in less time than is required by the shear-area method.

[9] Care, Pennsylvania Sugar Co., Philadelphia, Pa.

[9a] Received by the Secretary July 1, 1935.

As an example the writer will calculate the maximum deflection of the shaft shown in Fig. 29 by the shear-area method, to demonstrate that it is not the shortest. Furthermore, it is more complex than a comparable method presented by the writer[10] in that a simple differential equation must be used to obtain the required results, which may not appeal to every engineer.

As E is a constant it will be assumed equal to unity which will somewhat simplify the equations. To determine the end conditions of the mathematical beam the general moment equation with the left end as the origin, is,

$$\frac{d^2 y}{dx^2} = \phi_L - \frac{1}{2}(56.50\,x^2) - \frac{1}{2}(14.71\,x^2) + 961.2\,x \quad \ldots\ldots(101)$$

Integrating Equation (101):

$$6\,\frac{dy}{dx} = 6\,\phi_L\,x - 56.50\,x^3 - 14.71\,x^3 + 3\,(961.2\,x^2) \quad \ldots\ldots(102)$$

The moment equation as derived from the right end of the mathematical beam, is:

$$\frac{d^2 y}{dx^2} = \phi_R - \frac{1}{2}(90.68\,x^2) - \frac{1}{2}(19.24\,x^2) - \frac{1}{2}(2.267\,x^2) + 1\,072\,x \quad .(103)$$

Integrating Equation (103):

$$6\,\frac{dy}{dx} = 6\,\phi_R\,x - 90.68\,x^3 - 19.24\,x^3 - 2.267\,x^3 + 3\,(1\,072\,x^2) \quad ..(104)$$

Equate, six times, the two tangents of the mathematical beam at a point 28 in. from the left end, since the deflection of the real beam can be expressed by both equations at that point, thus:

$$6\,\phi_L\,x\Big]_0^{28} - 56.50\,x^3\Big]_5^{28} - 14.71\,x^3\Big]_0^{5} + 3\,(961.2\,x^2\Big]_0^{5}$$

$$= 6\,\phi_R\,x\Big]_0^{32} - 90.68\,x^3\Big]_{17}^{32} - 19.24\,x^3\Big]_{12}^{17} - 2.267\,x^3\Big]_0^{12} + 3\,(1\,072\,x)^2\Big]_0^{17} \quad .(105)$$

Substituting the limits of x and reducing Equation (105):

$$28\,\phi_L = 206\,700 + 1\,177 - 306 + 12\,020$$

$$= 32\,\phi_R - 495\,200 + 74\,250 - 15\,750 + 5\,541 - 653 + 154\,900. (106)$$

Reducing Equation (106):

$$28\,\phi_L - 193\,809 = 32\,\phi_R - 276\,912 \quad \ldots\ldots\ldots\ldots(107)$$

From the mathematical beam the total, ϕ_T, equals 33 477, and using the notation, $\phi_R = \phi_T - \phi_L$; then, from Equation (107):

$$28\,\phi_L - 193\,809 = 32(33\,477) - 32\,\phi_L - 276\,912 \quad \ldots\ldots(108)$$

Reducing Equation (108), $\phi_L = 16\,470$; and $\phi_R = 33\,477 - 16\,470 = 17\,007$. (All computations in this discussion were made with a 20-in. slide-rule.)

[10] "Shaft Deflections by the Method of Elastic Weights", by A. W. Fischer, *Product Engineering*, November, 1933, p. 428.

The moment of the mathematical beam is equal to zero at the section of maximum deflection, thus, at Section X–X:

$$M = 0 = 16\,740 - 56.50 \times 23\,(11.5 + x) - \tfrac{1}{2}\,(14.71\,x^2) + 961.2\,x. \quad (109)$$

From Equation (109) $x = 4.14$ in., which means that the point of maximum deflection of the real beam occurs 27.14 in. to the right of the left reaction (see Fig. 29).

Using the notation of the paper: $y_{max.} = \phi_L x - \tfrac{1}{2}\,I_x$, in which $x = 27.14$ in.; or, $y_{max.} = 16\,470(27.14) - \frac{1}{2}\Big[(56.50)\frac{23^3}{12} + 56.50\,(23)\,(15.64^2)$ $- 961.2\,(4.14^2) + \frac{14.71\,(4.14^3)}{3}\Big] = 447\,000 - 179\,500 = 267\,500$ in. when E equals unity. When E equals 29 000 000, the maximum deflection equals $\frac{267\,500}{29\,000\,000} = 0.009224$ in.

The deflection at a point 28 in. to the right of the left reaction from the left-hand part of Equation (107), is $28(16\,470) - 193\,809 = 267\,391$ in. when E equals unity, and when E equals $29(10^6)$, the deflection equals 0.009220.

From the foregoing computations the deflection at the point of zero shear of the real beam is found to be just a little less than the maximum deflection. On comparison with the solution of this problem which is preferred by the writer[10] it does not seem that the foregoing solution of the maximum deflection by the shear-area method is the shortest.

If Fig. 29 had been loaded with uniformly distributed loads of different values, then to solve for the maximum deflection the shear-area method would have been the shortest, and as the authors state it is suggested as particularly adapted to those problems involving distributed loads.

The shaft as given in the example actually has uniformly distributed loads of different values, but for the purpose of comparison it was considered as having no weight.

J. Charles Rathbun,[11] M. Am. Soc. C. E. (by letter).[11a]—In elementary textbooks on strength of materials the development of the beam theory is given, usually starting with the authors' Equation (2) and deriving the slope and deflection curves by direct integration. It is also shown that the loading, shear, and moment curves are related in the same manner as the moment divided by $E\,I$, the slope and deflection curves. It follows at once, with the usual assumptions of the beam theory and for a constant moment of inertia, that the five curves in Fig. 30 form a series in which each succeeding curve may be obtained by direct integration.

If the method of obtaining the equation of the $n + 1$-curve of this series from the n-curve is the same whether n is 1, 2, 3, or 4, one can obtain the

[11] Associate Prof., Civ. Eng., Coll. of the City of New York, New York, N. Y.

[11a] Received by the Secretary July 3, 1935.

fifth curve from the second one in the same way that he obtained the fourth from the first; or, he may obtain the fourth from the second in the same way that the third is obtained from the first. In each case the constants of integration must be taken care of by other means than those of pure mathematics. However, as shown by the authors in Equation (1), if the moment of inertia is not constant, the curves of Fig. 30(a) and Fig. 30(b) of the series do not have the same physical meaning when divided by the variable, I, as they have in the series of the previous paragraph. They must be considered as the first and second derivatives of the $\dfrac{M}{E\,I}$ - equation. The (d)-curve is the slope, whereas the (e)-curve is the deflection. With this second series equations are related to each other in the same way that they are in the first.

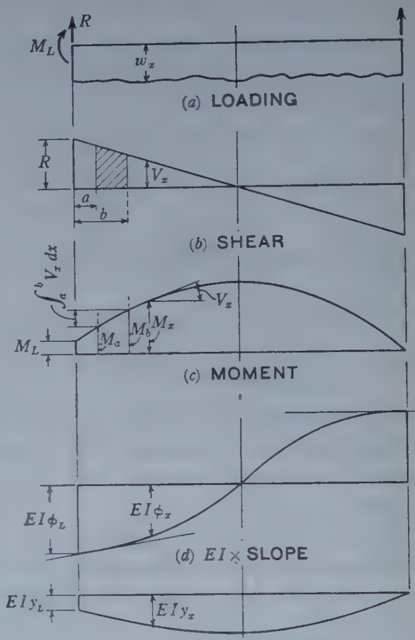

FIG. 30.

In order to take advantage of these well-known facts, one must keep the signs consistent as well as the units. The writer feels that inconsistencies have occurred in the several basic formulas derived by the authors and he has taken the liberty to re-state Equations (6), (7), (92), (93), (94), and (95), giving the assumptions under which the re-stated formulas are derived. It is expected that some of the differences between the two sets of formulas can be explained by differences of definitions both of terms and signs. It is hoped that the authors will clarify this phase of their paper in their closing discussion and will state definitely their assumptions as to signs. The writer has used the convention of analytic geometry that a dimension is positive if measured to the right or upward from the origin, whereas a force is positive if it acts in a positive direction—that is, upward. The origin is assumed at the left end of the beam. Curves (a) and (d) of Fig. 30 differ from those of Fig. 1 in sign possibly because of these assumptions. In the case of a sudden change in the formula of the load, or in the moment of inertia, the origin can often be shifted to advantage.

In Fig. 30 the area bounded by the curve and any two ordinates is equal to the difference between the corresponding ordinates in the next lower curve. This is the result of the method of obtaining the equation of the curve, by integration. It also follows that the units used in measuring the ordinate of any curve are those of the curve from which it is derived multiplied by feet; whence, if the ordinates of the loading curve (Fig. 30(a))

are in pounds per foot, those of the shear curve (Fig. 30(*b*)) are in units of pounds, and those of the moment curve (Fig. 30(*c*)) are in pound-feet; the $E\,I\,\phi$-curve (Fig. 30(*d*)) are in pound-feet^2; and, those of the $E\,I\,y$-curve (Fig. 30(*e*)) are in pound-feet.^{3} If one elects to divide by $E\,I$ and so use the second series, as the y-curve ordinates must be in feet, the units for the other curves follow at once with the (*d*)-curve ordinates being non-dimensional, the (*c*)-curve in feet^{-1}, the (*b*)-curve, or mathematical curve, in feet^{-2}, and the (*a*)-curve in feet^{-3}. Each term of the corresponding equation derived should conform to one or other of these systems of units, or the reason for not doing so should be evident. In any case each equation should be self-consistent in its units.

It has been shown that the relationship between Fig. 30(*b*) and Fig. 30(*d*) is the same as that between Fig. 30(*a*) and Fig. 30(*c*). In the first series the equation for Fig. (30*c*) is obtained (from the definition of moment) from that of Fig. 30(*a*) for the moment, $M_X = R\,X$, plus the moment of the loads about Point X (the load, w, is negative and this load moment, therefore, is negative in value). If x is taken as the distance from the load, $w\,dx$, to the point, X: $M_X = R\,X + \int_0^x w\,x\,dx$. It follows, then, from Fig. 30(*b*), that the equation for Fig. 30(*d*) is:

$$E\,I\,\phi_x = E\,I\,\phi_L + \int M\,dx = E\,I\,\phi_L + I\,A\bar{x} \quad \ldots\ldots\ldots(110)$$

or $\phi_x = \phi_L + \dfrac{A\bar{x}}{E}$, in which $A\bar{x}$ is the first moment of the area of the shear, divided by the I-curve (or mathematical beam curve) between $x = 0$ and $x = X$ about Point X. In this case, M_L is assumed to be zero. In the example shown in Fig. 30, ϕ_L, w, and, therefore, $\int^x w\,x\,dx$, are all negative in value whereas $A\bar{x}$ and $R\,X$ are positive. Equation (110) the writer feels should be used instead of the authors' Equation (6). Equations (6) and (7) apply only when $E\,I$ is a constant. If it is desired to consider I as a variable, Equation (110) becomes:

$$\phi_x = \phi_L + \frac{1}{E}\int_0^x \frac{M}{I}\,dx \quad \ldots\ldots\ldots\ldots\ldots\ldots(111)$$

or $\phi_x = \phi_L + \dfrac{A\bar{x}}{E}$. Integrating Equation (110) gives,

$$E\,I\,y = E\,I\,y_L + E\,I\int_0^X \phi_x\,dx = E\,I\,y_L + E\,I\,\phi_L\,X + I\int_0^X A\bar{x}\,dx$$

$$= E\,I\,y_L + E\,I\,\phi_L\,X + I\iint x\,dA\;dx$$

and dividing by the constant, $E\,I$,

$$y = y_L + \phi_L\,X + \frac{I_x}{2\,E} \quad \ldots\ldots\ldots\ldots\ldots\ldots\ldots(112)$$

In Equation (112), I_x is taken as the second moment or moment of inertia of the area under the mathematical-beam curve between the ordinates, $x = 0$ and $x = X$, about the ordinate throught Point X. The value of the authors' $\int A\bar{x}\,dx = \frac{I_x}{2}$ presents an interesting and a novel idea. The proof is quite simple. Equation (112) corresponds to the authors' Equation (7) when y_L is zero. If I is a variable, $y = y_L + \phi_L X + \frac{1}{E}\int\int \frac{M}{I}\,dx^2$ $= y_L + \phi_L X + \frac{I_x}{2\,E}$, as in Equation (112).

Apparently, the authors have assumed that EI is a constant in deriving Equations (92) to (95). The writer has obtained the following equations under the same assumption:

$$E\,I\,\phi_x = E\,I\,\phi_L + M_L X + \frac{R\,X^2}{2} + \int\int\int w\,dx^3$$

$$= E\,I\,\phi_L + M_L X + \frac{R\,X^2}{2} + \frac{1}{2}\int x^2\,(w\,dx)$$

and,

$$E\,I\,y = E\,I\,y_L + E\,I\,\phi_L\,X + M_L\frac{X^2}{2} + R\,\frac{X^3}{6}\int\int\int\int w\,dx^4$$

$$= E\,I\,y_L + E\,I\,\phi_L\,X + M_L\,\frac{X^2}{2} + \frac{R\,X^3}{6} + \frac{1}{6}\int x^3\,(w\,dx)$$

in which such terms as $\int x^2\,(w\,dx)$ and $\int x^3\,(w\,dx)$ may be interpreted as the second and third moments of the area under the load curve between $x = 0$ and $x = X$ about the ordinate through Point X. As R may be considered as a part of the load, and writing dW to represent the load whether concentrated as R, or distributed as $w\,dx$:

$$E\,I\,\phi_x = E\,I\,\phi_L + M_L\,X + \frac{1}{2}\int X^2\,dW$$

and,

$$E\,I\,y = E\,I\,y_L + E\,I\,\phi_L\,X + \frac{M_L\,X^2}{2} + \frac{1}{6}\int x^3\,dW$$

As dA and I_x are given definitions relative to the mathematical and shear curves and Q has not been defined by the authors these notations have not been incorporated in these equations. The subscript, L, for "left end" used by the authors is used in this discussion instead of the less definite, e, as the origin is always placed at the left end.

The writer takes issue with the authors in the case of the equations in a number of the examples particularly as to their inconsistency in units and

signs. This inconsistency makes it practically necessary to re-work the examples in order to connect their application with the ordinary beam theory and through them to connect the area-moment method with this theory. It is hoped that in their closing discussion the authors will clear up these points so that their work can be followed more readily.

It is understood that the following corrections in the paper as published in May, 1935, *Proceedings*, will be made before final publication in *Transactions*: In Equation (6), multiply the integrals by $\frac{1}{EI}$; in Equation (7), change θ to ϕ; in Equation (8), change θ_l to ϕ_v; in Equation (13), change M to ϕ; in Equation (26), multiply y by EI; on page 611, Line 5, change "Case 4" to "Case 3"; in Equation (37), change ϕ_y to ϕ_x; in Equation (40*b*), the last quantity should read "$-\frac{w}{EI} \times X \times \frac{x}{2} \times \frac{2x}{3}$"; in Equation (42), the last two quantities should read "$-\frac{PL}{8} \times \frac{L}{4} = \frac{5PL^2}{64EI}$"; in Equation (47), multiply Ey by I; in Equation (53), change $\frac{x^3}{3}$ to $\frac{x^3}{6}$; in Equations (76), (77), and (78), multiply ϕ_L by E; in Equations (80) and (81), change ϕ_A to ϕ_L; in Equation (82), change x to X; in Fig. (20*c*), the moment at the extreme right end will be M_3; in Equation (95) change ϕ_x to ϕ_e; and, in the lines following Equation (95), "$\phi_e = EI \times$ end slope"; and "$y_e = EI \times$ end deflection."

HAROLD R. KEPNER,[12] ASSOC. M. AM. SOC. C. E. (by letter).[12a]—Another analogy is presented in this paper, whereby structural problems involving the solution of the elastic curve equation may be simplified. Like the moment-area method and the column analogy it makes use of a dummy loading on a dummy structure, certain functions of which loading equal the desired functions of a real load on a real structure.

So far as the writer knows the analogy of the shear-area method has not been presented before, although the difficulties involved in the use of the moment area for distributed loads have indicated the desirability of some method involving the simpler shear curve.

A study of this paper has suggested a slightly different statement of the method as presented by the authors which seems more nearly to approach the "conjugate beam" method in its procedure. In spite of its limitations, the writer believes a brief presentation of this procedure may be worth while. Since the advantages of this analogy over those of the conjugate beam analogy seem to disappear for beams of varying cross-section, this procedure will be presented for the case of prismatic beams only, although its use is perfectly general if not always simple of computation.

---

[12] Associate Prof. of Eng., Utah State Agri. Coll., Logan, Utah.

[12a] Received by the Secretary July 11, 1935.

Statement.—If a dummy beam is loaded with the shear diagram from some real loading on a real (prismatic) beam, the following relations of load functions exist:

(1) The shear at a given section of the dummy beam equals the bending moment at the corresponding section of the real beam;

(2) The bending moment at a given section of the dummy beam, divided by $E\,I$ (modulus of elasticity and moment of inertia of a section of the real beam, respectively), equals the slope at the corresponding section of the real beam; and

(3) The second moment of the forces on one side of a given section of the dummy beam, divided by $2\,E\,I$, equals the deflection at the corresponding section of the real beam.

That these relations are true may be seen by a study of Equations (1) to (7). By "second moment" is meant what is commonly called "moment of inertia" and is computed as follows:

(*a*) For an area, the expressions for the moment of inertia of an area are applicable, are available in handbooks and textbooks, and, for simple figures, have been memorized by most engineers;

(*b*) For a single force, it is the product of the force by the square of the perpendicular distance from the force to the point in question; and

(*c*) For a couple, it is the product of the moment of the couple by twice the distance from its point of application to the point in question. That this is true for a couple may be shown as follows: Referring to Fig. 31, the second moment of the couple, $M = F\,a$ about Point O equals,

FIG. 31.

$$I_o = F\,(a + x)^2 - F\,x^2 = F\,a^2 - 2\,F\,a\,x + F\,x^2 - F\,x^2 = F\,a\,(a + 2\,x)$$

$$= 2\,x\,F\,a = 2\,x\,M \dots\dots\dots\dots\dots\dots\dots (113)$$

(Making a very small and F very large, without changing the moment, $M = F\,a$.)

The reactions at the supports of the dummy beam are either forces, couples, or a combination of forces and couples, and are determined by the conditions at the corresponding supports of the real beam. Table 1 shows how they are determined for several common types of beam. The symbols, V, M, ϕ, and y, represent the shear, bending moment, slope, and deflection at the given section of the real beam, and the primed symbols, V', M', and I', represent the shear, bending moment, and second moment, respectively, at the corresponding section of the dummy beam.

The signs used for both beams correspond to the convention in which upward forces on the left produce positive shear, and a beam bent concavely upward has positive bending moment. With a positive shear diagram taken as a downward load on the dummy beam, the sign of the second moment is the product of the sign of the bending moment by the sign of x and corre-

sponds to a positive slope on the real beam, down to the right, and to positive deflection downward. In order to illustrate the procedure several of the cases presented by the authors will serve as examples.

TABLE 1.—COMPUTATIONS OF REACTIONS FOR DUMMY BEAM

Type of Real Beam	REAL BEAM: Conditions at Left End	REAL BEAM	REAL BEAM: Conditions at Right End	DUMMY BEAM: Conditions at Left End	DUMMY BEAM	DUMMY BEAM: Conditions at Right End
Simple	$M_L = 0$ $\phi_L \neq 0$ $y_L = 0$	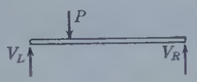	$M_R = 0$ $\phi_R \neq 0$ $y_R = 0$	$V'_L = 0$ $M'_L \neq 0$ $I'_L = 0$	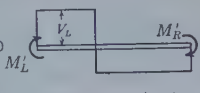 Reactions = 2 Couples	$V'_R = 0$ $M'_R \neq 0$ $I'_R = 0$
Cantilever	$M_L = 0$ $\phi_L \neq 0$ $y_L \neq 0$	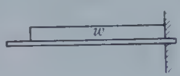	$M_R \neq 0$ $\phi_R = 0$ $y_R = 0$	$V'_L = 0$ $M'_L \neq 0$ $I'_L \neq 0$	 Reactions = 1 Force, 1 Couple	$V'_R \neq 0$ $M'_R = 0$ $I'_R = 0$
Fixed	$M_L \neq 0$ $\phi_L = 0$ $y_L = 0$	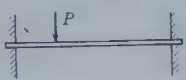	$M_R \neq 0$ $\phi_R = 0$ $y_R = 0$	$V'_L \neq 0$ $M'_L = 0$ $I'_L = 0$	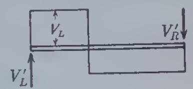 Reactions = 2 Forces	$V'_R \neq 0$ $M'_R = 0$ $I'_R = 0$
Continuous. Supports Level	$M_L \neq 0$ $\phi_L \neq 0$ $y_L = 0$		$M_R \neq 0$ $\phi_R \neq 0$ $y_R = 0$	$V'_L \neq 0$ $M'_L \neq 0$ $I'_L = 0$	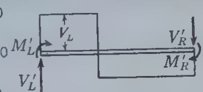 Reactions = 2 Forces, 2 Couples	$V'_R \neq 0$ $M'_R \neq 0$ $I'_R = 0$

Case 3.—Simple Beam with Concentrated Load Not at Mid-Span.—Making use of the condition of zero deflection at the right support and using the equivalent rectangles of Fig. 32(*c*) (the moment of inertia, I, of the rectangle about its base equals $\frac{b\,h^3}{3}$):

$$I'_R = 0 = (M'_L)\;(2\,L) - \left(\frac{Pa}{L}\right)\left(\frac{L^3}{3}\right) + \frac{P\,a^3}{3} = 0 \quad \ldots\ldots\ldots (114)$$

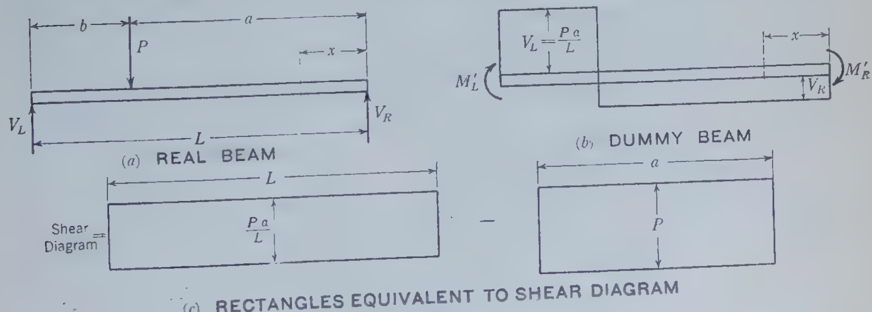

FIG. 32.

$$M'_L = \left(\frac{Pa}{6L}\right)(L^2 - a^2) = \left(\frac{Pab}{6L}\right)(L + a) \qquad (115)$$

$$\phi_L = \frac{M'_L}{EI} = \left(\frac{Pab}{6EI}\right)\left(\frac{(L + a)}{L}\right) \qquad (116)$$

and,

$$\phi_R = \left(\frac{-Pab}{6EI}\right)\left(\frac{(L + b)}{L}\right) \qquad (117)$$

The deflection, y, at a distance, x, from the right end is given by $\frac{I'_x}{2EI}$; as follows (when x is measured to the left the sign is negative):

$$I'_x = -(M'_R)(-2x) - \left(\frac{Pb}{L}\right)\left(\frac{x^3}{3}\right) = \left(\frac{2Pabx}{6L}\right)(L + b) - \frac{Pbx^3}{3L} = \left(\frac{Pbx}{3L}\right)(L^2 - b^2 - x^2) \qquad (118)$$

and,

$$y = \frac{I'_x}{2EI} = \left(\frac{Pbx}{6EIL}\right)(L^2 - b^2 - x^2) \qquad (119)$$

Since maximum deflection occurs where the slope, ϕ, is zero:

$$M'_x = 0 = -M'_R + \left(\frac{Pb}{L}\right)\left(\frac{x^2}{2}\right) = 0 \qquad (120)$$

$$\left(\frac{Pab}{6L}\right)(L + b) = \left(\frac{Pb}{L}\right)\left(\frac{x^2}{2}\right) \qquad (121)$$

$$x = \sqrt{\frac{a}{3}(L + b)} \qquad (122)$$

and,

$$y_m = \left(\frac{Pab}{9EIL}\right)\sqrt{\frac{a}{3}(L + b)^3} \qquad (123)$$

Case 11.—Fixed Beam with a Concentrated Load Not at the Mid-Span.—Making use of the conditions of zero slope and zero deflection at the right

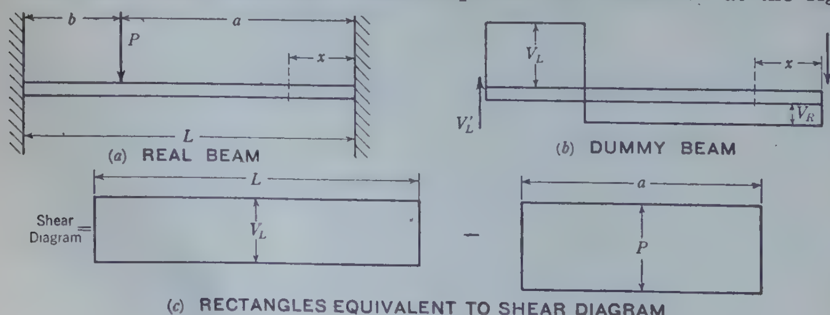

FIG. 33.

support and the equivalent rectangles (see Fig. 33): When $\phi_R = 0$, $M'_R = 0$,

$$V'_L L - \frac{V_L L^2}{2} + \frac{P a^2}{2} = 0 \qquad (124)$$

and, when $y'_R = 0$, $I'_R = 0$,

$$V'_L L^2 - \frac{V_L L^3}{3} + \frac{P a^3}{3} = 0 \qquad (125)$$

Eliminating V_L between Equations (124) and (125),

$$M_L = V'_L = \frac{P a^2 b}{L^2} \qquad (126)$$

and,

$$M_R = V'_R = \frac{P a b^2}{L^2} \qquad (127)$$

Then, by substitution in Equation (124),

$$V_L = \left(\frac{P a^2}{L^3}\right) (L + 2 b) \qquad (128)$$

and,

$$V_R = \left(\frac{P b^2}{L^3}\right) (L + 2 a) \qquad (129)$$

Points of inflection occur where $V' = 0$; hence:

$$\frac{P a^2 b}{L^2} - V_L x = 0 \qquad (130)$$

and,

$$\left(\frac{P a^2}{L^3}\right) (L + 2 b) x = \frac{P a^2 b}{L^2} \qquad (131)$$

If measured from the left end, $x = \frac{L b}{(L + 2 b)}$; and, if measured from the right end, $x = \frac{L a}{(L + 2 a)}$. Maximum deflection occurs where the slope, ϕ_x, is zero, hence:

$$M'_x = 0 = \frac{- P a b^2 x}{L^2} + \left(\frac{P b^2}{L^3}\right) (L + 2 a) \left(\frac{x^2}{2}\right) = 0 \qquad (132)$$

If measured from the right end, $x = \frac{2 a L}{(L + 2 a)}$, and,

$$I'_x = V'_R x^2 - V_R \frac{x^3}{3} = \frac{P a b^2 x^2}{L^2} - \left(\frac{P b^2}{L^3}\right) (L + 2 a) \left(\frac{x^3}{3}\right)$$

$$= \left(\frac{P b^2 x^2}{3 L^3}\right) (3 a L - 3 a x - b x) \qquad (133)$$

and the deflection equation, $y = \dfrac{I'_x}{2\,EI}$, becomes:

$$y = \left(\frac{P\,b^2\,x^2}{6\,E\,I\,L^3}\right)(3\,a\,L - 3\,a\,x - b\,x) \quad \ldots\ldots\ldots\ldots (134)$$

Substituting the value of x for maximum deflection, the expression becomes:

$$y_m = \frac{2\,P\,a^3\,b^2}{3\,EI\,(L + 2\,a)^2} \quad \ldots\ldots\ldots\ldots (135)$$

Cases 19 to 22.—Continuous Beam; Three-Moment Equation.—The right-hand side of the three-moment equation is the difference of two terms. The first equals the slope at the right end of a simple span of dimensions and loading of the left span of the continuous beam, multiplied by $6\,E$, and

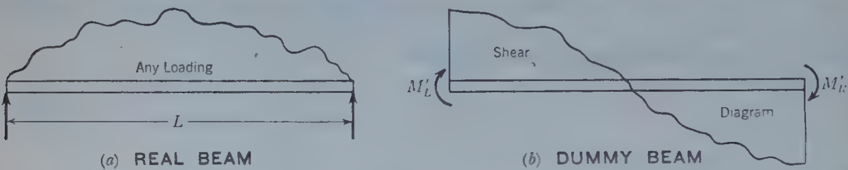

(a) REAL BEAM (b) DUMMY BEAM

FIG. 34.

the second term equals the slope at the left end of a simple span of the dimensions and loading of the right span of the continuous beam, multiplied by $6\,E$. Now, for a simple beam with any loading (see Fig. 34):

$$I'_L = 0 = (-M'_R)\,(2\,L) + I'_{LS} = 0 \quad \ldots\ldots\ldots\ldots (136)$$

$$M'_R = \frac{I'_{LS}}{2\,L} \quad \ldots\ldots\ldots\ldots (137)$$

$$\phi_R = \frac{I'_{LS}}{2\,E\,I\,L} \quad \ldots\ldots\ldots\ldots (138)$$

and,

$$\phi_L = \frac{I'_{RS}}{2\,E\,I\,L} \quad \ldots\ldots\ldots\ldots (139)$$

in which, I'_{RS} and I'_{LS} are the second moments of the shear diagram only, about the right and left supports, respectively.

Substituting these values for the slope, the general equation for three moments reads as follows, in terms of the second moments of the shear diagram for any loading:

$$\frac{M_1\,L_1}{I_1} + 2\,M_2\left(\frac{L_1}{I_1} + \frac{L_2}{I_2}\right) + \frac{M_3\,L_2}{I_2} = 6\,E\,\phi_{R1} - 6\,E\,\phi_{L2} = \frac{3\,I'_{L1}}{L_1\,I_1} - \frac{3\,I'_{R2}}{L_2\,I_2} \quad \ldots (140)$$

and for equal values of moment of inertia in both spans:

$$M_1\,L_1 + 2\,M_2\,(L_1 + L_2) + M_3\,L_2 = \frac{3\,I'_{L1}}{L_1} - \frac{3\,I'_{R2}}{L_2} \quad \ldots\ldots (141)$$

in which I'_{L1} and I'_{R2} are the second moments of the shear diagrams only, in the two spans, about the left and right outside supports, respectively.

Case 20.—Continuous Beam with Uniform Load Over Each Span.—Referring to Fig. 35 $\left(\text{the moment of inertia, } I\text{, of a triangle about its apex, is } \frac{b\,h^3}{4}\right)$:

$$I'_{LS} = \left(\frac{w\,L}{2}\right)\left(\frac{L^3}{3}\right) - (w\,L)\left(\frac{L^3}{4}\right) = -\frac{w\,L^4}{12} \quad \text{.......(142)}$$

and,

$$I'_{RS} = \frac{w\,L^4}{12} \quad \text{........................(143)}$$

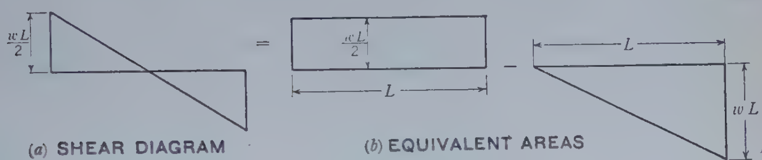

FIG. 35.

Equations (142) and (143) could also have been obtained by treating the shear diagram as a couple. Substituting these values for I'_{RS} and I'_{LS} in the three-moment equation, it becomes:

$$\frac{M_1 L_1}{I_1} + 2\,M_2\left(\frac{L_1}{I_1} + \frac{L_2}{I_2}\right) + \frac{M_3 L_2}{I_2} = -\frac{w_1 L^3_1}{4\,I_1} - \frac{w_2 L^3_2}{4\,I_2} \quad \text{...(144)}$$

or,

$$M_1 L_1 + 2\,M_2\,(L_1 + L_2) + M_3 L_2 = -\frac{w_1 L^3_1}{4} - \frac{w_2 L^3_2}{4} \quad \text{.....(145)}$$

It is hoped that the foregoing examples will serve to show the general procedure in applying the shear-area method in this manner and will also reveal its chief advantage, as stated by the authors; namely, the relative simplicity of calculating the second moment of shear areas composed of triangles and rectangles as compared with the first moment of parabolic segments of moment areas when uniformly distributed loads are involved. By the proper choice of equivalent areas a distributed load of any extent, or any arrangement of concentrated loads, may be handled simply. For loads of variable intensity and for beams of variable cross-section the dummy loading becomes quite as complex as that of the moment-area method. For beams of variable cross-section the loading curve is that of Equation (1) of the paper, and Statements (1), (2), and (3) of this discussion must be modified to take this into account. However, it is the writer's opinion that, for these more complicated cases, the classical methods involving integration, or approximate solutions involving the $\frac{M}{E\,I}$-diagram, might as well be used. It is worth

mentioning, perhaps, that the shear-area method has the pedagogical value inherent in all such analogies in that it provides the student with excellent drill in the fundamental relations and quantities of mechanics.

FRED L. PLUMMER,[13] ASSOC. M. AM. SOC. C. E. (by letter).[13a]—Engineers, in general, are not adequately familiar with the relations existing between load, shear, moment, slope, and deflection for continuous members subjected to lateral forces. Although most engineers may have had occasion to use Equations (146) and (147), at some time, relatively few have made any use of the companion Equations (148) and (149). In these equations all the symbols for slope:

$$EI\frac{dy}{dx} = \phi \qquad (146)$$

for moment:

$$EI\frac{d^2y}{dx^2} = M \qquad (147)$$

for shear:

$$EI\frac{d^3y}{dx^3} = V \qquad (148)$$

and, for load:

$$EI\frac{d^4y}{dx^4} = w \qquad (149)$$

have their usual significance. The authors indicate these relationships graphically in Fig. 1.

The wider use of the methods of "slope deflection" and "moment distribution", together with their many modifications, has created keen interest in methods of structural analysis during the past few years. Since these methods of analysis are based on a study of distortions, it is natural that interest in methods of determining distortions and deflections should be equally stimulated. The writer has been amazed by the extent of this interest as evidenced by the attendance of designing engineers and architects in the vicinity of Cleveland, Ohio, at special classes devoted to the study of the various methods of determining stresses and deflections for statically indeterminate structures.

The authors have performed a double service to the profession, therefore, first by describing the successive relationships between load, shear, moment, slope, and deflection, and then demonstrating how these relationships may be used to develop alternates to the "moment-area" method of determining slopes and deflections. The writer has solved several problems by both the "shear-area" and the "moment-area" methods, and finds that he prefers the latter method. This decision may be due, however, to the fact that he has been familiar with this method for a much longer period.

---

[13] Assoc. Prof., Structural Eng., Case School of Applied Science, Cleveland, Ohio.

[13a] Received by the Secretary July 17, 1935.

In all such "shorthand" methods of analogy, a set of rules may be established and followed blindly, thereby "grinding out" the required results with little mental effort and possibly with little appreciation of the physical significance of the process. It is quite proper that such methods be developed. The routine labor required for many similar designs may thus be lightened materially. It is also important, however, that the young engineer first familiarize himself with the physical meaning of his process so that he may use it when, and only when, it is entirely applicable.

The writer would have preferred that the authors omit several of the routine examples, substituting in their place a more complete development of the theoretical principles illustrated.

AMERICAN SOCIETY OF CIVIL ENGINEERS

Founded November 5, 1852

DISCUSSIONS

STRUCTURAL BEAMS IN TORSION

Discussion

By Messrs. Harold E. Wessman, and F. B. Seely and W. J. Putnam

Harold E. Wessman,[15] Assoc. M. Am. Soc. C. E. (by letter).[15a]—Structural engineers seem to be displaying an increasing interest in the effects of torsional resistance on stresses in structural members. This curiosity does not restrict itself solely to the member in torsion, but also embraces study of the resulting effects on bending moments of connecting members. The paper is a timely contribution to the subject. Although the problem is more apparent in the monolithic reinforced concrete building frame, it occurs also in steel structures where some connections insure full continuity and practically all types of connections develop at least a modicum of restraint.

In most structural units torsion may prove to be quite unimportant. One is not justified in dismissing it, however, simply because he considers it unimportant. Every one is prone to do this at times with knotty problems, because it is the easiest course. It is better to be an "agnostic" rather than an "atheist" in such matters, however, until a basis of scientific research, both analytical and physical, justifies conclusions. In the matter of torsion, that basis will be provided by papers such as this one and additional researches involving other structural cross-sections and their relation to the structure as a whole.

The writer has suggested that torsion may fall into the category of knotty problems. It is complex, both in its broad aspects and in its details. A thorough consideration of torsion in the field of structures takes the problem of analysis away from planar confines and puts it in the space realm. This will discourage many from further consideration of the subject because, as a rule, structural engineers prefer to be "two-dimensional analysts," despite the fact that they live in a space world.

Note.—The paper by Inge Lyse, M. Am. Soc. C. E., and Bruce G. Johnston, Jun. Am. Soc. C. E., was published in April, 1935, *Proceedings*. Discussion on this paper has appeared in *Proceedings*, as follows: April 1935, by Messrs. H. M. Westergaard and R. D. Mindlin, and Joseph B. Reynolds.

[15] Assoc. Prof., Dept. of Structural Eng. and Mechanics, Coll. of Eng., Univ. of Iowa. Iowa City, Iowa.

[15a] Received by the Secretary May 2, 1935.

The details of the problem, likewise, are not simple of solution. One needs only to look at the disagreement apparent in Fig. 9 to confirm this statement. Various difficulties are involved in the study of torsion stresses in a single twisted unit, quite apart from those which come to light when one considers related effects in connecting members.

As the authors note, only a few simple cross-sections, such as the circle, ellipse, rectangle, square, equilateral triangle, and certain hollow sections, are susceptible to pure mathematical analysis. The membrane analogy, or soap bubble, is called upon to serve as an aid in the solution of other sections, such as the familiar rolled steel shapes used in structural practice. It is difficult, however, to get accurate measurements of the slopes of the soap bubble at the boundaries because of the curving or "meniscus" effect of the film. Since the slope of the film at the boundary is a measure of the unit shear stress at corresponding points, the modification in curvature makes accurate interpretation somewhat diffcult. The materials testing laboratory is another aid for the determination of the torsion constant by twisting actual specimens; but it is difficult to "look inside" the beam to find out what happens, and at points on the exterior at fillets, it is hard to measure strains.

This paper emphasizes the co-operation possible between mathematical analysis, mathematical aids such as the membrane analogy, and the physical testing laboratory. The preceding comments by the writer indicate briefly that this co-operation is necessary in securing an answer to torsion problems. The authors are to be congratulated for using all the available tools at their command.

It is unfortunate, however, that they did not present their soap film tests in more detail. It would be interesting to know precisely how they determined the volume under the film and the coefficients, α, in Fig. 7. Was any attempt made to obtain an independent curve for stress concentration at fillets similar to those in Fig. 9 (which exhibit a considerable lack of agreement both in values and trends)? At the ratio, $\frac{r}{n} = 0.40$, the percentage increase of stress in fillets ranges from about 45 to 140. At the ratio, $\frac{r}{n} = 1.00$, the range is from 25 to 90 per cent. For ratios of $\frac{r}{n} > 1$, Westergaard's and Mindlin's curve and Taylor's soap film tests,[36] portrayed in Fig. 9, show increasing values of stress concentration. All other curves continue the downward trend. In other words, they conform to the thesis that an increase in the radius of the fillet always reduces the stress concentration. Cushman's soap film tests[13] were not carried far enough to give values in the range, $1 < \frac{r}{n} < 2$, although the general trend is downward.

Incidentally, the following question may be raised at this point: "Are the ordinates in Fig. 9, 'Percentage of Increase of Stress in Fillets,' or do they

[36] Technical Repts., Advisory Committee for Aeronautics, No. 33, June, 1917 (Rept. covers experimental work with soap films by Messrs. A. A. Griffith and G. I. Taylor).

[13] "Shearing Stresses in Torsion and Bending by Membrane Analogy," by P. A. Cushman, Doctoral Dissertation, Univ. of Michigan, 1932.

actually give 'Percentage of Increase of Stress Concentration Factor'"? This question is pertinent, because, as the fillet size increases, the torsion constant also increases; hence, for a given twisting moment, the stress at the fillet might actually decrease, even if the ratio of stresses, $\frac{\tau_m}{\tau_o}$, increases. It is to be noted that Equation (67) is expressed in terms of this ratio. Föppl, who derives an equation from a consideration of Stokes' theorem, expresses results in terms of a similar ratio.[11]

If the authors plotted contours to determine the volume under each film for different fillet radii, the following procedure would give an approximate check on the curves in Fig. 9 with little additional labor. Even if contours were not plotted, the determination of a slope at one point on the fillet near the edge, but far enough away to eliminate edge influence, should not take much additional time, considering the extent of the laboratory testing that was done.

In Fig. 30(a), Section OA bisects the fillet, and Fig. 30(b) shows a profile of the section. The differential equation of curvature in terms of the

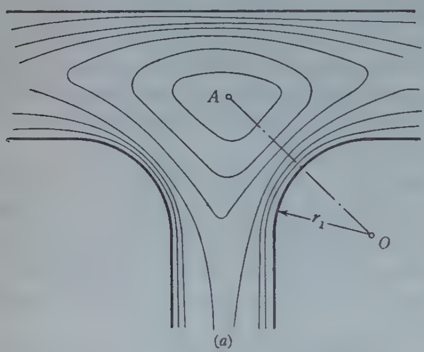

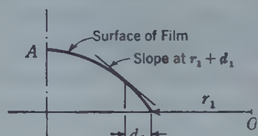

FIG. 30.

stress function for torsion is given by the authors in Equation (1). This equation, of course, follows directly from the differential equation of equilibrium of forces expressed in terms of displacement rather than stress. Moreover, it is the same as the one for curvature of the soap bubble surface, except that the constant, $2\,G\,\theta$, is replaced by the constant, $\frac{p}{S}$, in which p is the unit pressure normal to the surface of the film, and S is the constant tension in the film.

In polar co-ordinates, Equation (1) becomes,

$$\frac{\partial^2 F}{\partial r^2} + \frac{1}{r}\,\frac{\partial F}{\partial r} + \frac{1}{r^2}\,\frac{\partial^2 F}{\partial \theta^2} = C \quad\ldots\ldots\ldots\ldots\ldots\ldots(91)$$

in which C is the constant, $-2\,G\,\theta$, or $-\frac{p}{S}$.

[11] "Drang und Zwang," by A. and L. Föppl, Second Edition, Vol. 2, 1928, p. 73.

For a surface of revolution, $\frac{\partial F}{\partial \theta} = 0$ and Equation (91) takes the simpler form,

$$\frac{\partial^2 F}{\partial r^2} + \frac{1}{r}\frac{\partial F}{\partial r} = C \qquad (92)$$

The solution of this differential equation is,

$$F = \frac{Cr^2}{4} + A \log r + B \qquad (93)$$

The equation for the slope, which measures the unit shear is,

$$\frac{\partial F}{\partial r} = \frac{Cr}{2} + \frac{A}{r} \qquad (94)$$

At the fillet of a rolled section, part of the soap film is approximately a surface of revolution with its axis passing through the center of the fillet; contours over this part will be parallel to the edge of the fillet, as in Fig. 30(*a*). Radius r in Equation (94) is, therefore, the radius relative to the center of the fillet. The value of the constant, C, has already been noted. It only remains for Constant A to be evaluated. In one approximate solution proposed, A is found by assuming that the slope is zero at a distance, $\frac{n}{2}$, in from the edge of the fillet,[12] and that the surface is one of revolution for at least this same distance in from the edge. The assumption of zero slope at the distance noted is open to question.

By an inspection of contours, or by one or two measurements, either of slope or of elevation, F, of the surface, at a point a small definite distance in from the edge, the authors could have obtained a finite value for the slope, $\frac{\partial F}{\partial r}$, at a finite distance from the center of the fillet. By substituting this in Equation (94), the constant, A, can then be evaluated more closely.

The writer realizes that this involves fairly precise measurement. One might also raise the question, "Why not measure the slope right at the edge and get the shear stress at the critical point directly"? If one can eliminate edge influence on curvature, this would be the logical solution. The writer suggests the preceding steps, however, to get away from edge influence and to obtain a more accurate determination of the constant, A. He ventures to predict that the resulting curve for the stress concentration factor will exhibit a rising trend for values of $\frac{r}{n} > 1$.

F. B. SEELY,[17] ESQ., AND W. J. PUTNAM,[18] ESQ. (by letter).[18a]—It may be of value to study the results of the experiments discussed in this paper, on the

[12] "Theory of Elasticity," by S. Timoshenko, 1934, p. 259.

[17] Head, Dept. of Theoretical and Applied Mechanics, Coll. of Eng., Univ. of Illinois, Urbana, Ill.

[18] Prof. of Theoretical and Applied Mechanics, Coll. of Eng., Univ. of Illinois, Urbana, Ill.

[18a] Received by the Secretary May 18, 1935.

torsional properties of H-beams and I-beams, in connection with the results of somewhat similar, but less exhaustive, tests on several rolled steel channels conducted by the writers in 1930.

For a bar or shaft having a circular cross-section, the relation between the twisting moment, T, and the angle of twist per unit of length, θ, as given by Equation (4), is $T = J\ G\ \theta$. Similarly, the authors point out that for members having non-circular cross-sections, Equation (4) becomes $T = K\ G\ \theta$ (see Equation (5)), in which K is the torsion constant for the given section. For a narrow rectangle Saint Venant gave the approximate value of $K = \frac{1}{3}\ n^3\ b$ (see Equation (6)) in which n is the short dimension and b the long dimension of the rectangle. Likewise, for a section made up of narrow rectangles, such as a ship channel, the approximate value of K for the entire section is $K = \Sigma(\frac{1}{3}\ n^3\ b)$; but for a (trapezodial) section with sloping sides, such as the flanges of most rolled steel channels, the value of K is expressed by Equations (9) and (10) of the paper.

For a channel section, then, the expression for K, would be,

$$K = \frac{1}{3}\ w^3\ d + 2\ \frac{b}{12}\ (m + n)\ (m^2 + n^2) \ldots\ldots\ldots\ldots (95)$$

in which the symbols are identified by reference to Fig. 31. As noted by the authors, the value of K is proportional to the volume under a soap film that is stretched across an opening of the same shape as that of the cross-section, the soap film being inflated slightly by a difference of pressure on the two sides of the film. In Equation (95) the factor corresponding to the "hump" or "hill" that occurs in the soap film at the junctions of the flanges and web is omitted. The "end loss" corresponding to the "sloping down" of the soap film to meet the edges of the short dimensions of the rectangular or trapezodial sections, is also omitted. In their studies, the writers concluded that corrections for these two effects could be omitted in view of the deviation of the actual dimensions of rolled sections from the tabular handbook values. Furthermore, these effects in a channel section are relatively less than in an I-section or in an H-section.

Fig. 31.

Comparison of Test and Calculated Values of K.—Four channels ranging in depth from 6 to 15 in., as listed in Table 5 were tested as free-ended members in pure torsion to determine the torsional constant, K, from Equation (4), namely,

$$K = \frac{1}{G} \times \frac{T}{\theta} \ldots\ldots\ldots\ldots (96)$$

The value of G was taken to be 12 000 000 lb per sq in.; T was measured in a 23 000 in-lb torsion machine, and the angle of twist, $\phi = \theta\ L$, in a given length, L, was measured by means of a 20-in. level bar on flat bars attached to the top flange of the channel, as shown in Fig. 32.

TABLE 5.—TEST RESULTS AND COMPUTED VALUES FOR PURE TORSION IN CHANNEL SECTIONS

Channel	Torsion Constant, K		Shearing Stresses in Web and Flange			
	Test value (Equation (96))	Computed value (Equation (95))	Test value of $E\epsilon$	$\tau = \sigma = 0.8 \times$ Column (4) (see Equation (97))	Computed value of τ (Equation (98))	Approximate maximum value of τ in flange (Equation (99))
(1)	(2)	(3)	(4)	(5)	(6)	(7)
6-In., 15.3-Lb:*						
Web	0.206	0.201	$2.00T$	$1.60T$	$1.69T$	......
Flange			$2.43T$	$1.94T$	$1.93T$	$2.18T$
6-In., 15.5-Lb:†						
Web	0.400	0.405	$1.72T$	$1.38T$	$1.38T$	......
Flange			$1.48T$	$1.18T$	$0.847T$	$1.20T$
10-In., 15.3-Lb:						
Web	0.256	0.203	$1.54T$	$1.23T$	$1.18T$	......
Flange			$2.25T$	$1.80T$	$2.15T$	$3.11T$
15-In., 33.9-Lb:						
Web	1.08	0.951	$0.593T$	$0.474T$	$0.420T$	......
Flange			$0.838T$	$0.670T$	$0.685T$	$0.947T$

* Ship channel. † Heavy channel.

The relations between T and ϕ for several lengths along a 10-in., 15.3-lb channel are shown in Fig. 33(a). The values of K found from the curves

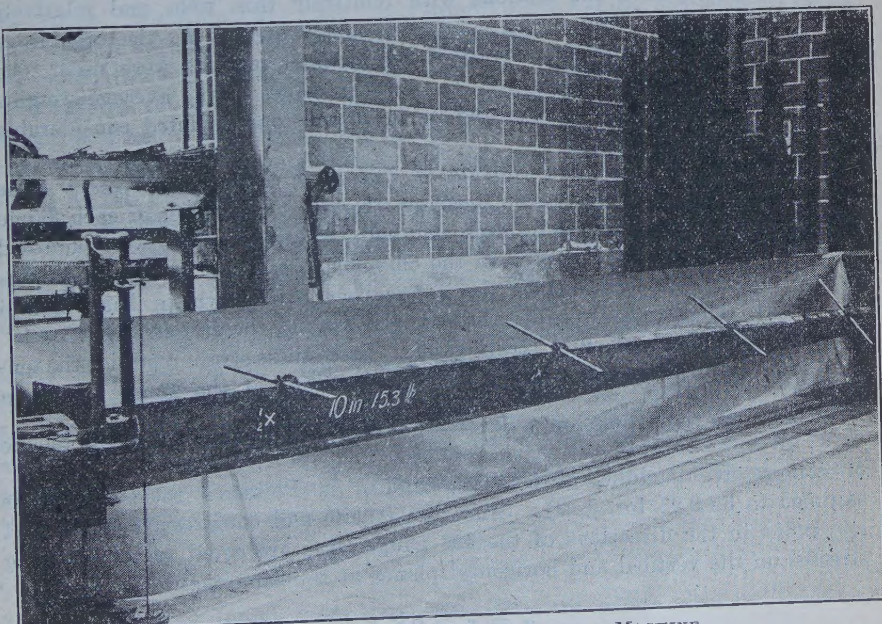

FIG. 32.—VIEW OF CHANNEL IN TESTING MACHINE.

similar to those shown in Fig. 33(*a*), together with the values of K computed from Equation (95), are given in Table 5, Column (3) for each of the four channels tested. It will be observed that the values computed from Equation (95) are not in close agreement with the values obtained from test results

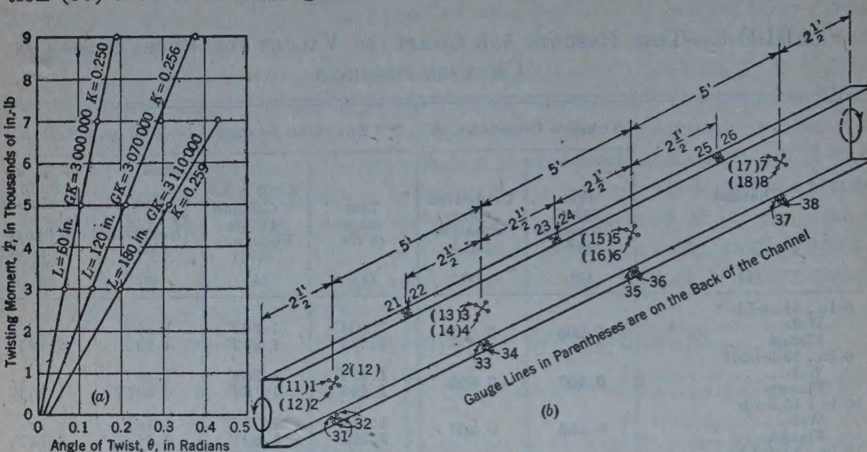

FIG. 33.—LOCATION OF 2-INCH GAUGE LINES ON 10-INCH, 15.3-POUND CHANNEL SUBJECTED TO PURE TORSION.

(Column (2), Table 5), but they indicate that Equation (95) may be used satisfactorily for approximate results. The computed values in Column (3) that deviate most from the test values apply to the 10-in. and the 15-in. channels, which have the sections with relatively thin webs and relatively thick and tapering flanges. In computing the values of K, the tabular or handbook values of the dimensions of the channel sections were used. All the channels tested checked closely the tabular values of the average weights per foot of length, but some of the linear dimensions deviated considerably from the tabular dimensions.

Comparison of Test and Calculated Values of Shearing Stresses.—The approximate values of the elastic shearing stresses at the center of each flange and at the center of the web on each channel at several sections were obtained by measuring the elastic strains in the channels caused by twisting moments at the ends. The locations of the gauge lines are shown in Fig. 32 and Fig. 33(*b*). The stresses were determined by measuring the unit strains, ϵ, on 45° gauge lines by means of a 2-in. strain-gauge. From these strain readings the tensile and compressive unit stresses in the directions of the gauge lines can be found from the expression, $\sigma = \dfrac{E\,\epsilon}{1 + \mu} = 0.8\,E\,\epsilon$, in which E is the tensile or compressive modulus of elasticity and μ is Poisson's ratio (which is assumed to be 0.25 for steel). Since the tensile and compressive stresses at any point in the directions of the 45° gauge lines are equal to the shearing stresses on the vertical and horizontal planes at the same point,

$$\sigma = \tau = 0.8\,E\,\epsilon \ldots\ldots\ldots\ldots\ldots\ldots\ldots\ldots (97)$$

The relations between the twisting or torsional moment, T, and the values of ϵ (or of $E\ \epsilon$, in which E is assumed to be 30 000 000 lb per sq in.) for several gauge lines are shown in Fig. 34. Similar curves were found for all the gauge lines on all the channels tested. The average of the values of $E\ \epsilon$ and the

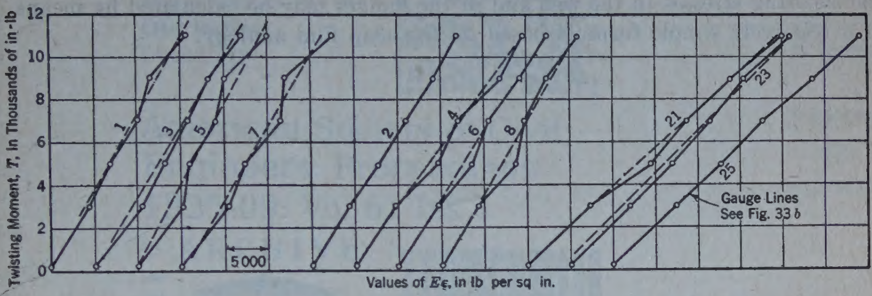

FIG. 34.

corresponding values of τ and σ in the web and flanges of each of the four channels tested, are shown in Table 5, together with the calculated values of the shearing stresses from the equation,

$$\tau = \frac{T\ t}{K} \quad \ldots\ldots\ldots\ldots\ldots\ldots\ldots\ldots\ldots (98)$$

in which t is the thickness of the section at the location of the gauge line (see Fig. 31). It will be observed that Equation (98) is consistent with the soap film analogy. The larger t becomes, the more will the soap film puff up; the greater will be the slope of the film; and, therefore, the greater the shearing stress. Equation (98) yields only approximate values, but leads to useful and reliable results as may be seen from Table 5, in which it is shown that the calculated and test results are in reasonably satisfactory agreement (compare Column (5) and Column (6)). It should be noted that since the strain-gauge used had a 2-in. gauge length, the stresses obtained from the measured strains are the average in the region of the point considered rather than the stress at the given point.

The computed values in Column (6), Table 5, that deviate most from the test values apply to the 6-in. 15.5-lb, and the 10-in. 15.3-lb channels. For these sections the 2-in. gauge line included too much of the relatively short flange width for satisfactory stress determinations at the point considered.

The maximum value of τ in the flange (not considering the stress at the fillet) would be (on the basis of the soap film analogy) at the point where the largest inscribed circle is tangent to the face of the flange, since the soap film would have the greatest slope at this point; the maximum shearing stress would occur, therefore, at about the point, A, Fig. 31. The approximate value of the maximum shearing unit stress on the outside face of the flange, should, then, be given by the equation,

$$\tau = \frac{T\ m}{K} \quad \ldots\ldots\ldots\ldots\ldots\ldots\ldots\ldots\ldots (99)$$

The values of τ found from Equation (99) are given also in Table 5, Column (7).

The results of these tests of rolled steel channels in pure torsion are in substantial agreement with the results of the similar but more exhaustive tests of I-beams and H-beams presented in the paper under discussion, in showing that reasonably reliable values of the angles of twist of the members and of the shearing stresses in the web and in the flanges may be calculated by means of a relatively simple formula based on the soap film analogy.